

Stochastic Convergence Rates and Applications of Adaptive Quadrature in Bayesian Inference

Blair Bilodeau¹ Alex Stringer² Yanbo Tang³

¹Department of Statistical Sciences, University of Toronto

²Department of Statistics and Actuarial Science, University of Waterloo

³Department of Mathematics, Imperial College London

Abstract

We provide the first stochastic convergence rates for a family of adaptive quadrature rules used to normalize the posterior distribution in Bayesian models. Our results apply to the uniform relative error in the approximate posterior density, the coverage probabilities of approximate credible sets, and approximate moments and quantiles, therefore guaranteeing fast asymptotic convergence of approximate summary statistics used in practice. The family of quadrature rules includes adaptive Gauss-Hermite quadrature, and we apply this rule in two challenging low-dimensional examples. Further, we demonstrate how adaptive quadrature can be used as a crucial component of a modern approximate Bayesian inference procedure for high-dimensional additive models. The method is implemented and made publicly available in the `aghq` package for the R language, available on CRAN.

* Authors listed alphabetically.

Contents

1	Introduction	4
2	Preliminaries	6
2.1	Bayesian Inference	6
2.2	Numerical Quadrature	6
2.3	Adaptive Quadrature	8
2.4	Approximate Bayesian Inference	8
3	Convergence Rates	9
3.1	Approximate Posterior	10
3.2	Approximate Posterior Summaries	11
3.3	Proof Sketch of Theorem 1	11
4	Low-Dimensional Parameter Spaces	12
4.1	Example: Modelling Infectious Disease Spread	12
4.2	Example: Estimating the Mass of the Milky Way	15
5	High-Dimensional Parameter Spaces	17
5.1	High-Dimensional Approximation Method	18
5.2	Example: Zero-Inflated Geostatistical Binomial Regression	19
6	Discussion	21
A	Regularity Assumptions	26
B	Proof of Theorem 1	27
B.1	Quantifying Accuracy for Approximate Bayesian Inference	27
B.2	Proof of Lemma 2	30
B.3	Proof of Lemma 3	35
C	Proof of Lemma 4	37
C.1	Bounding Term 1 of Eq. (21)	44
C.2	Bounding Term 2 of Eq. (21)	45
C.3	Bounding Term 3 of Eq. (21)	45
C.4	Bounding Term 4 of Eq. (21)	46
C.5	Bounding Term 5 of Eq. (21)	47
C.6	Bounding Term 6 of Eq. (21)	48
C.7	Bounding Term 7 of Eq. (21)	49
C.8	Combining the Bounds on Eq. (21)	49
C.9	Laplace Approximation Proof ($k = 1$)	51
D	Proofs of Convergence Rates for Approximate Posterior Summaries	52
D.1	Proofs for Exact Integration of Approximate Posterior	52
D.2	Proofs for Approximating Marginal Posterior Density	54
D.3	Proofs for Approximating Marginal Posterior Expectation	56

E	Computational Considerations	58
E.1	The aghq Package	58
E.2	Computing Posterior Summaries	61
E.3	Software Package Versions	62
E.4	Automatic Differentiation	62
E.5	Optimization Software	63
F	Simulations	63
G	Further detail for Section 5.2	64
G.1	MCMC Results	64
G.2	MCMC Results with β Fixed	66
G.3	Empirical Accuracy of AGHQ	66
H	Glossary of Commonly Used Terms	70

1. Introduction

The central challenge of Bayesian inference is computing the *posterior distribution*, which requires evaluating an integral—the *normalizing constant* or *marginal likelihood*—that is intractable in all but the simplest models. *Numerical quadrature* (or *cubature* in multiple dimensions) comprises a range of techniques for approximating deterministic integrals via function evaluations at finitely many points, and is a mature field of study in applied mathematics; see Davis and Rabinowitz (1975) for an overview. However, in Bayesian inference, the integrand is necessarily changing with the observed data, and consequently fixed quadrature rules can perform arbitrarily poorly by failing to capture the shifting mass of the integrand. To address this limitation, *adaptive quadrature* techniques based on shifting and scaling fixed quadrature rules using the mode and curvature of the integrand have been proposed in Bayesian inference since at least Naylor and Smith (1982). More recently, adaptive quadrature has been employed as a fundamental component of approximate Bayesian inference in the popular INLA framework (Rue et al. 2009), for integrating out random effects (Pinheiro and Bates 1995; Cagnone and Monari 2013), and in the context of Bayesian inversion (Schillings and Schwab 2016). In the present work, we study stochastic convergence rates as the sample size tends to infinity for fixed parameter dimension and number of quadrature points. Theorem 1 and its corollaries provide the first stochastic convergence rates for the error in normalizing Bayesian posterior densities with adaptive quadrature, and for computing approximate moments and marginal densities.

Despite its broad applicability and usage by practitioners, relatively little is known about the theoretical properties of adaptive quadrature for Bayesian inference. Naylor and Smith (1982) discuss the practical application of what Tierney and Kadane (1986) call *adaptive Gauss–Hermite quadrature* (AGHQ) in Bayesian inference, arguing that it is a useful tool for normalizing posterior distributions and computing approximate summary statistics, but do not provide any theoretical guarantees on its accuracy. Tierney and Kadane (1986) use AGHQ to renormalize a Laplace approximation (which itself corresponds to AGHQ with a single quadrature point) of the marginal posterior density, however they do not discuss the effect that the error introduced by this numerical renormalization may have on their convergence rate. Kass et al. (1990) rigorously establish convergence rates for the Laplace approximation in Bayesian inference, but their proof only applies to one-dimensional parameters, and they do not provide results for AGHQ with multiple quadrature points. More recently, for a specific, restricted class of one-dimensional functions that vary only through a scaling parameter n , Jin and Andersson (2020) expand upon the work of Liu and Pierce (1994) to show that AGHQ with $k \in \mathbb{N}$ quadrature points converges at relative rate $\mathcal{O}(n^{-\lfloor (k+2)/3 \rfloor})$, and comment that this rate holds in multiple dimensions using a specific extension of the univariate rule.

In statistical problems, the integrand varies through n both as a scaling factor and the data observed at time n , which is not captured by the class of functions considered by Liu and Pierce (1994) and Jin and Andersson (2020). A *stochastic convergence* perspective is needed in order to quantify the behaviour of AGHQ when used in fitting any statistical model, including when used to approximate the normalizing constant in Bayesian inference. Beyond the univari-

ate Laplace analysis by Kass et al. (1990), a stochastic convergence perspective is also taken by Schillings and Schwab (2016) in the context of Bayesian inversion of operator equations, where they study convergence as the variance of the data tends to zero. Dick et al. (2019) study Bayesian PDE inversion using a Quasi-Monte Carlo variant of numerical quadrature. As is standard in the numerical analysis literature, they suppose that the data (rather than the model) satisfies certain regularity conditions, and provide a convergence rate as the number of quadrature points tends to infinity. Convergence limits as the data variability tends to zero and as the number of quadrature points tends to infinity for a fixed data sequence are both distinct from the asymptotic statistics perspective we take of letting the sample size n tend to infinity, and our results explicitly identify the effect of k on the approximation error.

In this work, we quantify the stochastic error of using adaptive quadrature rules to approximate the posterior distribution and summary statistics based on it. We demonstrate that the crucial property of AGHQ is that the underlying quadrature rule, Gauss-Hermite quadrature, exactly integrates the product of the Gaussian density and any polynomial of *total order* $2k - 1$ or less for a well-chosen integer k in p dimensions; we call this property $\mathcal{P}(k, p)$ (see Definition 1). More precisely, under standard regularity assumptions, we prove that if the posterior normalizing constant is approximated using the adaptive form of *any* quadrature rule that satisfies $\mathcal{P}(k, p)$, then the relative error of the approximate normalizing constant to the true normalizing constant converges in probability at rate $\mathcal{O}_P(n^{-\lfloor (k+2)/3 \rfloor})$, where n is the number of observed data points (Theorem 1). The main technical contribution that enables this result is a precise quantification of how well the posterior distribution locally approximates a Gaussian distribution as a function of the data.

We further describe how to approximate marginal posterior densities and moments using a second application of AGHQ, and show that the convergence rate is preserved for the error of these approximate summary statistics (Corollaries 2 and 3). For approximate quantiles and credible sets, we show that the rate is preserved in the ideal case where one can exactly integrate the AGHQ approximation (Corollary 4), and provide a computational method to approximate these. We include a simulation study (Appendix F) that illustrates the stochastic nature of the convergence rates and demonstrates an example of a simple model in which our stated rate is achieved in finite samples empirically.

To illustrate the breadth of models for which adaptive quadrature provides a useful tool for inference, in Section 4 we directly apply the method to two challenging examples that satisfy the conditions of our theoretical results. For a distance-based, individual-level model for the spread of infectious disease, we show that the results obtained using AGHQ are nearly identical to those obtained via traditional sampling-based approaches by Almutiry et al. (2020), at a substantial reduction in computational time. Additionally, we apply AGHQ to estimate the mass of the Milky Way galaxy using multivariate position and velocity measurements of star clusters and a complex astrophysical model.

In addition to the low-dimensional examples of Section 4, in Section 5 we demonstrate the applicability of adaptive quadrature for high-dimensional models by employing it within a broader method to fit a complex zero-inflated geostatistical binomial regression model, which

we use to infer the spatial risk of contracting a certain tropical disease in West Africa, and for which Bayesian inferences had not previously been made. This example is particularly challenging and is not compatible with INLA or (to our knowledge) any other existing (non-MCMC) framework for making approximate Bayesian inferences, and we discuss some observed difficulties with applying MCMC to it as well.

AGHQ and the corresponding high-dimensional method are implemented in the `aghq` package in the R statistical programming language, made publicly available on the CRAN package repository. All code for the examples and simulations in the present paper is available at <https://github.com/awstringer1/aghq-paper-code>. For more details on `aghq`, see the vignette by Stringer (2021).

2. Preliminaries

2.1. Bayesian Inference

Suppose that we observe a dataset $\mathbf{Y}^{(n)} = (\mathbf{Y}_1, \dots, \mathbf{Y}_n) \subseteq \mathbb{R}^d$ generated from some unknown probability distribution. We fix a *model* for the data defined by a *parameter space* $\Theta \subseteq \mathbb{R}^p$ and *likelihood* $\pi(\mathbf{Y}^{(n)} \mid \boldsymbol{\theta})$. Often, the model assumes independent and identically distributed (i.i.d.) data, in which case the likelihood factors into $\pi(\mathbf{Y}^{(n)} \mid \boldsymbol{\theta}) = \prod_{i=1}^n \pi(\mathbf{Y}_i \mid \boldsymbol{\theta})$, but we do not require this restriction. Further, we do not require that the model be well-specified; the only constraint on the data-generating distribution is that it satisfies certain regularity assumptions for the chosen model.

For some *prior density* $\pi(\cdot)$ on Θ , the object of inferential interest is the *posterior density*

$$\pi(\boldsymbol{\theta} \mid \mathbf{Y}^{(n)}) = \frac{\pi(\boldsymbol{\theta}, \mathbf{Y}^{(n)})}{\int_{\Theta} \pi(\boldsymbol{\theta}', \mathbf{Y}^{(n)}) d\boldsymbol{\theta}'}, \quad (1)$$

where $\pi(\boldsymbol{\theta}, \mathbf{Y}^{(n)}) = \pi(\boldsymbol{\theta})\pi(\mathbf{Y}^{(n)} \mid \boldsymbol{\theta})$ is the *unnormalized posterior density*. Inference for $\boldsymbol{\theta}$ is based upon point and interval estimates computed from $\pi(\boldsymbol{\theta} \mid \mathbf{Y}^{(n)})$.

All posterior summaries (marginals, moments, quantiles, etc.) require knowledge of the normalized posterior distribution, which requires computing the denominator of Eq. (1), referred to as the *marginal likelihood* or *normalizing constant*,

$$\pi(\mathbf{Y}^{(n)}) = \int_{\Theta} \pi(\boldsymbol{\theta}', \mathbf{Y}^{(n)}) d\boldsymbol{\theta}'.$$

The computation of this integral—as well as the further integration required to compute posterior summary statistics—is typically not analytically tractable, so inference is instead conducted using integral approximations.

2.2. Numerical Quadrature

A *quadrature rule* for approximating an integral $F = \int f(\boldsymbol{\theta}) d\boldsymbol{\theta}$ of a function $f : \Theta \rightarrow \mathbb{R}$ is a collection of *points* $\mathcal{Q} \subseteq \Theta$ and a *weight function* $\omega : \mathcal{Q} \rightarrow \mathbb{R}$, and is denoted by $\mathfrak{R}(\mathcal{Q}, \omega)$. The approximate integral under such a rule is denoted by

$$\tilde{F}_{(\mathcal{Q}, \omega)} = \sum_{z \in \mathcal{Q}} f(z) \omega(z),$$

which we denote by just \widetilde{F} when $\mathfrak{R}(\mathcal{Q}, \omega)$ is clear. Often, quadrature rules are designed to be exact for specific functions of interest, most often polynomials. A p -dimensional polynomial P , defined by

$$P(x_1, \dots, x_p) = \sum_{t=1}^T a_t \prod_{d=1}^p x_d^{j_{t,d}}$$

for some $T \in \mathbb{N}$, $(a_1, \dots, a_T) \in \mathbb{R}^T$, and $(j_{t,1}, \dots, j_{t,p})_{t \in [T]} \subseteq \mathbb{N}^p$, is said to have *total order* $\max_{t \in [T]} \sum_{d=1}^p j_{t,d}$ (Heiss and Winschel 2008).

Definition 1. For any $k, p \in \mathbb{N}$, a quadrature rule $\mathfrak{R}(\mathcal{Q}, \omega)$ satisfies $\mathcal{P}(k, p)$ if for all p -dimensional polynomials $P : \Theta \rightarrow \mathbb{R}$ of total order $2k - 1$ or less,

$$\int_{\Theta} \phi(\boldsymbol{\theta}; 0, \mathbf{I}_p) P(\boldsymbol{\theta}) d\boldsymbol{\theta} = \sum_{z \in \mathcal{Q}} \phi(z; 0, \mathbf{I}_p) P(z) \omega(z), \quad (2)$$

where $\phi(\boldsymbol{\theta}; 0, \mathbf{I}_p)$ is the standard p -dimensional Gaussian density.

The choice of the multivariate Gaussian density in Definition 1 is strategic, since in many parametric models the posterior distribution asymptotically (in sample size) converges to a Gaussian distribution by the Bernstein von Mises theorem (van der Vaart 1998, Chapter 10). For a non-standard limit, another baseline density can be used in place of the Gaussian in Definition 1, but we do not consider such models at present.

Consider the univariate case (i.e., $p = 1$) with $\Theta = \mathbb{R}$. For $k \in \mathbb{N}$, let H_k be the k^{th} Hermite polynomial, defined for all $z \in \mathbb{R}$ by

$$H_k(z) = (-1)^k e^{z^2/2} \frac{d^k e^{-z^2/2}}{dz^k}, \quad (3)$$

and denote its zeroes by z_1^*, \dots, z_k^* . These zeroes are distinct, symmetric about 0, and include 0 if and only if k is odd. The Gauss–Hermite quadrature (GHQ) rule uses the points $\mathcal{Q} = (z_j^*)_{j \in [k]}$ and the weight function

$$\omega(z_j^*) = \frac{k!}{[H_{k+1}(z_j^*)]^2 \phi(z_j^*)}, \quad (4)$$

where $\phi(\cdot)$ denotes the standard normal density. It is well known (e.g., Eq. (3.6.11) of Davis and Rabinowitz 1975) that GHQ satisfies $\mathcal{P}(k, 1)$ using the smallest number of points k possible. Hence, a naive application of GHQ for integrating f may be expected to perform well in the case that f is centred at $\theta = 0$ and $f(\theta)/\phi(\theta)$ is well-approximated by a univariate polynomial of total order $2k - 1$ or less. For a strict subset $\Theta \subset \mathbb{R}$, there exist finite interval Gauss quadrature rules (Section 2.7 of Davis and Rabinowitz, 1975; Theorem 1 of Bojanov and Petrov, 2001) that satisfy $\mathcal{P}(k, p)$.

Quadrature rules in p dimensions are formed by combining a univariate quadrature rule for each dimension. The most common combination technique is the *product rule*. If $\mathcal{Q} \subseteq \mathbb{R}$ is a collection of univariate quadrature points with weight function $\omega : \mathbb{R} \rightarrow \mathbb{R}$, the product rule induced multivariate quadrature rule is defined by $\mathcal{Q} = \mathcal{Q}^p$ and $\omega(\mathbf{z}) = \prod_{j=1}^p \omega(z_{i_j})$ for any

$\mathbf{z} = (z_{i_1}, \dots, z_{i_p}) \in \mathcal{Q}$. GHQ with the product rule satisfies $\mathcal{P}(k, p)$ (see Section 5.6 of Davis and Rabinowitz 1975), and requires k^p quadrature points. Sparse rules are also available that satisfy $\mathcal{P}(k, p)$, see Section 3.

In addition to $\mathcal{P}(k, p)$, a commonly desired property of quadrature rules is that they are *symmetric*, which we formalize now in the context of our problem. We note that GHQ with both product rule and the sparse rule we consider is symmetric, and hence restricting ourselves to symmetric rules is benign.

Definition 2. $\mathfrak{R}(\mathcal{Q}, \omega)$ is symmetric if for all $\mathbf{z} \in \mathcal{Q}$, $-\mathbf{z} \in \mathcal{Q}$ and $\omega(\mathbf{z}) = \omega(-\mathbf{z})$.

For Bayesian inference, we are interested in integrating functions that depend on $\mathbf{Y}^{(n)}$, such as $f(\boldsymbol{\theta}) = \pi(\boldsymbol{\theta}, \mathbf{Y}^{(n)})$. A limitation of numerical quadrature rules is that the points and weights remain fixed regardless of the shape and location of $\pi(\boldsymbol{\theta}, \mathbf{Y}^{(n)})$. As $n \rightarrow \infty$, standard Bayesian asymptotic theory (van der Vaart 1998, Ch. 10) guarantees that with high probability over $\mathbf{Y}^{(n)}$, the posterior mode concentrates to some $\boldsymbol{\theta}^*$ and the variance at the mode tends to 0. Consequently, any fixed rule will miss most of the mass of $\pi(\boldsymbol{\theta}, \mathbf{Y}^{(n)})$, and this problem worsens as $n \rightarrow \infty$. A procedure that explicitly *adapts* to the changing location and shape of the posterior density is necessary to obtain statistical performance guarantees that hold assuming only standard regularity conditions on the model.

2.3. Adaptive Quadrature

Naylor and Smith (1982) introduced a technique that was eventually named *adaptive* Gauss-Hermite quadrature (AGHQ) by Tierney and Kadane (1986), which we extend here to adaptive quadrature in general.

Given a function f to integrate (which one expects is well-approximated by a Gaussian density), define the mode, curvature at the mode, and Cholesky decomposition of the inverse curvature by

$$\hat{\boldsymbol{\theta}} = \arg \max_{\boldsymbol{\theta} \in \Theta} f(\boldsymbol{\theta}); \quad \mathbf{H}(\hat{\boldsymbol{\theta}}) = -\partial_{\boldsymbol{\theta}}^2 \log f(\hat{\boldsymbol{\theta}}); \quad [\mathbf{H}(\hat{\boldsymbol{\theta}})]^{-1} = \hat{\mathbf{L}}\hat{\mathbf{L}}^\top. \quad (5)$$

While we focus on the Cholesky decomposition for concreteness, any other matrix decomposition of this form could be used in our results. For any quadrature rule $\mathfrak{R}(\mathcal{Q}, \omega)$, the adapted integral approximation under this rule is

$$\tilde{F}_{(\mathcal{Q}, \omega)}^A = |\hat{\mathbf{L}}| \sum_{\mathbf{z} \in \mathcal{Q}} f(\hat{\mathbf{L}}\mathbf{z} + \hat{\boldsymbol{\theta}}) \omega(\mathbf{z}).$$

2.4. Approximate Bayesian Inference

We will use adaptive quadrature to approximate three integrals for Bayesian inference: the normalizing constant to obtain an approximate posterior density, and then the further integration needed to obtain approximate marginal posterior densities and moments. For any approximation $\tilde{\pi}(\mathbf{Y}^{(n)})$ of $\pi(\mathbf{Y}^{(n)})$, the approximate posterior distribution is

$$\tilde{\pi}(\boldsymbol{\theta} | \mathbf{Y}^{(n)}) = \frac{\pi(\boldsymbol{\theta}, \mathbf{Y}^{(n)})}{\tilde{\pi}(\mathbf{Y}^{(n)})}. \quad (6)$$

First, to approximate the normalizing constant, denote the analogous quantities of Eq. (5) for the function $f(\boldsymbol{\theta}) = \pi(\boldsymbol{\theta}, \mathbf{Y}^{(n)})$ by $\widehat{\boldsymbol{\theta}}_n$, $\mathbf{H}_n(\widehat{\boldsymbol{\theta}}_n)$, and $\widehat{\mathbf{L}}_n$. Then, for any quadrature rule $\mathfrak{R}(\mathcal{Q}, \boldsymbol{\omega})$, the adapted approximate normalizing constant under this rule is

$$\widetilde{\pi}_{(\mathcal{Q}, \boldsymbol{\omega})}^A(\mathbf{Y}^{(n)}) = |\widehat{\mathbf{L}}_n| \sum_{\mathbf{z} \in \mathcal{Q}} \pi(\widehat{\mathbf{L}}_n \mathbf{z} + \widehat{\boldsymbol{\theta}}_n, \mathbf{Y}^{(n)}) \boldsymbol{\omega}(\mathbf{z}). \quad (7)$$

When $\mathfrak{R}(\mathcal{Q}, \boldsymbol{\omega})$ is GHQ, the adaptive form is AGHQ by definition, and we denote the approximate normalizing constant by $\widetilde{\pi}^{\text{AGHQ}}(\mathbf{Y}^{(n)})$. When $k = 1$, $\mathbf{z} = 0$ and $\boldsymbol{\omega}(\mathbf{z}) = (2\pi)^{p/2}$, so the AGHQ approximation is actually a Laplace approximation (Tierney and Kadane 1986) and may be applied to integrals of any dimension without computational difficulties. In Section 5, we provide an example of how to combine AGHQ on low-dimensional parameters of interest with a Laplace approximation for high-dimensional nuisance parameters.

Second, to approximate the marginal posterior distribution, we apply AGHQ twice. Suppose the parameter can be decomposed into $\boldsymbol{\theta} = (\boldsymbol{\psi}, \boldsymbol{\lambda})$ where $\boldsymbol{\psi} \in \mathbb{R}^q$, and we are interested in computing the marginal posterior density at $\boldsymbol{\psi} = \boldsymbol{\psi}_0$,

$$\pi(\boldsymbol{\psi}_0 | \mathbf{Y}^{(n)}) = \frac{\int \pi(\boldsymbol{\psi}_0, \boldsymbol{\lambda}, \mathbf{Y}^{(n)}) d\boldsymbol{\lambda}}{\int \pi(\boldsymbol{\theta}, \mathbf{Y}^{(n)}) d\boldsymbol{\theta}}.$$

Define $\widehat{\boldsymbol{\theta}}_n^{\boldsymbol{\psi}_0} = \arg \max_{\boldsymbol{\theta} \in \Theta(\boldsymbol{\psi}_0)} \pi(\boldsymbol{\psi}_0, \boldsymbol{\lambda}, \mathbf{Y}^{(n)})$ for $\Theta(\boldsymbol{\psi}_0) = \{\boldsymbol{\theta} \in \Theta : \boldsymbol{\theta} = (\boldsymbol{\psi}_0, \boldsymbol{\lambda})\}$, $\mathbf{H}_n^{\boldsymbol{\psi}_0}(\boldsymbol{\theta}) = -\partial_{\boldsymbol{\lambda}}^2 \log \pi(\boldsymbol{\psi}_0, \boldsymbol{\lambda}, \mathbf{Y}^{(n)})$, and $\mathbf{H}_n^{\boldsymbol{\psi}_0}(\widehat{\boldsymbol{\theta}}_n^{\boldsymbol{\psi}_0})^{-1} = \widehat{\mathbf{L}}_n^{\boldsymbol{\psi}_0} (\widehat{\mathbf{L}}_n^{\boldsymbol{\psi}_0})^\top$. Then, given a fixed $\mathfrak{R}(\mathcal{Q}, \boldsymbol{\omega})$ and $\mathfrak{R}(\mathcal{Q}', \boldsymbol{\omega}')$ of dimensions p and $p - q$ respectively, the approximate marginal density is

$$\widetilde{\pi}(\boldsymbol{\psi}_0 | \mathbf{Y}^{(n)}) = \frac{|\widehat{\mathbf{L}}_n^{\boldsymbol{\psi}_0}| \sum_{\mathbf{z}' \in \mathcal{Q}'} \pi \left((0, \widehat{\mathbf{L}}_n^{\boldsymbol{\psi}_0} \mathbf{z}'^\top)^\top + \widehat{\boldsymbol{\theta}}_n^{\boldsymbol{\psi}_0}, \mathbf{Y}^{(n)} \right) \boldsymbol{\omega}'(\mathbf{z}')}{|\widehat{\mathbf{L}}_n| \sum_{\mathbf{z} \in \mathcal{Q}} \pi(\widehat{\mathbf{L}}_n \mathbf{z} + \widehat{\boldsymbol{\theta}}_n, \mathbf{Y}^{(n)}) \boldsymbol{\omega}(\mathbf{z})}, \quad (8)$$

which we denote by $\widetilde{\pi}^{\text{AGHQ}}(\boldsymbol{\psi}_0 | \mathbf{Y}^{(n)})$ when both rules correspond to AGHQ.

Third, let $g : \Theta \rightarrow \mathbb{R}_+$ be any nonnegative function satisfying $\int g(\boldsymbol{\theta}) \pi(\boldsymbol{\theta}) d\boldsymbol{\theta} < \infty$. Denote the analogous quantities of Eq. (5) for the function $f(\boldsymbol{\theta}) = \pi^g(\boldsymbol{\theta}, \mathbf{Y}^{(n)}) = \pi(\boldsymbol{\theta}, \mathbf{Y}^{(n)}) g(\boldsymbol{\theta})$ by $\widehat{\boldsymbol{\theta}}_n^g$, $\mathbf{H}_n^g(\boldsymbol{\theta})$, and $\widehat{\mathbf{L}}_n^g$, when they exist (see Appendix D.3). Then, given a fixed $\mathfrak{R}(\mathcal{Q}, \boldsymbol{\omega})$, define

$$\widetilde{\mathbb{E}}[g(\boldsymbol{\theta}) | \mathbf{Y}^{(n)}] = \frac{|\widehat{\mathbf{L}}_n^g| \sum_{\mathbf{z} \in \mathcal{Q}} \pi^g(\widehat{\mathbf{L}}_n^g \mathbf{z} + \widehat{\boldsymbol{\theta}}_n^g, \mathbf{Y}^{(n)}) \boldsymbol{\omega}(\mathbf{z})}{|\widehat{\mathbf{L}}_n| \sum_{\mathbf{z} \in \mathcal{Q}} \pi(\widehat{\mathbf{L}}_n \mathbf{z} + \widehat{\boldsymbol{\theta}}_n, \mathbf{Y}^{(n)}) \boldsymbol{\omega}(\mathbf{z})}, \quad (9)$$

which we denote by $\widetilde{\mathbb{E}}^{\text{AGHQ}}[g(\boldsymbol{\theta}) | \mathbf{Y}^{(n)}]$ when the rule is AGHQ.

3. Convergence Rates

In this section, we provide stochastic convergence rates for adaptive quadrature applied to Bayesian inference as well as stochastic convergence rates for various summary statistics of inferential interest. All proofs are deferred to the appendix. We denote probability under the true data-generating distribution by \mathbb{P}_n^* , and use C to denote a generic constant in n that may otherwise depend on p , k , and the universal constants in Appendix A.

3.1. Approximate Posterior

Theorem 1. *Suppose there exists $m \geq 4$ such that the likelihood of the data $\pi(\mathbf{Y}^{(n)} \mid \boldsymbol{\theta})$ is m -times differentiable as a function of $\boldsymbol{\theta}$ and the regularity assumptions of Appendix A hold. For $1 \leq k \leq \lfloor m/2 \rfloor$, if $\mathfrak{R}(\mathcal{Q}, \omega)$ is a symmetric quadrature rule satisfying $\mathcal{P}(k, p)$ then*

$$\lim_{n \rightarrow \infty} \mathbb{P}_n^* \left(\left| \frac{\pi(\mathbf{Y}^{(n)})}{\tilde{\pi}_{(\mathcal{Q}, \omega)}^{\mathcal{A}}(\mathbf{Y}^{(n)})} - 1 \right| \leq C n^{-\lfloor \frac{k+2}{3} \rfloor} \right) = 1.$$

Remark 1. *For AGHQ with $k = 1$, Theorem 1 recovers the known $\mathcal{O}_P(n^{-1})$ rate for the Laplace approximation (Kass et al. 1990). \triangleleft*

Remark 2. *If $k > \lfloor m/2 \rfloor$ the rate for $k = \lfloor m/2 \rfloor$ applies; this can be seen by reproducing the proof with a Taylor expansion of order m rather than one of order $2k$. \triangleleft*

The following corollary demonstrates the utility of Theorem 1, and follows immediately from the algebra of Appendix B.1 and the definition of $\tilde{\pi}_{(\mathcal{Q}, \omega)}^{\mathcal{A}}(\boldsymbol{\theta} \mid \mathbf{Y}^{(n)})$.

Corollary 1. *Under the conditions of Theorem 1,*

$$\lim_{n \rightarrow \infty} \mathbb{P}_n^* \left(\sup_{\boldsymbol{\theta} \in \Theta} \left| \frac{\pi(\boldsymbol{\theta} \mid \mathbf{Y}^{(n)})}{\tilde{\pi}_{(\mathcal{Q}, \omega)}^{\mathcal{A}}(\boldsymbol{\theta} \mid \mathbf{Y}^{(n)})} - 1 \right| \leq C n^{-\lfloor \frac{k+2}{3} \rfloor} \right) = 1$$

and

$$\lim_{n \rightarrow \infty} \mathbb{P}_n^* \left(\left\| \pi(\cdot \mid \mathbf{Y}^{(n)}) - \tilde{\pi}_{(\mathcal{Q}, \omega)}^{\mathcal{A}}(\cdot \mid \mathbf{Y}^{(n)}) \right\|_{\text{TV}} \leq C n^{-\lfloor \frac{k+2}{3} \rfloor} \right) = 1.$$

The results of this section apply to any symmetric quadrature rule satisfying $\mathcal{P}(k, p)$. In our applications, we focus on AGHQ defined using the product rule due to its simplicity and the fact that we have provided a robust implementation in the `aghq` package. It is of interest to compare alternatives empirically, such as the nested rule considered by Genz and Keister (1996), which is a Gaussian extension of the Gauss–Kronrod–Patterson construction.

Further, for multidimensional posteriors, our theoretical results apply to symmetric quadrature rules based on “sparse grids” as long as they satisfy $\mathcal{P}(k, p)$. For example, Smolyak’s quadrature rule satisfies this criteria (Heiss and Winschel 2008, Theorem 1), which reduces the dependence on the dimension from exponential to polynomial asymptotically. For specific k and p , however, sparse rules may actually be more computationally intensive than the product rule; for example, when $k = 5$ and $p = 2$, the product rule uses 25 quadrature points while the Smolyak rule uses 55.

The convergence rate depends directly on the number of quadrature points as follows. If one uses a product rule extension, then k^p quadrature points are needed to satisfy $\mathcal{P}(k, p)$. Hence, if the model is of dimension p and one uses a product rule extension with $|\mathcal{Q}|$ quadrature points, the convergence rate will be $n^{-\lfloor (|\mathcal{Q}|^{1/p} + 2)/3 \rfloor}$.

3.2. Approximate Posterior Summaries

We now show that the convergence rate of Theorem 1 is realized for the approximations to marginal distributions and moments. Refer to Section 2.4 for definitions and see Appendix E.2 for computational details.

Corollary 2. *Fix the value of ψ_0 . Suppose the conditions in Theorem 1 are satisfied when replacing all instances of θ with (ψ_0, λ) , θ^* with some constant $\theta_{\psi_0}^* = (\psi_0, \lambda_{\psi_0}^*)$, \mathbf{H}_n with $\mathbf{H}_n^{\psi_0}$ and $B_{\theta^*}^p(\cdot)$ with $B_{\lambda_{\psi_0}^*}^{p-q}(\cdot)$. Then*

$$\lim_{n \rightarrow \infty} \mathbb{P}_n^* \left(\left| \frac{\pi(\psi_0 \mid \mathbf{Y}^{(n)})}{\tilde{\pi}(\psi_0 \mid \mathbf{Y}^{(n)})} - 1 \right| \leq C n^{-\lfloor \frac{k+2}{3} \rfloor} \right) = 1.$$

Corollary 3. *Suppose $g : \Theta \rightarrow \mathbb{R}_+$ satisfies assumptions (M1) through (M3) from Appendix D.3. Then, if the conditions of Theorem 1 also hold,*

$$\lim_{n \rightarrow \infty} \mathbb{P}_n^* \left(\left| \frac{\mathbb{E}[g(\theta) \mid \mathbf{Y}^{(n)}]}{\tilde{\mathbb{E}}[g(\theta) \mid \mathbf{Y}^{(n)}]} - 1 \right| \leq C n^{-\lfloor \frac{k+2}{3} \rfloor} \right) = 1.$$

Both Corollaries 2 and 3 require additional assumptions to be verified. In Appendices D.2 and D.3, we show that (a) Corollary 2 applies to all values of ψ_0 in a $n^{-1/2}$ -neighbourhood of the unrestricted posterior mean (Proposition 1) and (b) Corollary 3 applies to all marginal posterior moments (Proposition 2).

3.3. Proof Sketch of Theorem 1

Finally, we provide a brief sketch of the proof of Theorem 1 to highlight the intuition for how convergence rates of the posterior inform the ultimate approximation error rate, and contrast our result with previous analyses of adaptive quadrature rules.

Proof sketch (informal) of Theorem 1. The proof quantifies the rate at which the posterior behaves locally Gaussian with polynomial error, combines this with the polynomial exactness property $\mathcal{P}(k, p)$, and then quantifies that the contribution to the posterior mass outside of this local neighbourhood is negligible with high probability. Specifically, the proof of Theorem 1 is composed of demonstrating that the following key facts hold with high probability asymptotically. We refer to the corresponding formal statements by their location in the appendix.

- (1) There exists a neighbourhood centered at a fixed parameter with radius defined by the curvature of the likelihood such that the likelihood is exponentially small outside of the neighbourhood. See Lemma 6 for the precise statement.
- (2) Within this neighbourhood, there exists a smaller neighbourhood with radius decaying at rate $\sqrt{\log(n)}/n$ such that the likelihood is polynomially small within the annulus outside of the shrinking neighbourhood. See Lemma 7 for the precise statement.

- (3) A Taylor series expansion (with order depending on k) of the unnormalized posterior provides an accurate polynomial approximation within the shrinking neighbourhood. See the proof of Lemma 4 for details. \square

The two most relevant works to our result are Kass et al. (1990) and Jin and Andersson (2020). We now contrast our proof with the analyses in both to highlight our technical contribution. First, we note that all of these works have only proved results for specifically AGHQ, while we have distilled the rate down to a simpler set of assumptions satisfied by more rules. Second, Kass et al. (1990) only prove the $k = p = 1$ case. They remark $p > 1$ is trivial, however, multivariate Taylor expansions lead to a product of sums rather than simply a sum of products, which consequently must be further upper bounded (see Eq. (20)).

Third, for the $k > 1$ case, higher-order derivatives are required, and Jin and Andersson (2020) sketch a proof for a limited class of functions in this setting. However, their analysis requires limiting assumptions that rule out posterior functions. Specifically, Jin and Andersson (2020) (inheriting the assumptions of Liu and Pierce 1994) only allow integrands of the form $\exp\{n\ell(\boldsymbol{\theta})\}$ rather than $\exp\{n\ell_n(\boldsymbol{\theta})\}$, meaning ℓ cannot depend on n and consequently also cannot depend on data; this eliminates *all* log-likelihoods.

Finally, neither Jin and Andersson (2020) nor Liu and Pierce (1994) provide an explicit argument for the order of the remainder terms from a Taylor series expansion. Handling these remainder terms is highly nontrivial, as can be seen by the proofs in Kass et al. (1990) and our appendix. Specifically, this requires a) identifying whether the remainder term is odd or even, b) controlling the higher-order derivatives of the likelihood at various distances from the target parameter (undefined for Jin and Andersson 2020), and c) applying probabilistic concentration results depending on the order of the remainder (also undefined for Jin and Andersson 2020, who take a deterministic approach).

4. Low-Dimensional Parameter Spaces

In the next two sections, we complement the theoretical results of Section 3 through three challenging examples, demonstrating the attractive computational properties of AGHQ for approximate Bayesian inference. In all of the examples, the quadrature rule we use is AGHQ with the product rule extension to multiple dimensions. Because MCMC is arguably the most widely researched method for making approximate Bayesian inferences, and enjoys robust implementation in open-source software, we pay attention to the practical advantages of AGHQ compared to state of the art MCMC methods for the chosen examples.

4.1. Example: Modelling Infectious Disease Spread

We consider the popular *Susceptible, Infectious, Removed* (SIR) model for infectious disease spread as implemented in the `EpiILMCT` package in R (Almutiry et al. 2020). Despite the low dimension of the parameter space, MCMC is the methodology of choice for fitting these models, leading to long run times and the need for specialized tuning and practical assessment of

Table 1: Posterior summaries are reported for AGHQ applied to the infectious disease data of Section 4.1. Comparison with MCMC is reported using the Kolmogorov-Smirnov (KS) distance. Mean, SD, and quantiles for α are multiplied by 100.

k	Mean		SD		2.5%		97.5%		KS	
	α	β	α	β	α	β	α	β	α	β
3	1.21	1.31	0.239	0.148	0.829	1.06	1.70	1.63	0.0326	0.0362
5	1.20	1.30	0.232	0.152	0.750	0.982	1.60	1.55	0.0234	0.0258
7	1.20	1.30	0.233	0.153	0.758	0.984	1.67	1.59	0.0133	0.0129
9	1.20	1.30	0.233	0.153	0.759	0.985	1.66	1.58	0.0139	0.0131
11	1.20	1.30	0.233	0.153	0.758	0.984	1.66	1.58	0.0126	0.0158
13	1.20	1.30	0.233	0.153	0.757	0.984	1.66	1.58	0.0168	0.0157
MCMC	1.20	1.30	0.228	0.151	0.761	0.986	1.65	1.58	-	-

convergence. We demonstrate here that AGHQ gives fast and stable results that closely match the output of MCMC in a small fraction of the run time.

Almutiry et al. (2020) consider an outbreak of Tomato Spotted Wilt Virus in $n = 520$ plants. Plants were grown on an even grid and checked for the virus every 14 days, a total of 7 times. There were $n_0 = 327$ plants infected by the end of the study period. For each plant we observe infection times $I_1 \leq \dots \leq I_{n_0}$ and $I_i = \infty$ for $i = n_0 + 1, \dots, n$. Plants may infect other plants while they are infected, and we observe associated removal times $R_i, i \in [n]$ where a plant is no longer infectious. The likelihood function for these observed infection and removal times is given by

$$\pi(\mathbf{I}, \mathbf{R} | \alpha, \beta) = \prod_{j=2}^{n_0} \left(\sum_{i: I_i < I_j \leq R_i} \lambda_{ij} \right) \exp \left\{ - \sum_{i=1}^{n_0} \sum_{j=1}^n [\min(R_i, I_j) - \min(I_i, I_j)] \lambda_{ij} \right\},$$

where $\lambda_{ij} = \alpha d_{ij}^{-\beta}$ is the *infectivity rate*: the rate at which an infectious plant i passes the disease to a susceptible plant j . Here d_{ij} is the Euclidean distance between plants i and j , and $\alpha, \beta > 0$ are the parameters of inferential interest. Independent Exponential(.01) priors are placed on α, β . As discussed in Appendix E, we transform the parameters as $\theta_1 = \log \alpha$ and $\theta_2 = \log \beta$, perform the quadrature on this transformed scale, and then transform back when reporting results.

Fig. 1 shows the posterior density estimates obtained using $k = 3, 5$, and 7 , and a comparison to a long MCMC run. The $k = 5$ and 7 results are visually indistinguishable from the density obtained through MCMC (and each other). Table 1 makes this more precise, with comparisons of posterior summaries of interest for $k = 3, 5, 7, 9, 11, 13$.

Table 2 shows the dramatic improvement in run time of AGHQ, as measured by the number of MCMC iterations (not including any time spent tuning the sampler) that could have been run in the same amount of time as it took to run the full AGHQ procedure. Running MCMC for the maximum such number of iterations resulted in all such iterations being marked as divergent

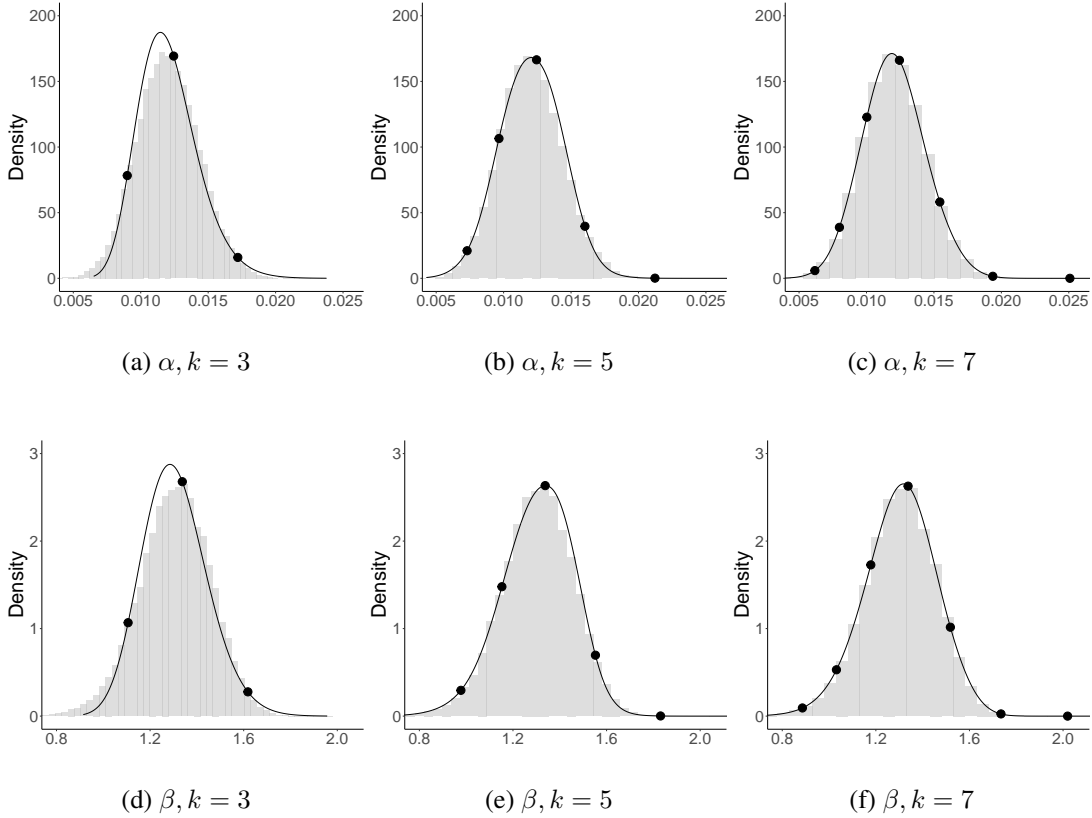


Figure 1: AGHQ (\bullet , $—$) and MCMC (\blacksquare) results for the infectious disease data of Section 4.1.

Table 2: Median (over 100 replications) run times to compute the marginal posteriors of both α and β using AGHQ for the infectious disease data of Section 4.1. Effective iterations are the number of MCMC iterations that could have been performed in the same time it took to run AGHQ, calculated based on a maximum run time of 84 seconds for 10,000 MCMC iterations using 4 parallel chains in `tmbstan`.

k	3	5	7	9	11	13
Time (Seconds)	0.101	0.160	0.224	0.285	0.357	0.441
Effective Iterations	12	19	27	34	42	52

and NaN estimates for the number of effective parameters. This demonstrates the substantial computational gains attained by AGHQ in this simple example when compared to MCMC.

In practice, choosing k remains an open question. As helpfully suggested by a referee, one strategy is to fit the model with successively increasing k until inferences no longer change with k . Table 1 shows this occurring for the infectious disease example, where up to $k = 13$ was fit, with similar estimates from about $k = 7$ or so. Adding up the first row of Table 2, we see that the total time for this entire strategy is about 1.568 seconds, or 186 total MCMC iterations, still a dramatic computational gain.

4.2. Example: Estimating the Mass of the Milky Way

Estimating the mass of the Milky Way Galaxy (hereafter the ‘‘Galaxy’’) is of importance to astrophysicists interested in determining the amount of Dark Matter in the universe, among other things. Eadie and Harris (2016) describe a probabilistic model for estimating and, importantly, quantifying uncertainty in the mass of the Galaxy using Bayesian inference. They use three-dimensional observed position and velocity measurements of star clusters in orbit of the Galaxy within a probabilistic physical model whose parameters determine the mass of the Galaxy at any radial distance from its centre. The parameters are subject to nonlinear constraints and are found to have strongly correlated, highly skewed posteriors with mode lying on or near the boundary of the parameter space (Eadie and Harris 2016). Care is required in implementing AGHQ for this problem.

The choice of priors was observed to have a substantial effect on inference in this problem (Eadie and Harris 2016), and a large body of knowledge on how to do this is available from the underlying physics. Eadie and Harris (2016) consider many different choices of priors and subsets of their data and the effect that this has on the estimated mass of the Galaxy. They use MCMC for inference, where each new model fit in their application requires careful tuning and assessment of the chains as well as potentially inconvenient run times. We find that AGHQ exhibits fast and stable performance in this challenging problem, although we note that our present implementation with `tmbstan` (software that was not available at the time Eadie and Harris 2016, was written) seems to avoid some of the reported challenges with MCMC as well. Nonetheless, this example serves to illustrate the application of AGHQ in a challenging applied problem.

Let $\mathbf{Y}_i = (y_{i1}, y_{i2}, y_{i3})$ denote the three measurements for each star cluster: position, radial velocity, and tangential velocity relative to the centre of the Galaxy (referred to as *galactocentric* measurements), and let the full matrix of data be $\mathbf{Y}^{(n)} = \{\mathbf{Y}_i : i \in [n]\}$. There are $n = 70$ clusters with complete measurements. The probability density for \mathbf{Y}_i is

$$f(\mathbf{Y}_i; \Psi_0, \gamma, \alpha, \beta) = \frac{L_i^{-2\beta} \mathcal{E}_i^{\frac{\beta(\gamma-2)}{\gamma} + \frac{\alpha}{\gamma} - \frac{3}{2}} \Gamma\left(\frac{\alpha}{\gamma} - \frac{2\beta}{\gamma} + 1\right)}{\sqrt{8\pi^3} 2^{-2\beta} \Psi_0^{-\frac{2\beta}{\gamma} + \frac{\alpha}{\gamma}} \Gamma\left(\frac{\beta(\gamma-2)}{\gamma} + \frac{\alpha}{\gamma} - \frac{1}{2}\right)},$$

where $L_i = y_{i1}y_{i3}$, $\mathcal{E}_i = \Psi_0 y_{i1}^{1-\gamma} - (y_{i2}^2 + y_{i3}^2)/2$, and $i \in [n]$. The parameters $\Xi = (\Psi_0, \gamma, \alpha, \beta)$ determine the mass of the Galaxy at radial distance r kiloparsecs (kpc) from its centre according

Table 3: Comparison of AGHQ with $k = 5$ to MCMC using the KS distance for the astronomy data of Section 4.2.

Param.	Ψ_0	γ	α	β
KS(AGHQ,MCMC)	0.00872	0.00844	0.0358	0.00739

to $M(r) = \Psi_0 \gamma r^{1-\gamma}$. While $M(r)$ only directly depends on Ψ_0 and γ , its posterior will depend indirectly on all four parameters due to correlation between them.

Eadie and Harris (2016) consider many different strongly informative priors for the four model parameters. We choose one configuration of theirs: $\Psi_0 \sim \text{Unif}(1, 200)$, $\gamma \sim \text{Unif}(0.3, 0.7)$, $\alpha - 3 \sim \text{Gamma}(1, 4.6)$, and $\beta \sim \text{Unif}(-0.5, 1)$. The parameters are further subject to nonlinear constraints $\alpha > \gamma$, $\alpha > \beta(2 - \gamma) + \gamma/2$, and $\mathcal{E}_i > 0, i \in [n]$.

We find the following transformations convenient in this example:

$$\theta_j = \log \left(-\log \left[\frac{\Xi_j - a_j}{b_j - a_j} \right] \right), j = 1, 2, 4, \quad \theta_3 = \log(\alpha - 3),$$

where (a_j, b_j) are the endpoints of the uniform prior for Ξ_j . We let $\boldsymbol{\theta} = (\theta_1, \theta_2, \theta_3, \theta_4)$ and normalize the posterior $\pi(\boldsymbol{\theta} | \mathbf{Y}^{(n)})$ using AGHQ with $k = 5$. We emphasize that these transformations are not required to apply the theoretical results of Section 3, and refer the reader to Appendix E for further discussion about implementation. To find the posterior mode accounting for the remaining non-linear constraints, we perform a constrained optimization using the IPOPT software (Wachter and Biegler 2006) with derivatives of the log-likelihood and constraints provided by the TMB software (Kristensen et al. 2016).

Figs. 2 and 3 show the marginal posteriors of Ξ and Fig. 3 the posterior mean and standard deviation of $M(r)$ respectively using $k = 5$, and hence Theorem 1 prescribes an $\mathcal{O}_P(n^{-2})$ relative error rate. The total computation time for the optimization, quadrature, and computation of marginal posteriors was around 1.3 seconds on a modern laptop using the aghq package. Table 3 shows the estimated KS statistic between the AGHQ and MCMC approximate empirical CDFs. AGHQ is generally quite accurate, with slight disagreement in the middle of the posterior for α , although the tail appears accurately estimated, which is reflected both visually in Fig. 2 and numerically in Table 3.

An interesting computational challenge emerges in this example: we observe that using a larger number of quadrature points to satisfy $k > 5$ results in points outside the constraint regions and is hence infeasible. A similar challenge is observed when computing the marginal posterior for β , and in this case only we report results of a simpler method based on reuse of the original adapted points. These challenges may be due to the low sample size: \mathbf{H}_n^{-1} has a wide spectrum that causes the quadrature points to be spread far apart. As n becomes larger this spectrum would be expected to become smaller and hence a larger number of quadrature points may be expected to lie inside the constraint region. However, we reiterate that $k = 5$ still yields a very fast $\mathcal{O}_P(n^{-2})$ relative error rate by Theorem 1 as well as empirically accurate results in this example (Table 3).

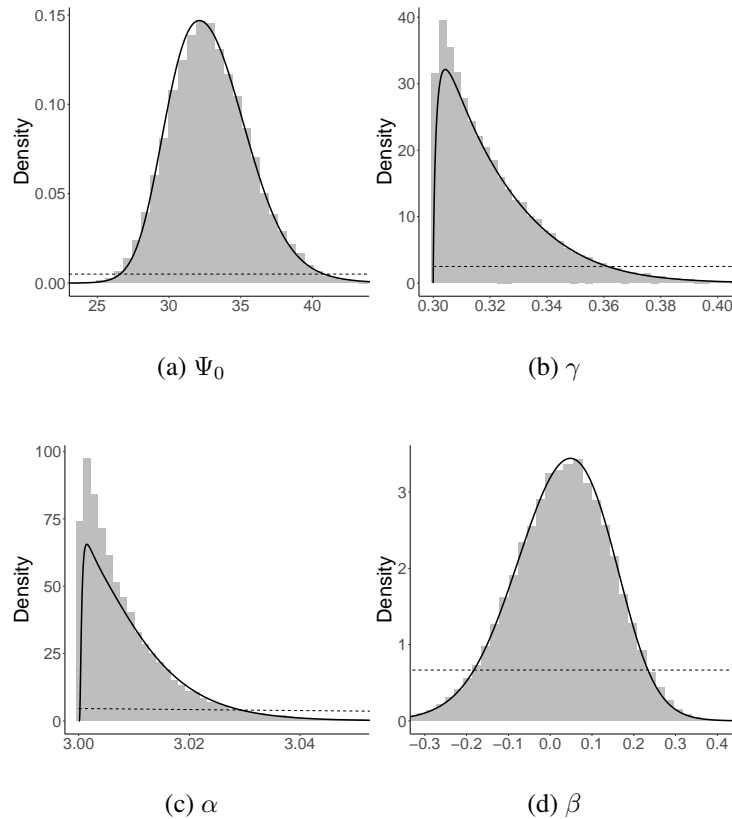


Figure 2: (a) – (d): prior (---), and AGHQ (—) and MCMC (■) approximate posterior distributions for the four parameters from the astronomy data of Section 4.2. The marginal posteriors for γ (b) and α (c) are particularly skewed, and the approximation appears very accurate in the tails of both distributions, which is important for accurately quantifying uncertainty using marginal credible intervals.

5. High-Dimensional Parameter Spaces

Adaptive quadrature is an increasingly popular technique in modern Bayesian statistics as one important component of more complicated methods for approximate posterior inference in models with high-dimensional parameter spaces. In this section we demonstrate the use of one such type of method, based on the INLA method of Rue et al. (2009), through fitting a spatial model for zero-inflated counts, for which MCMC-based inference is observed to be challenging.

The methods described in this section have no known convergence theory, and their usefulness in applied Bayesian statistics makes development of such theory a topic of substantial current interest. Theorem 1, which describes the convergence properties of the adaptive quadrature rules used at the core of these methods, is a first step in this direction.

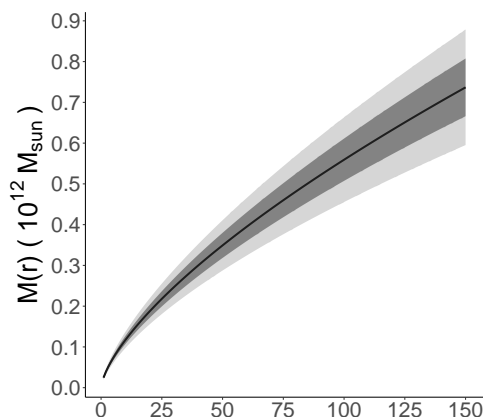


Figure 3: AGHQ estimated posterior mean mass (—), relative to the mass of the sun, of the Milky Way galaxy as a function of radial distance from galaxy centre (kpc), with one- (■) and two- (■) standard deviation bands for the astronomy data of Section 4.2.

5.1. High-Dimensional Approximation Method

Consider a parameter vector $(\mathbf{w}, \boldsymbol{\theta})$ where $\boldsymbol{\theta} \in \mathbb{R}^p$ and $\mathbf{w} \in \mathbb{R}^m$ with $p \ll m$. Bayesian inferences for these parameters are made using the posterior distributions:

$$\begin{aligned}\pi(\boldsymbol{\theta} | \mathbf{Y}^{(n)}) &= \frac{\int \pi(\mathbf{w}, \boldsymbol{\theta}, \mathbf{Y}^{(n)}) d\mathbf{w}}{\int \int \pi(\mathbf{w}, \boldsymbol{\theta}, \mathbf{Y}^{(n)}) d\mathbf{w} d\boldsymbol{\theta}}, \\ \pi(\mathbf{w} | \mathbf{Y}^{(n)}) &= \int \pi(\mathbf{w} | \boldsymbol{\theta}, \mathbf{Y}^{(n)}) \pi(\boldsymbol{\theta} | \mathbf{Y}^{(n)}) d\boldsymbol{\theta}.\end{aligned}$$

It is assumed that p is small enough to make it computationally feasible to directly apply adaptive quadrature to $d\boldsymbol{\theta}$ integrals, but that m is large enough for this to be infeasible for $d\mathbf{w}$ integrals, even using sparse grids or other non-product rule extensions to multiple dimensions. This occurs, for example, in hierarchical models (Kass and Steffey 1989; Rue et al. 2009; Wood et al. 2016; Geirsson et al. 2020; Section 5.2) where \mathbf{w} typically relate to the mean response, and $\boldsymbol{\theta}$ are variance components.

For any fixed $\boldsymbol{\theta}$, Tierney and Kadane (1986) suggest approximating $\pi(\boldsymbol{\theta} | \mathbf{Y}^{(n)}) \approx \tilde{\pi}_{\text{LA}}^{\text{AGHQ}}(\boldsymbol{\theta} | \mathbf{Y}^{(n)})$ by first approximating $\int \pi(\mathbf{w}, \boldsymbol{\theta}, \mathbf{Y}^{(n)}) d\mathbf{w} \approx \tilde{\pi}_{\text{LA}}(\boldsymbol{\theta}, \mathbf{Y}^{(n)})$ using AGHQ with $k = 1$ (a Laplace approximation), and then renormalizing the result using numerical integration, for which they also use AGHQ in their experiments. Stringer et al. (2021) combine this approximation with a Gaussian approximation $\pi(\mathbf{w} | \boldsymbol{\theta}, \mathbf{Y}^{(n)}) \approx \tilde{\pi}_{\text{G}}(\mathbf{w} | \boldsymbol{\theta}, \mathbf{Y}^{(n)})$, obtaining

$$\tilde{\pi}(\mathbf{w} | \mathbf{Y}^{(n)}) \approx \int \tilde{\pi}_{\text{G}}(\mathbf{w} | \boldsymbol{\theta}, \mathbf{Y}^{(n)}) \tilde{\pi}_{\text{LA}}^{\text{AGHQ}}(\boldsymbol{\theta} | \mathbf{Y}^{(n)}) d\boldsymbol{\theta}. \quad (10)$$

The integration in Eq. (10) is approximated with the same AGHQ points and weights used to obtain $\tilde{\pi}_{\text{LA}}^{\text{AGHQ}}(\boldsymbol{\theta} | \mathbf{Y}^{(n)})$, so that $\tilde{\pi}(\mathbf{w} | \mathbf{Y}^{(n)})$ corresponds to a discrete mixture of Gaussian approximations with weights determined by AGHQ. Inferences for \mathbf{w} are then made by sampling

from this Gaussian mixture. The INLA method of Rue et al. (2009) uses an alternative adaptive quadrature rule for the renormalization, and then another Laplace approximation to approximate the marginal distributions $\pi(w_j|\boldsymbol{\theta}, \mathbf{Y}^{(n)})$.

There is a growing body of evidence suggesting that approximations based on Eq. (10) give results empirically similar to those returned by MCMC and other methods (Rue et al. 2009; Brown 2011; Taylor and Diggle 2014; Stringer et al. 2021; Wood 2020) in faster computational times. In Section 5.2 we show an example of a model for which a state-of-the-art MCMC algorithm runs for days and fails to converge (Appendix G.1) to a suitable solution, while Eq. (10) provides a potentially suitable (Appendix G.3) solution in minutes. However, we stress that the convergence properties of Eq. (10) are not known, and the apparent practical utility of this approximation makes establishing such properties an important area of research. Because AGHQ is used several times in the computation of Eq. (10), Theorem 1 is a first step towards this broader goal.

5.2. Example: Zero-Inflated Geostatistical Binomial Regression

Diggle and Giorgi (2016) introduce a zero-inflated geostatistical binomial regression model, where both the incidence rate and suitability of infection (zero-inflation probability) varies spatially. They argue that such models are of substantial importance in the mapping of tropical diseases, and make frequentist inferences for the parameters of interest. Here we make Bayesian inferences for the spatial patterns in incidence and suitability of infection of a tropical disease in Nigeria and Cameroon, based on a dataset of subjects who tested positive in $n = 190$ villages in this region (Giorgi et al. 2018). Data are obtained from the `loa1oa` object in the `geostatsp` package (Brown 2011). A simpler model that does not allow for zero-inflation has been fit using INLA (Brown 2011) as well as MCMC and maximum likelihood (Giorgi and Diggle 2017). To our knowledge, no previous Bayesian implementation of this zero-inflated model exists.

We apply Eq. (10) to fit this model. Let $0 \leq y_i \leq N_i, i \in [n]$ represent the counts of people infected and total number of people in the i^{th} village out of the $n = 190$ included in the data, and let $\mathbf{s}_i \in \mathbb{R}^2$ denote the geographical coordinates of this village. For every location $\mathbf{s} \in \mathbb{R}^2$, let $\phi(\mathbf{s})$ denote the probability that this location is capable of disease transmission (the *suitability* probability), and $p(\mathbf{s})$ denote the probability that transmission occurs at this location, conditional on it being suitable (the *incidence* probability). Diggle and Giorgi (2016) stress the practical importance of allowing observed zero counts $y_i = 0$ to either be *haphazard* zeroes arising from sampling variability, or *structural* zeroes arising from a location being unsuitable for disease transmission. They also discuss how this makes joint inference of the underlying spatial fields governing suitability and incidence very challenging. The full model is

$$\begin{aligned} \mathbb{P}[Y_i = y_i | p(\mathbf{s}_i), \phi(\mathbf{s}_i)] &= [1 - \phi(\mathbf{s}_i)] \mathbf{I}(y_i = 0) + \phi(\mathbf{s}_i) \times \text{Binomial}[y_i; N_i, p(\mathbf{s}_i)], \\ \log \left[\frac{\phi(\mathbf{s})}{1 - \phi(\mathbf{s})} \right] &= \beta_{\text{suit}} + u(\mathbf{s}); \quad \log \left[\frac{p(\mathbf{s})}{1 - p(\mathbf{s})} \right] = \beta_{\text{inc}} + v(\mathbf{s}), \quad \mathbf{s} \in \mathbb{R}^2 \\ u(\cdot) | \boldsymbol{\theta} &\sim \mathcal{GP}(0, \mathbf{C}_{\boldsymbol{\theta}}); \quad v(\cdot) | \boldsymbol{\theta} \sim \mathcal{GP}(0, \mathbf{C}_{\boldsymbol{\theta}}), \end{aligned}$$

where the unknown functions $u(\cdot), v(\cdot)$ are modelled as independent Gaussian Processes with

the same Matérn covariance function, \mathbf{C}_θ , with $\theta = (\sigma, \rho)$ and the two intercepts are given independent Gaussian priors with variance 1000. We assign σ and ρ^{-2} independent exponential priors satisfying $\mathbb{P}(\rho < 200\text{km}) = \mathbb{P}(\sigma < 4) = 97.5\%$, following Brown (2011) and Fuglstad et al. (2019).

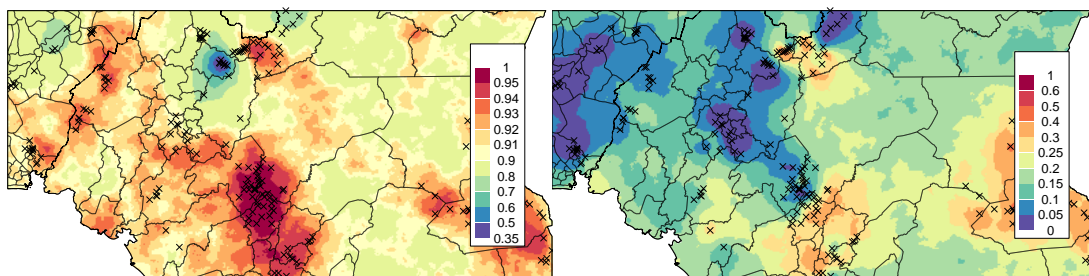
Inference for $u(\cdot)$ and $v(\cdot)$ is based on their values at the observed locations \mathbf{s}_i , and then posterior distributions for their values at any new location $\mathbf{s} \in \mathbb{R}^2$ are obtained using standard methods for spatial interpolation. Define $\mathbf{U} = \{u(\mathbf{s}_i) : i \in [n]\}$, $\mathbf{V} = \{v(\mathbf{s}_i) : i \in [n]\}$, and let $\mathbf{w} = (\mathbf{U}, \beta_{\text{suit}}, \mathbf{V}, \beta_{\text{inc}}) \in \mathbb{R}^m$, $m = 2n + 2$. The Gaussian process priors on $u(\cdot)|\theta$ and $v(\cdot)|\theta$ imply that $\mathbf{U}|\theta \sim \mathbf{N}[0, \Sigma(\theta)]$ and $\mathbf{V}|\theta \sim \mathbf{N}[0, \Sigma(\theta)]$ independently, where $[\Sigma(\theta)]_{ij} = \mathbf{C}_\theta(\|\mathbf{s}_i - \mathbf{s}_j\|)$, $i, j \in [n]$. To infer $\mathbf{U}^* \equiv \{u(\mathbf{s}_t^*) : t \in [T]\}$ and $\mathbf{V}^* \equiv \{v(\mathbf{s}_t^*) : t \in [T]\}$ for any set of new locations $\{\mathbf{s}_t^* : t \in [T]\} \subseteq \mathbb{R}^2$, we simulate from the predictive distribution $(\mathbf{U}^*, \mathbf{V}^*)|\mathbf{Y}$ by first drawing \mathbf{w} from $\tilde{\pi}(\mathbf{w}|\mathbf{Y}^{(n)})$ using standard methods (Rue 2001), and then sampling from $(\mathbf{U}^*, \mathbf{V}^*)|\mathbf{w}$ using existing algorithms for conditional simulation of Gaussian fields, implemented in the `geostatsp` (Brown 2011) and `RandomFields` (Schlather et al. 2015) packages.

We fit the model using AGHQ with $k = 7$ and the approximations described in Section 5.1, and show the resulting spatial interpolations on a fine grid in Fig. 4. Total computation time for parameter estimation was 225 seconds. The predicted incidence probabilities appear visually similar to those reported by Brown (2011) and Giorgi and Diggle (2017) for the simpler model without zero-inflation, and the novel plot of predicted suitability probabilities identifies a cluster of villages that have a low posterior probability of being suitable for transmission. Owing to the lack of available convergence theory in this problem, we include a brief simulation study in Appendix G.3 to assess the empirical accuracy of this procedure for this model and these data.

To better illustrate the difficulty of fitting this model with existing methods, we fit the model using MCMC by running the “NUTS” sampler (Hoffman and Gelman 2014) through the `tmbstan` package (Monnahan and Kristensen 2018) using the default settings. Eight chains of 10,000 iterations each (including a 1,000 iteration warmup) were run in parallel on a remote server at a total “wall” computation time of 66 hours. The resulting chains exhibited divergent transitions according to STAN’s built in diagnostics. We investigated this in Appendix G.1, finding that β_{suit} is poorly identified by the sampler. We ran both Eq. (10) and MCMC with β_{suit} and β_{inc} fixed at their estimated posterior means obtained from the initial fit of Eq. (10). This sampler converged without warnings in just over 19 hours for 10,000 iterations. The Kolmogorov-Smirnov (KS) statistics for the difference between approximate marginal CDFs from MCMC and Eq. (10) indicate that the two procedures provide mostly comparable inferences, with disagreement in a small number of villages. See Appendix G.2 for further details. We re-iterate that MCMC did not produce a complete answer for β_{suit} in this problem.

Inferences made using Eq. (10) produce a complete answer in around three and a half minutes on a modern server for this problem of substantial practical importance (Diggle and Giorgi 2016). In this same problem and on the same hardware, MCMC either (a) runs for almost a day and produces an incomplete answer, or (b) runs for almost 3 days and fails. This example illustrates why these types of approximations have such high potential value in applied

Figure 4: AGHQ estimated posterior mean (a) suitability probabilities and (b) incidence rates for the loa1oa example of Section 5.



(a) $\mathbb{E} [\phi(\cdot) | \mathbf{Y}^{(n)}]$

(b) $\mathbb{E} [\phi(\cdot) \times p(\cdot) | \mathbf{Y}^{(n)}]$

statistics, and why convergence theory for Eq. (10) is of such importance. Theorem 1 provides a first step towards this goal.

6. Discussion

Using standard regularity assumptions, we have provided the first stochastic convergence rate for adaptive quadrature in Bayesian inference, and showed that this rate applies to the approximate normalizing constant, posterior density, moments, and marginal densities. Using our R package `aghq`, available on CRAN, we demonstrated the use of AGHQ for Bayesian inference in two challenging low-dimensional models and one high-dimensional model. We now briefly discuss five open problems for the theory of adaptive quadrature in Bayesian inference.

First, computing approximate quantiles and credible sets requires further integration of the approximate posterior over a subset of the parameter space, and hence a quadrature rule is needed that satisfies a truncated version of $\mathcal{P}(p, k)$. Providing a robust method for this computation with corresponding theoretical guarantees (analogous to Corollaries 2 and 3) will complete the justification of using AGHQ for all facets of Bayesian inference in low-dimensional models. The current implementation uses an interpolation-based method with no theoretical guarantees, but appears to provide reasonable output in challenging examples. Second, for high-dimensional models, the current implementation uses a Gaussian approximation and an adaptive quadrature approximation with reused points and weights. Providing full theoretical guarantees for the output of this entire procedure remains an open problem, and will not only validate the use of the `aghq` package for such models but also provide the first theoretical guarantees for INLA-like methods; we believe that Theorem 1 is an important first step towards this goal. Third, our theoretical guarantees are all asymptotic and worst-case subject to the reg-

ularity assumptions. A challenging open problem is to provide theoretical guarantees that hold for finite samples and adapt to properties such as smoothness and sparsity, leading to improved performance for “benign” data and models. Fourth, a principled choice of k in any given practical application, for any given data set, remains an open problem. The recommendation from Section 4.1 is feasible due to the fast run time of AGHQ, and a more formally-motivated approach based on this could lead to a clearer and more useful practical recommendation. Lastly, developing methods with comparable accuracy to AGHQ that are computationally feasible in very high dimensions remains a challenging open problem.

Acknowledgements

BB acknowledges support from an NSERC Canada Graduate Scholarship and the Vector Institute. AS acknowledges support from an NSERC Postgraduate Scholarship and the Centre for Global Health Research at St. Michael’s Hospital, Toronto, Canada. YT acknowledges support from an NSERC Postgraduate Scholarship and the Vector Institute. We thank Jeffrey Negrea, Nancy Reid, Daniel Roy, and Jamie Stafford for helpful comments and suggestions.

References

- Almutiry, W., V. Warriyar K.V, and R. Deardon (2020). Continuous time individual-level models of infectious disease: EpiILMCT. arXiv:2006.00135v1.
- Bojanov, B. and P. P. Petrov (2001). Gaussian interval quadrature formula. *Numerische Mathematik* 87, 625–643.
- Braun, M. (2014). trustOptim: An R package for trust region optimization with sparse Hessians. *Journal of Statistical Software* 60, 1–16.
- Brown, P. (2011). Model-based geostatistics the easy way. *Journal of Statistical Software* 73, 423–498.
- Cagnone, S. and P. Monari (2013). Latent variable models for ordinal data by using the adaptive quadrature approximation. *Computational Statistics* 28, 597–619.
- Carpenter, B., A. Gelman, M. D. Hoffman, D. Lee, B. Goodrich, M. Betancourt, M. Brubaker, J. Guo, P. Li, and A. Riddell (2017). Stan: A probabilistic programming language. *Journal of Statistical Software* 76.
- Davis, P. J. and P. Rabinowitz (1975). *Methods of Numerical Integration*. Academic Press.
- Dick, J., R. N. Gantner, Q. T. Le Gia, and C. Schwab (2019). Higher order quasi-Monte Carlo integration for Bayesian PDE inversion. *Computers and Mathematics with Applications* 77, 144–172.
- Diggle, P. J. and E. Giorgi (2016). Model-based geostatistics for prevalence mapping in low-resource settings. *Journal of the American Statistical Association* 111, 1096–1120.

- Duvenaud, D. and R. P. Adams (2015). Black-box stochastic variational inference in five lines of Python. *NIPS Workshop on Black-box Learning and Inference*.
- Eadie, G. M. and W. E. Harris (2016). Bayesian mass estimates of the Milky Way: the dark and light sides of parameter assumptions. *The Astrophysical Journal* 829.
- Falbel, D. and J. Luraschi (2020). *torch: tensors and neural networks with 'GPU' acceleration*. R package version 0.1.1.
- Fan, J. and J. Lv (2008). Sure independence screening for ultrahigh dimensional feature space. *Journal of the Royal Statistical Society, Series B: Statistical Methodology* 70, 849–911.
- Fuglstad, G.-A., D. Simpson, F. Lindgren, and H. Rue (2019). Constructing priors that penalize the complexity of Gaussian random fields. *Journal of the American Statistical Association* 114, 445–452.
- Gabry, J., D. Simpson, A. Vehtari, M. Betancourt, and A. Gelman (2019). Visualization in Bayesian workflow. *Journal of the Royal Statistical Society, Series A: Statistics in Society* 182, 389–402.
- Geirsson, O. P., B. Hrafnkelsson, D. Simpson, and H. Sigurdarson (2020). LGM split sampler: An efficient MCMC sampling scheme for latent Gaussian models. *Statistical Science* 35, 218–233.
- Genz, A. and B. D. Keister (1996). Fully symmetric interpolatory rules for multiple integrals over infinite regions with Gaussian weight. *Journal of Computational and Applied Mathematics* 71, 299–309.
- Geyer, C. J. (2020). *trust: Trust Region Optimization*. R package version 0.1-8.
- Giorgi, E. and P. J. Diggle (2017). PrevMap: An R package for prevalence mapping. *Journal of Statistical Software* 78.
- Giorgi, E., D. K. Schluter, and P. J. Diggle (2018). Bivariate geostatistical modelling of the relationship between Loa loa prevalence and intensity of infection. *Environmetrics* 29.
- Heiss, F. and V. Winschel (2008). Likelihood approximation by numerical integration on sparse grids. *Journal of Econometrics* 144, 62–80.
- Hoffman, M. D. and A. Gelman (2014). The no-U-turn sampler: Adaptively setting path lengths in Hamiltonian Monte Carlo. *Journal of Machine Learning Research* 15, 1593–1623.
- Jin, S. and B. Andersson (2020). A note on the accuracy of adaptive Gauss–Hermite quadrature. *Biometrika* 107, 737–744.

- Kass, R. and D. Steffey (1989). Approximate Bayesian inference in conditionally independent hierarchical models (parametric empirical Bayes models). *Journal of the American Statistical Association* 84, 717–726.
- Kass, R. E., L. Tierney, and J. B. Kadane (1990). The validity of posterior expansions based on Laplace’s method. *Bayesian and Likelihood Methods in Statistics and Econometrics*, 473–488.
- Kristensen, K., A. Nielson, C. W. Berg, H. Skaug, and B. M. Bell (2016). TMB: automatic differentiation and Laplace approximation. *Journal of Statistical Software* 70.
- Liu, Q. and D. A. Pierce (1994). A note on Gauss-Hermite quadrature. *Biometrika* 81, 624–629.
- Margossian, C. C., A. Vehtari, D. Simpson, and R. Agrawal (2020). Hamiltonian Monte Carlo using an adjoint-differentiated Laplace approximation. *arXiv:2004.12550v3*.
- Monnahan, C. and K. Kristensen (2018). No-U-turn sampling for fast Bayesian inference in ADMB and TMB: Introducing the adnuts and tmbstan R packages. *PLOS ONE* 13, 1–10.
- Naylor, J. and A. F. M. Smith (1982). Applications of a method for the efficient computation of posterior distributions. *Journal of the Royal Statistical Society, Series C: Applied Statistics* 31, 214–225.
- Pinheiro, J. C. and D. M. Bates (1995). Approximations to the log-likelihood function in the nonlinear mixed-effects model. *Journal of computational and Graphical Statistics* 4, 12–35.
- Rue, H. (2001). Fast sampling of Gaussian Markov random fields. *Journal of the Royal Statistical Society, Series B: Statistical Methodology* 63, 325–338.
- Rue, H., S. Martino, and N. Chopin (2009). Approximate Bayesian inference for latent Gaussian models by using integrated nested Laplace approximations. *Journal of the Royal Statistical Society, Series B: Statistical Methodology* 71, 319–392.
- Schillings, C. and C. Schwab (2016). Scaling limits in computational Bayesian inversion. *ESAIM: Mathematical Modelling and Numerical Analysis* 50, 1825–1856.
- Schlather, M., A. Malinowski, P. J. Menck, M. Oesting, and K. Storkorb (2015). Analysis, simulation and prediction of multivariate random fields with package randomfields. *Journal of Statistical Software* 63.
- Stringer, A. (2021). Implementing adaptive quadrature for Bayesian inference: the aghq package. *arXiv:2101.04468*.
- Stringer, A., P. Brown, and J. Stafford (2021). Approximate Bayesian inference for case crossover models. *Biometrics* 77, 785–795.

- Tang, Y. and N. Reid (2020). Modified likelihood root in high dimensions. *Journal of the Royal Statistical Society, Series B: Statistical Methodology* 82, 1349–1369.
- Taylor, B. M. and P. J. Diggle (2014). INLA or MCMC? A tutorial and comparative evaluation for spatial prediction in log-Gaussian Cox processes. *Journal of Statistical Computation and Simulation* 84, 2266–2284.
- Tierney, L. and J. B. Kadane (1986). Accurate approximations for posterior moments and marginal densities. *Journal of the American Statistical Association* 81, 82–86.
- van der Vaart, A. W. (1998). *Asymptotic Statistics*. Cambridge University Press.
- Wachter, A. and L. T. Biegler (2006). On the implementation of a primal-dual interior point filter line search algorithm for large-scale nonlinear programming. *Mathematical Programming* 106, 25–57.
- Winkelbauer, A. (2012). Moments and absolute moments of the normal distribution. arXiv:1209.4340.
- Wood, S. (2020). Simplified integrated nested Laplace approximation. *Biometrika* 107, 223–230.
- Wood, S., N. Pya, and B. Säfken (2016). Smoothing parameter and model selection for general smooth models. *Journal of the American Statistical Association* 111, 1548–1575.
- Yao, Z., A. Gholami, K. Keutzer, and M. W. Mahoney (2020). Pyhessian: Neural networks through the lens of the hessian. arXiv:1912.07145v3.

A. Regularity Assumptions

We state here some more notation and the required modelling assumptions for Theorem 1. The log-likelihood of a parameter $\boldsymbol{\theta} \in \mathbb{R}^p$ is denoted by $\ell_n(\boldsymbol{\theta}; \mathbf{Y}^{(n)}) = \log \pi(\mathbf{Y}^{(n)} | \boldsymbol{\theta})$. When the dependence on the data is clear, we may use $\ell_n(\boldsymbol{\theta})$ for brevity. Denote the log-posterior (unnormalized) by $\ell_n^\pi(\boldsymbol{\theta}) = \log \pi(\boldsymbol{\theta}, \mathbf{Y}^{(n)}) = \ell_n(\boldsymbol{\theta}) + \log \pi(\boldsymbol{\theta})$. The maximum likelihood estimator is $\boldsymbol{\theta}_n^{\text{MLE}} = \arg \max_{\boldsymbol{\theta} \in \Theta} \ell_n(\boldsymbol{\theta})$, and the posterior mode is $\widehat{\boldsymbol{\theta}}_n = \arg \max_{\boldsymbol{\theta} \in \Theta} \ell_n^\pi(\boldsymbol{\theta})$. The negative Hessian of the log-posterior is

$$\mathbf{H}_n(\boldsymbol{\theta}) = -\frac{\partial^2}{\partial \boldsymbol{\theta} \partial \boldsymbol{\theta}^\top} \ell_n^\pi(\boldsymbol{\theta}).$$

Further, we make frequent use of the Cholesky decomposition of the inverse curvature of the log-posterior at $\widehat{\boldsymbol{\theta}}_n$, which for symmetric, positive-definite $\mathbf{H}_n(\widehat{\boldsymbol{\theta}}_n)$ is the unique lower-triangular matrix that satisfies

$$\left[\mathbf{H}_n(\widehat{\boldsymbol{\theta}}_n) \right]^{-1} = \widehat{\mathbf{L}}_n \widehat{\mathbf{L}}_n^\top.$$

For any $x_0 \in \mathbb{R}^p$ and $\delta > 0$, let $B_{x_0}^p(\delta) = \{x \in \mathbb{R}^p : \|x - x_0\|_2 < \delta\}$ denote the open ball in \mathbb{R}^p of radius δ centred at x_0 with respect to the Euclidean norm. Let $\phi(x; \boldsymbol{\mu}, \boldsymbol{\Sigma})$ denote the multivariate normal density evaluated at x with mean $\boldsymbol{\mu}$ and variance $\boldsymbol{\Sigma}$. For a positive-definite $p \times p$ matrix A , let $\lambda_1(A) \geq \dots \geq \lambda_p(A) > 0$ denote its ordered eigenvalues. For any $f : \mathbb{R}^p \rightarrow \mathbb{R}$, $\boldsymbol{\alpha} \subseteq \mathbb{N}^p$, and $\mathbf{x} \in \mathbb{R}^p$, we define

$$|\boldsymbol{\alpha}| = \sum_{j=1}^p \alpha_j, \quad \boldsymbol{\alpha}! = \prod_{j=1}^p \alpha_j!, \quad \mathbf{x}^\alpha = \mathbf{x}_\alpha = \prod_{j=1}^p x_j^{\alpha_j}, \text{ and}$$

$$\partial^\alpha f(\mathbf{x}) = \partial x_1^{\alpha_1} \partial x_2^{\alpha_2} \dots \partial x_p^{\alpha_p} f(\mathbf{x}) = \frac{\partial^{|\boldsymbol{\alpha}|} f(\mathbf{x})}{\partial x_1^{\alpha_1} \partial x_2^{\alpha_2} \dots \partial x_p^{\alpha_p}}.$$

For any data-generating distribution \mathbb{P}_n^* , we say the following assumptions hold if there exist $\delta > 0$ and $\boldsymbol{\theta}^* \in \Theta$ such that all five statements are true.

Assumption 1. *There exists $m, M > 0$ such that for all $\boldsymbol{\alpha} \subseteq \mathbb{N}^p$ with $0 \leq |\boldsymbol{\alpha}| \leq m$,*

$$\lim_{n \rightarrow \infty} \mathbb{P}_n^* \left[\sup_{\boldsymbol{\theta} \in B_{\boldsymbol{\theta}^*}^p(\delta)} \left| \partial^\alpha \ell_n^\pi(\boldsymbol{\theta}) \right| < nM \right] = 1.$$

Assumption 2. *There exist $0 < \underline{\eta} \leq \bar{\eta} < \infty$ such that*

$$\lim_{n \rightarrow \infty} \mathbb{P}_n^* \left[n\underline{\eta} \leq \inf_{\boldsymbol{\theta} \in B_{\boldsymbol{\theta}^*}^p(\delta)} \lambda_p(\mathbf{H}_n(\boldsymbol{\theta})) \leq \sup_{\boldsymbol{\theta} \in B_{\boldsymbol{\theta}^*}^p(\delta)} \lambda_1(\mathbf{H}_n(\boldsymbol{\theta})) \leq n\bar{\eta} \right] = 1.$$

Assumption 3. *There exists $b > 0$ such that*

$$\lim_{n \rightarrow \infty} \mathbb{P}_n^* \left[\sup_{\boldsymbol{\theta} \in [B_{\boldsymbol{\theta}^*}^p(\delta)]^c} \ell_n(\boldsymbol{\theta}) - \ell_n(\boldsymbol{\theta}^*) \leq -nb \right] = 1.$$

Assumption 4. For any $\beta > 0$ and function $G(n)$ such that $\lim_{n \rightarrow \infty} G(n) = \infty$,

$$\lim_{n \rightarrow \infty} \mathbb{P}_n^* \left[\frac{\sqrt{n}}{G(n)} \left\| \hat{\boldsymbol{\theta}}_n - \boldsymbol{\theta}^* \right\|_2 > \beta \right] = 0.$$

Assumption 5. There exist $0 < c_1 < c_2 < \infty$ such that

$$c_1 \leq \inf_{\boldsymbol{\theta} \in B_{\boldsymbol{\theta}^*}^p(\delta)} \pi(\boldsymbol{\theta}) \leq \sup_{\boldsymbol{\theta} \in B_{\boldsymbol{\theta}^*}^p(\delta)} \pi(\boldsymbol{\theta}) \leq c_2.$$

Remark 3. Assumptions 1, 2, and 5 are standard assumptions that can be found in the asymptotic literature. Assumption 3 corresponds to a consistency condition for the MLE (see the paragraph before Theorem 8 in Kass et al. 1990). Assumption 4 is implied by $n^{1/2}$ the consistency of the MLE and Assumption 5. In the presence of Assumption 5, Assumptions 1 to 4 are equivalent to analogous assumptions on the log-likelihood and the MLE. \triangleleft

Remark 4. Our assumptions are similar to those found in Section 3 of Kass et al. (1990), with the exception that the number of derivatives we require can potentially be higher since $k \geq 1$, and our assumptions hold in probability rather than almost surely. \triangleleft

Remark 5. Assumptions 1–2 (where $m \geq 2$ in Assumption 1) and 4–5 are sufficient to imply the Bernstein-von Mises theorem holds for our model, meaning that the posterior distribution is asymptotically Gaussian. Using Theorem 10.1 in van der Vaart (1998), the conditions on the model are: differentiability in quadratic mean, invertability of the Fisher information matrix at $\boldsymbol{\theta}^*$, continuity and positivity of the prior distribution at $\boldsymbol{\theta}^*$, and finally the existence of tests ζ_n such that for every $\epsilon > 0$:

$$\lim_{n \rightarrow \infty} \mathbb{P}_n^* \zeta_n = 0 \quad \text{and} \quad \lim_{n \rightarrow \infty} \sup_{\|\boldsymbol{\theta} - \boldsymbol{\theta}^*\|_2 \geq \epsilon} (1 - \zeta_n) = 0.$$

Assumptions 1, 2 and 5 directly imply the first three conditions, as for the final requirement, let

$$\zeta_n = \mathbb{I} \left\{ \left\| \boldsymbol{\theta}_n^{\text{MLE}} - \boldsymbol{\theta}^* \right\|_2 > \frac{\log(n)}{n^{1/2}} \right\},$$

then by Assumption 4 this sequence of test satisfies the final condition. \triangleleft

B. Proof of Theorem 1

B.1. Quantifying Accuracy for Approximate Bayesian Inference

We measure the accuracy of a normalizing-constant approximation by the *relative error*,

$$E_{\text{rel}}(\mathbf{Y}^{(n)}) = \left| \frac{\pi(\mathbf{Y}^{(n)})}{\tilde{\pi}(\mathbf{Y}^{(n)})} - 1 \right|.$$

Since we are ultimately interested in summary statistics of the posterior for Bayesian inference, we require further integration of the approximate posterior density. To measure this error, we use the *total variation error*,

$$E_{\text{TV}}(\mathbf{Y}^{(n)}) = \sup_{\mathcal{K} \in \mathcal{B}(\mathbb{R}^p)} \left| \int_{\mathcal{K}} \tilde{\pi}(\boldsymbol{\theta} | \mathbf{Y}^{(n)}) - \pi(\boldsymbol{\theta} | \mathbf{Y}^{(n)}) d\boldsymbol{\theta} \right|.$$

Fortunately, by the definition of $\tilde{\pi}(\boldsymbol{\theta} \mid \mathbf{Y}^{(n)})$, $E_{\text{TV}}(\mathbf{Y}^{(n)})$ simplifies to

$$\begin{aligned} \sup_{\mathcal{K} \in \mathcal{B}(\mathbb{R}^p)} \left| \int_{\mathcal{K}} \tilde{\pi}(\boldsymbol{\theta} \mid \mathbf{Y}^{(n)}) - \pi(\boldsymbol{\theta} \mid \mathbf{Y}^{(n)}) d\boldsymbol{\theta} \right| &= \left| \frac{1}{\tilde{\pi}(\mathbf{Y}^{(n)})} - \frac{1}{\pi(\mathbf{Y}^{(n)})} \right| \sup_{\mathcal{K} \in \mathcal{B}(\mathbb{R}^p)} \left| \int_{\mathcal{K}} \pi(\boldsymbol{\theta}, \mathbf{Y}^{(n)}) d\boldsymbol{\theta} \right| \\ &= \left| \frac{1}{\tilde{\pi}(\mathbf{Y}^{(n)})} - \frac{1}{\pi(\mathbf{Y}^{(n)})} \right| \underbrace{\int_{\Theta} \pi(\boldsymbol{\theta}, \mathbf{Y}^{(n)}) d\boldsymbol{\theta}}_{\pi(\mathbf{Y}^{(n)})} \\ &= \left| \frac{\pi(\mathbf{Y}^{(n)})}{\tilde{\pi}(\mathbf{Y}^{(n)})} - 1 \right|, \end{aligned}$$

so $E_{\text{TV}}(\mathbf{Y}^{(n)}) = E_{\text{rel}}(\mathbf{Y}^{(n)})$ and it suffices to analyse $E_{\text{rel}}(\mathbf{Y}^{(n)})$.

Finally, the choice of positioning the approximation in the numerator or denominator in the definition of $E_{\text{rel}}(\mathbf{Y}^{(n)})$ does not affect the discussion of asymptotic rates, as is made clear in the following Lemma.

Lemma 1. *For any sequences of random variables (A_n) and (B_n) such that*

- a) $\mathbb{P}_n(A_n > 0) = \mathbb{P}_n(B_n > 0) = 1$ for all n , and
- b) there exists $r > 0$ and $C > 0$ satisfying

$$\lim_{n \rightarrow \infty} \mathbb{P}_n \left(\left| \frac{A_n}{B_n} - 1 \right| \leq Cn^{-r} \right) = 1,$$

it holds that

$$\lim_{n \rightarrow \infty} \mathbb{P}_n \left(\left| \frac{B_n}{A_n} - 1 \right| \leq 2Cn^{-r} \right) = 1.$$

Proof of Lemma 1. By assumption $\mathbb{P}_n(A_n = 0) = \mathbb{P}_n(B_n = 0) = 0$ for all n , so in what follows we work on the event $\{|A_n| > 0\} \cap \{|B_n| > 0\}$. For any $z \in [0, 1)$, $\frac{1}{1-z} \geq 1+z$. So, for all $n > (2C)^{1/r}$,

$$\begin{aligned} \mathbb{P}_n \left(\frac{B_n}{A_n} < 1 - 2Cn^{-r} \right) &= \mathbb{P}_n \left(\frac{A_n}{B_n} \geq [1 - 2Cn^{-r}]^{-1} \right) \\ &\leq \mathbb{P}_n \left(\frac{A_n}{B_n} \geq 1 + 2Cn^{-r} \right) \\ &\leq \mathbb{P}_n \left(\left| \frac{A_n}{B_n} - 1 \right| \geq Cn^{-r} \right). \end{aligned}$$

Similarly, for any $z \in [0, 1]$, $\frac{1}{1+z} \leq 1 - z/2$. So, for all $n > (2C)^{1/r}$,

$$\begin{aligned} \mathbb{P}_n \left(\frac{B_n}{A_n} > 1 + 2Cn^{-r} \right) &= \mathbb{P}_n \left(\frac{A_n}{B_n} \leq [1 + 2Cn^{-r}]^{-1} \right) \\ &\leq \mathbb{P}_n \left(\frac{A_n}{B_n} \leq 1 - Cn^{-r} \right) \\ &\leq \mathbb{P}_n \left(\left| \frac{A_n}{B_n} - 1 \right| \geq Cn^{-r} \right). \end{aligned}$$

Thus,

$$\begin{aligned}
 & \lim_{n \rightarrow \infty} \mathbb{P}_n \left(\left| \frac{B_n}{A_n} - 1 \right| > 2Cn^{-r} \right) \\
 &= \lim_{n \rightarrow \infty} \mathbb{P}_n \left(\frac{B_n}{A_n} > 1 + 2Cn^{-r} \cup \frac{B_n}{A_n} < 1 - 2Cn^{-r} \right) \\
 &\leq \lim_{n \rightarrow \infty} \mathbb{P}_n \left(\frac{B_n}{A_n} > 1 + 2Cn^{-r} \right) + \lim_{n \rightarrow \infty} \mathbb{P}_n \left(\frac{B_n}{A_n} < 1 - 2Cn^{-r} \right) \\
 &\leq 2 \lim_{n \rightarrow \infty} \mathbb{P}_n \left(\left| \frac{A_n}{B_n} - 1 \right| \geq Cn^{-r} \right) \\
 &= 0.
 \end{aligned}$$

□

Theorem 1. *Suppose there exists $m \geq 4$ such that the likelihood of the data $\pi(\mathbf{Y}^{(n)} \mid \boldsymbol{\theta})$ is m -times differentiable as a function of $\boldsymbol{\theta}$ and the regularity assumptions of Appendix A hold. For $1 \leq k \leq \lfloor m/2 \rfloor$, if $\mathfrak{R}(\mathcal{Q}, \boldsymbol{\omega})$ is a symmetric quadrature rule satisfying $\mathcal{P}(k, p)$ then*

$$\lim_{n \rightarrow \infty} \mathbb{P}_n^* \left(\left| \frac{\pi(\mathbf{Y}^{(n)})}{\tilde{\pi}_{(\mathcal{Q}, \boldsymbol{\omega})}^A(\mathbf{Y}^{(n)})} - 1 \right| \leq C n^{-\lfloor \frac{k+2}{3} \rfloor} \right) = 1.$$

The proof of Theorem 1 follows directly from the combination of the following two lemmas.

Lemma 2. *Under Assumptions 1 to 5, for all $1 \leq k \leq \lfloor m/2 \rfloor$, if $\mathfrak{R}(\mathcal{Q}, \boldsymbol{\omega})$ is a quadrature rule satisfying $\mathcal{P}(k, p)$ then there exists a constant $C > 0$ such that*

$$\lim_{n \rightarrow \infty} \mathbb{P}_n^* \left(\frac{|\pi(\mathbf{Y}^{(n)}) - \tilde{\pi}_{(\mathcal{Q}, \boldsymbol{\omega})}^A(\mathbf{Y}^{(n)})|}{\pi(\mathbf{Y}^{(n)} \mid \hat{\boldsymbol{\theta}}_n)} \leq C \frac{1}{n^{p/2 + \lfloor (k+2)/3 \rfloor}} \right) = 1.$$

Lemma 3. *Under Assumptions 2, 4, and 5, for all $1 \leq k \leq \lfloor m/2 \rfloor$, if $\mathfrak{R}(\mathcal{Q}, \boldsymbol{\omega})$ is a quadrature rule satisfying $\mathcal{P}(k, p)$ then there exists a constant $C > 0$ such that*

$$\lim_{n \rightarrow \infty} \mathbb{P}_n^* \left(\frac{\tilde{\pi}_{(\mathcal{Q}, \boldsymbol{\omega})}^A(\mathbf{Y}^{(n)})}{\pi(\mathbf{Y}^{(n)} \mid \hat{\boldsymbol{\theta}}_n)} \geq C \frac{1}{n^{p/2}} \right) = 1.$$

The rest of this section is devoted to proving Lemmas 2 and 3. For notational simplicity in the multivariate case, we adopt Einstein notation for tensor products throughout our proofs. In particular, when upper and lower indices appear twice in a term, this will denote summation over the relevant range of this index. For example, if $\mathbf{a}, \mathbf{b} \in \mathbb{R}^p$, then

$$\mathbf{a}_i \mathbf{b}^i = \sum_{i=1}^p a_i b_i = \mathbf{a}^\top \mathbf{b}.$$

More specifically, we use this in the context of multivariate Taylor expansions. That is, for any $j \in [p]$,

$$a_{i_1 \dots i_j} \partial^{i_1 \dots i_j} f(x) = \sum_{i_1, \dots, i_j \in [p]} (a_{i_1} \dots a_{i_j}) \times \left(\partial_{x_{i_1}} \dots \partial_{x_{i_j}} f(x) \right).$$

Finally, to account for the constants in a Taylor series, we introduce the new notation:

$$a_{[i_1 \dots i_j]}! \partial^{i_1 \dots i_j} f(x) = \sum_{i_1, \dots, i_j \in [p]} \frac{1}{i_1! \dots i_j!} (a_{i_1} \dots a_{i_j}) \times \left(\partial_{x_{i_1}} \dots \partial_{x_{i_j}} f(x) \right).$$

To ease notational burden when writing large polynomials, we also define for $b > 3$:

$$\begin{aligned} \tau_{<b}^{(j)} &= \left\{ (t_3, \dots, t_{2k}) \in \mathbb{Z}_+^{2k-3} \mid \sum_{s=3}^{2k} t_s = j \text{ and } \sum_{s=3}^{2k} st_s \leq b-1 \right\}, \\ \tau_{=b}^{(j)} &= \left\{ (t_3, \dots, t_{2k}) \in \mathbb{Z}_+^{2k-3} \mid \sum_{s=3}^{2k} t_s = j \text{ and } \sum_{s=3}^{2k} st_s = b \right\}, \\ \tau_{\geq b}^{(j)} &= \left\{ (t_3, \dots, t_{2k}) \in \mathbb{Z}_+^{2k-3} \mid \sum_{s=3}^{2k} t_s = j \text{ and } \sum_{s=3}^{2k} st_s \geq b \right\}. \end{aligned}$$

The significance of only considering $s \geq 3$ is made clear in Appendix C, but arises from considering only the higher-order terms of a Taylor series expansion. We also use $\tau(\mathbf{t}) = \sum_{s=3}^{2k} st_s$ for any $\mathbf{t} = (t_3, \dots, t_{2k}) \in \mathbb{Z}_+^{2k-3}$.

B.2. Proof of Lemma 2

Fix arbitrary $\gamma > 0$ (to be tuned at the end as a function of p and k) and let $\gamma_n = \gamma \sqrt{(\log n)/n}$ for each $n \in \mathbb{N}$. First, expand the fraction of interest, giving

$$\begin{aligned} & \frac{\left| \pi(\mathbf{Y}^{(n)}) - \tilde{\pi}_{(\mathcal{Q}, \omega)}^{\mathcal{A}}(\mathbf{Y}^{(n)}) \right|}{\pi(\mathbf{Y}^{(n)} \mid \hat{\boldsymbol{\theta}}_n)} \\ &= \frac{\left| \int_{\Theta} \pi(\boldsymbol{\theta}) \pi(\mathbf{Y}^{(n)} \mid \boldsymbol{\theta}) d\boldsymbol{\theta} - |\hat{\mathbf{L}}_n| \sum_{z \in \mathcal{Q}} \omega(z) \pi(\hat{\mathbf{L}}_n z + \hat{\boldsymbol{\theta}}_n) \pi(\mathbf{Y}^{(n)} \mid \boldsymbol{\theta} = \hat{\mathbf{L}}_n z + \hat{\boldsymbol{\theta}}_n) \right|}{\pi(\mathbf{Y}^{(n)} \mid \hat{\boldsymbol{\theta}}_n)} \\ &= \pi(\hat{\boldsymbol{\theta}}_n) \left| \int_{\Theta} \exp \left\{ \ell_n^\pi(\boldsymbol{\theta}) - \ell_n^\pi(\hat{\boldsymbol{\theta}}_n) \right\} d\boldsymbol{\theta} \right. \\ & \quad \left. - |\hat{\mathbf{L}}_n| \sum_{z \in \mathcal{Q}} \omega(z) \exp \left\{ \ell_n^\pi(\hat{\mathbf{L}}_n z + \hat{\boldsymbol{\theta}}_n) - \ell_n^\pi(\hat{\boldsymbol{\theta}}_n) \right\} \right|, \end{aligned}$$

which after splitting the region of integration and applying the triangle inequality is:

$$\begin{aligned} & \leq \pi(\hat{\boldsymbol{\theta}}_n) \left| \int_{B_{\hat{\boldsymbol{\theta}}_n}^p(\gamma_n)} \exp \left\{ \ell_n^\pi(\boldsymbol{\theta}) - \ell_n^\pi(\hat{\boldsymbol{\theta}}_n) \right\} d\boldsymbol{\theta} \right. \\ & \quad \left. - |\hat{\mathbf{L}}_n| \sum_{z \in \mathcal{Q}} \omega(z) \exp \left\{ \ell_n^\pi(\hat{\mathbf{L}}_n z + \hat{\boldsymbol{\theta}}_n) - \ell_n^\pi(\hat{\boldsymbol{\theta}}_n) \right\} \right| \\ & \quad + \pi(\hat{\boldsymbol{\theta}}_n) \int_{[B_{\hat{\boldsymbol{\theta}}_n}^p(\gamma_n)]^c} \exp \left\{ \ell_n^\pi(\boldsymbol{\theta}) - \ell_n^\pi(\hat{\boldsymbol{\theta}}_n) \right\} d\boldsymbol{\theta}. \end{aligned} \tag{11}$$

Our strategy is to upper bound Eq. (11) using a few key quantities, and then show that the regularity assumptions imply these quantities are of the correct order with probability tending to 1. Specifically, we use

$$\widehat{M}_n = \sup_{\alpha: |\alpha| \leq m} \sup_{\theta \in B_{\widehat{\theta}_n}^p(\bar{z}|\widehat{\mathbf{L}}_n|\gamma_n)} \left| \partial^\alpha \ell_n^\pi(\theta) \right|, \quad \bar{\eta}_n = \frac{\lambda_1(\mathbf{H}_n(\widehat{\theta}_n))}{n}, \quad \text{and} \quad \underline{\eta}_n = \frac{\lambda_p(\mathbf{H}_n(\widehat{\theta}_n))}{n},$$

where $\bar{z} = \sup_{z \in \mathcal{Q}} \|z\|_2 < \infty$.

We use these quantities to state the following result, which handles the primary technical difficulties for proving Theorem 1. We defer its proof to Appendix C.

Lemma 4. *For all $1 \leq k \leq \lfloor m/2 \rfloor$, if $\mathfrak{R}(\mathcal{Q}, \omega)$ is a quadrature rule satisfying $\mathcal{P}(k, p)$ then there exists a constant $C_{k,p} > 0$ depending only on p and k such that for all $n \in \mathbb{N}$ it holds \mathbb{P}_n^* -a.s. that*

$$\begin{aligned} & \left| \int_{B_{\widehat{\theta}_n}^p(\gamma_n)} \exp \left\{ \ell_n^\pi(\theta) - \ell_n^\pi(\widehat{\theta}_n) \right\} d\theta - |\widehat{\mathbf{L}}_n| \sum_{z \in \mathcal{Q}} \omega(z) \exp \left\{ \ell_n^\pi(\widehat{\mathbf{L}}_n z + \widehat{\theta}_n) - \ell_n^\pi(\widehat{\theta}_n) \right\} \right| \\ & \leq C_{k,p} \left(\left(\frac{\bar{\eta}_n}{\underline{\eta}_n} \right)^{p/2} + 1 \right) n^{-p/2} \\ & \quad \times \left[\max_{j \in [\kappa]} \max_{t \in \tau_{\geq 2k}^{(j)}} (\widehat{M}_n)^j (\underline{\eta}_n n)^{-\tau(t)/2} + \max_{t \in \tau_{\geq 3(\kappa+1)+1\{2k=2 \pmod{3}\}}^{(\kappa+1)}} (\widehat{M}_n)^{\kappa+1} (\underline{\eta}_n n)^{-\tau(t)/2} \right. \\ & \quad \left. + (\underline{\eta}_n)^{-1/2} \max_{j \in \{0\} \cup [\kappa]} (\widehat{M}_n)^j n^{-\frac{\gamma^2 \eta_n + 2}{4}} + \widehat{\Lambda}_n (\widehat{M}_n)^{\kappa+2} \max_{t \in \tau_{\geq 3(\kappa+2)}^{(\kappa+2)}} (\underline{\eta}_n n)^{-\tau(t)/2} \right], \end{aligned} \tag{12}$$

where

$$\begin{aligned} \widehat{\Lambda}_n = & \left[\left(\frac{\bar{\eta}_n}{\underline{\eta}_n} \right)^{p/2} \exp \left\{ (2k) p^{2k} \max\{1, \gamma^{2k}\} \widehat{M}_n \left(\frac{\log(n)}{n} \right)^{3/2} \right\} \right. \\ & \left. + \exp \left\{ (2k) p^{2k} \max\{1, \bar{z}^{2k}\} \widehat{M}_n \max \left\{ (\underline{\eta}_n n)^{-3/2}, (\underline{\eta}_n n)^{-k} \right\} \right\} \right] \end{aligned}$$

and κ is the smallest integer such that $3(\kappa + 1) \geq 2k$.

We then want to make use of the following, which provides the necessary convergence for each of the quantities used in Lemma 4.

Lemma 5. *Under Assumptions 1, 2, 4, and 5, the following hold:*

- i) $\lim_{n \rightarrow \infty} \mathbb{P}_n^* \left(\underline{\eta} \leq \underline{\eta}_n \leq \bar{\eta}_n \leq \bar{\eta} \right) = 1.$
- ii) $\lim_{n \rightarrow \infty} \mathbb{P}_n^* \left(\widehat{M}_n \leq nM \right) = 1.$

$$\text{iii) } \lim_{n \rightarrow \infty} \mathbb{P}_n^* \left(\pi(\widehat{\boldsymbol{\theta}}_n) \leq c_2 \right) = 1.$$

Proof of Lemma 5.

i) By Assumption 4, $\lim_{n \rightarrow \infty} \mathbb{P}_n^* \left(\widehat{\boldsymbol{\theta}}_n \in B_{\boldsymbol{\theta}^*}^p(\delta) \right) = 1$. Thus,

$$\begin{aligned} \lim_{n \rightarrow \infty} \mathbb{P}_n^* (\overline{\eta}_n \leq \overline{\eta}) &= \lim_{n \rightarrow \infty} \mathbb{P}_n^* \left(\frac{\lambda_1(\mathbf{H}_n(\widehat{\boldsymbol{\theta}}_n))}{n} \leq \overline{\eta} \right) \\ &\geq \lim_{n \rightarrow \infty} \mathbb{P}_n^* \left(\widehat{\boldsymbol{\theta}}_n \in B_{\boldsymbol{\theta}^*}^p(\delta), \sup_{\boldsymbol{\theta} \in B_{\boldsymbol{\theta}^*}^p(\delta)} \frac{\lambda_1(\mathbf{H}_n(\boldsymbol{\theta}))}{n} \leq \overline{\eta} \right) \\ &= 1, \end{aligned}$$

where the last step uses Assumption 2. The inequality for $\underline{\eta}_n$ is proven in the same fashion.

ii) First, recall that $|\widehat{\mathbf{L}}_n| \leq (\underline{\eta}_n n)^{-p/2}$. By i), we have

$$\lim_{n \rightarrow \infty} \mathbb{P}_n^* \left((\underline{\eta}_n n)^{-p/2} \leq (\underline{\eta} n)^{-p/2} \right) = 1.$$

That is, for all $\varepsilon > 0$,

$$\lim_{n \rightarrow \infty} \mathbb{P}_n^* \left(\overline{\mathbf{z}}|\widehat{\mathbf{L}}_n|t \vee \gamma_n < \varepsilon \right) = 1,$$

so by Assumption 4 again,

$$\lim_{n \rightarrow \infty} \mathbb{P}_n^* \left(B_{\widehat{\boldsymbol{\theta}}_n}^p(\overline{\mathbf{z}}|\widehat{\mathbf{L}}_n| \vee \gamma_n) \subseteq B_{\boldsymbol{\theta}^*}^p(\delta) \right) = 1.$$

Thus,

$$\begin{aligned} &\lim_{n \rightarrow \infty} \mathbb{P}_n^* \left(\widehat{M}_n \leq nM \right) \\ &= \lim_{n \rightarrow \infty} \mathbb{P}_n^* \left(\sup_{\boldsymbol{\alpha}: |\boldsymbol{\alpha}| \leq m} \sup_{\boldsymbol{\theta} \in B_{\widehat{\boldsymbol{\theta}}_n}^p(\overline{\mathbf{z}}|\widehat{\mathbf{L}}_n| \vee \gamma_n)} \left| \partial^{\boldsymbol{\alpha}} \ell_n^\pi(\boldsymbol{\theta}) \right| \leq nM \right) \\ &\geq \lim_{n \rightarrow \infty} \mathbb{P}_n^* \left(B_{\widehat{\boldsymbol{\theta}}_n}^p(\overline{\mathbf{z}}|\widehat{\mathbf{L}}_n| \vee \gamma_n) \subseteq B_{\boldsymbol{\theta}^*}^p(\delta), \sup_{\boldsymbol{\alpha}: |\boldsymbol{\alpha}| \leq m} \sup_{\boldsymbol{\theta} \in B_{\boldsymbol{\theta}^*}^p(\delta)} \left| \partial^{\boldsymbol{\alpha}} \ell_n^\pi(\boldsymbol{\theta}) \right| \leq nM \right) \\ &= 1, \end{aligned}$$

where the last step uses Assumption 1.

iii) This follows directly from Assumptions 4 and 5. □

Now, if $\underline{\eta} \leq \underline{\eta}_n \leq \overline{\eta}_n \leq \overline{\eta}$ and $\widehat{M}_n \leq nM$, for large enough n it holds that $\widehat{\Lambda}_n \leq 2$, so we

can further upper bound the RHS of Eq. (12) to obtain

$$\begin{aligned} & \left| \int_{B_{\hat{\theta}_n}^p(\gamma_n)} \exp \left\{ \ell_n^\pi(\boldsymbol{\theta}) - \ell_n^\pi(\hat{\boldsymbol{\theta}}_n) \right\} d\boldsymbol{\theta} - |\hat{\mathbf{L}}_n| \sum_{\mathbf{z} \in \mathcal{Q}} \boldsymbol{\omega}(\mathbf{z}) \exp \left\{ \ell_n^\pi(\hat{\mathbf{L}}_n \mathbf{z} + \hat{\boldsymbol{\theta}}_n) - \ell_n^\pi(\hat{\boldsymbol{\theta}}_n) \right\} \right| \\ & \leq C n^{-p/2} \left[\max_{j \in [\kappa]} \max_{\mathbf{t} \in \tau_{\geq 2k}^{(j)}} n^{j-\tau(\mathbf{t})/2} + \max_{\mathbf{t} \in \tau_{\geq 3(\kappa+1)+\mathbb{I}\{2k=2 \pmod{3}\}}^{(\kappa+1)}} n^{\kappa+1-\tau(\mathbf{t})/2} \right. \\ & \quad \left. + \max_{j \in \{0\} \cup [\kappa]} n^{j-\frac{\gamma^2 \eta + 2}{4}} + \max_{\mathbf{t} \in \tau_{\geq 3(\kappa+2)}^{(\kappa+2)}} n^{\kappa+2-\tau(\mathbf{t})/2} \right] \end{aligned}$$

for some constant $C > 0$ that depends on p and k as well as $\underline{\eta}$, $\bar{\eta}$, and M .

Clearly, we can take γ arbitrarily large to make the third term as small (polynomially) as we desire. Upon inspection, the first term is maximized at $j = \kappa$ and $\tau(\mathbf{t}) = 2k$, the second term is maximized at $\tau(\mathbf{t}) = 3(\kappa + 1) + \mathbb{I}\{2k = 2 \pmod{3}\}$, and the fourth term is maximized at $\tau(\mathbf{t}) = 3(\kappa + 2)$. Thus,

$$\begin{aligned} & \left| \int_{B_{\hat{\theta}_n}^p(\gamma_n)} \exp \left\{ \ell_n^\pi(\boldsymbol{\theta}) - \ell_n^\pi(\hat{\boldsymbol{\theta}}_n) \right\} d\boldsymbol{\theta} - |\hat{\mathbf{L}}_n| \sum_{\mathbf{z} \in \mathcal{Q}} \boldsymbol{\omega}(\mathbf{z}) \exp \left\{ \ell_n^\pi(\hat{\mathbf{L}}_n \mathbf{z} + \hat{\boldsymbol{\theta}}_n) - \ell_n^\pi(\hat{\boldsymbol{\theta}}_n) \right\} \right| \\ & \leq C n^{-p/2} \left[\frac{1}{n^{k-\kappa}} + \frac{\mathbb{I}\{2k \neq 2 \pmod{3}\}}{n^{(\kappa+1)/2}} + \frac{\mathbb{I}\{2k = 2 \pmod{3}\}}{n^{(\kappa+1)/2+1/2}} + \frac{1}{n^{(\kappa+2)/2}} \right]. \end{aligned} \quad (13)$$

Now, recall that κ is chosen to be the smallest integer such that $3(\kappa + 1) \geq 2k$. There are three cases to consider. If $2k = 0 \pmod{3}$, then $\kappa = 2k/3 - 1$, if $2k = 1 \pmod{3}$, then $\kappa = (2k - 1)/3$, and if $2k = 2 \pmod{3}$, then $\kappa = (2k - 2)/3$. Substituting this into Eq. (13) gives

$$\begin{aligned} & \left| \int_{B_{\hat{\theta}_n}^p(\gamma_n)} \exp \left\{ \ell_n^\pi(\boldsymbol{\theta}) - \ell_n^\pi(\hat{\boldsymbol{\theta}}_n) \right\} d\boldsymbol{\theta} - |\hat{\mathbf{L}}_n| \sum_{\mathbf{z} \in \mathcal{Q}} \boldsymbol{\omega}(\mathbf{z}) \exp \left\{ \ell_n^\pi(\hat{\mathbf{L}}_n \mathbf{z} + \hat{\boldsymbol{\theta}}_n) - \ell_n^\pi(\hat{\boldsymbol{\theta}}_n) \right\} \right| \\ & \leq C n^{-p/2} \left[\frac{\mathbb{I}\{2k = 0 \pmod{3}\}}{n^{k/3}} + \frac{\mathbb{I}\{2k = 1 \pmod{3}\}}{n^{(k+1)/3}} + \frac{\mathbb{I}\{2k = 2 \pmod{3}\}}{n^{(\kappa+2)/3}} \right] \\ & = C n^{-p/2 - \lfloor \frac{k+2}{3} \rfloor}. \end{aligned}$$

So, in conjunction with Lemma 5, this controls the first term on the RHS of Eq. (11). For the second term of the RHS, Lemmas 6 and 7 (stated below) together complete the proof of Lemma 2 by taking γ large enough (in k). \square

Lemma 6. *Under Assumptions 3 and 5,*

$$\lim_{n \rightarrow \infty} \mathbb{P}_n^* \left[\int_{[B_{\hat{\theta}_n^*}^p(\delta)]^c} \exp \left\{ \ell_n^\pi(\boldsymbol{\theta}) - \ell_n^\pi(\hat{\boldsymbol{\theta}}_n) \right\} d\boldsymbol{\theta} \leq \frac{e^{-nb}}{c_1} \right] = 1,$$

Proof of Lemma 6. Since $\widehat{\boldsymbol{\theta}}_n$ maximizes ℓ_n^π ,

$$\begin{aligned} \int_{[B_{\boldsymbol{\theta}^*}^p(\delta)]^c} \exp\{\ell_n^\pi(\boldsymbol{\theta}) - \ell_n^\pi(\widehat{\boldsymbol{\theta}}_n)\} d\boldsymbol{\theta} &\leq \int_{[B_{\boldsymbol{\theta}^*}^p(\delta)]^c} \frac{\pi(\boldsymbol{\theta})}{\pi(\boldsymbol{\theta}^*)} \exp\{\ell_n(\boldsymbol{\theta}) - \ell_n(\boldsymbol{\theta}^*)\} d\boldsymbol{\theta} \\ &\leq \frac{1}{\pi(\boldsymbol{\theta}^*)} \sup_{\boldsymbol{\theta}' \in [B_{\boldsymbol{\theta}^*}^p(\delta)]^c} \exp\{\ell_n(\boldsymbol{\theta}') - \ell_n(\boldsymbol{\theta}^*)\} \int_{\Theta} \pi(\boldsymbol{\theta}) d\boldsymbol{\theta} \\ &= \frac{1}{\pi(\boldsymbol{\theta}^*)} \sup_{\boldsymbol{\theta}' \in [B_{\boldsymbol{\theta}^*}^p(\delta)]^c} \exp\{\ell_n(\boldsymbol{\theta}') - \ell_n(\boldsymbol{\theta}^*)\}. \end{aligned}$$

The result then follows by applying Assumptions 3 and 5. \square

Lemma 7. *Under Assumptions 2 to 5, there exists a constant $C > 0$ such that*

$$\lim_{n \rightarrow \infty} \mathbb{P}_n^* \left[\int_{[B_{\widehat{\boldsymbol{\theta}}_n}^p(\gamma_n)]^c \cap B_{\boldsymbol{\theta}^*}^p(\delta)} \exp\{\ell_n^\pi(\boldsymbol{\theta}) - \ell_n^\pi(\widehat{\boldsymbol{\theta}}_n)\} d\boldsymbol{\theta} \leq C \frac{1}{n^{\widehat{\gamma}_n^2 \eta / 4 + p/2}} \right] = 1.$$

Proof of Lemma 7. Using a second order Taylor expansion for each $\boldsymbol{\theta} \in [B_{\widehat{\boldsymbol{\theta}}_n}^p(\gamma_n)]^c \cap B_{\boldsymbol{\theta}^*}^p(\delta)$ gives

$$\exp\{\ell_n^\pi(\boldsymbol{\theta}) - \ell_n^\pi(\widehat{\boldsymbol{\theta}}_n)\} = \exp\left\{-\frac{1}{2}(\boldsymbol{\theta} - \widehat{\boldsymbol{\theta}}_n)^\top \mathbf{H}_n(\boldsymbol{\vartheta}_n^\theta)(\boldsymbol{\theta} - \widehat{\boldsymbol{\theta}}_n)\right\},$$

where $\boldsymbol{\vartheta}_n^\theta = \widehat{\tau}_\theta \widehat{\boldsymbol{\theta}}_n + (1 - \widehat{\tau}_\theta)\boldsymbol{\theta}$ for some $\widehat{\tau}_\theta \in [0, 1]$. Consider the case where $\widehat{\boldsymbol{\theta}}_n \in B_{\boldsymbol{\theta}^*}^p(\gamma_n)$. This implies that, since $\gamma_n \rightarrow 0$, for large enough n

$$\begin{aligned} &\sup_{\boldsymbol{\theta} \in B_{\boldsymbol{\theta}^*}^p(\delta)} \|\boldsymbol{\vartheta}_n^\theta - \boldsymbol{\theta}^*\|_2 \\ &= \sup_{\boldsymbol{\theta} \in B_{\boldsymbol{\theta}^*}^p(\delta)} \left\| \widehat{\tau}_\theta \widehat{\boldsymbol{\theta}}_n + (1 - \widehat{\tau}_\theta)\boldsymbol{\theta} - \widehat{\tau}_\theta \boldsymbol{\theta}^* - (1 - \widehat{\tau}_\theta)\boldsymbol{\theta}^* \right\|_2 \\ &\leq \sup_{\boldsymbol{\theta} \in B_{\boldsymbol{\theta}^*}^p(\delta)} \widehat{\tau}_\theta \gamma_n + (1 - \widehat{\tau}_\theta)\delta \\ &\leq \delta. \end{aligned}$$

Thus, letting $\underline{\eta}_n^* = \inf_{\boldsymbol{\theta} \in B_{\boldsymbol{\theta}^*}^p(\delta)} \lambda_p(\mathbf{H}_n(\boldsymbol{\theta}))/n$, we have

$$\sup_{\boldsymbol{\theta} \in B_{\boldsymbol{\theta}^*}^p(\delta)} (\boldsymbol{\theta} - \widehat{\boldsymbol{\theta}}_n)^\top \mathbf{H}_n(\boldsymbol{\vartheta}_n^\theta)(\boldsymbol{\theta} - \widehat{\boldsymbol{\theta}}_n) \geq \underline{\eta}_n^* n (\boldsymbol{\theta} - \widehat{\boldsymbol{\theta}}_n)^\top (\boldsymbol{\theta} - \widehat{\boldsymbol{\theta}}_n).$$

That is,

$$\begin{aligned}
 & \int_{[B_{\hat{\boldsymbol{\theta}}_n}^p(\gamma_n)]^c \cap B_{\boldsymbol{\theta}^*}^p(\delta)} \exp\{\ell_n^\pi(\boldsymbol{\theta}) - \ell_n^\pi(\hat{\boldsymbol{\theta}}_n)\} d\boldsymbol{\theta} \\
 & \leq \int_{[B_{\hat{\boldsymbol{\theta}}_n}^p(\gamma_n)]^c \cap B_{\boldsymbol{\theta}^*}^p(\delta)} \exp\left\{-\frac{\underline{\eta}_n^* n}{2}(\boldsymbol{\theta} - \hat{\boldsymbol{\theta}}_n)^\top(\boldsymbol{\theta} - \hat{\boldsymbol{\theta}}_n)\right\} d\boldsymbol{\theta} \\
 & \leq \int_{[B_{\hat{\boldsymbol{\theta}}_n}^p(\gamma_n)]^c} \exp\left\{-\frac{\underline{\eta}_n^* n}{2}(\boldsymbol{\theta} - \hat{\boldsymbol{\theta}}_n)^\top(\boldsymbol{\theta} - \hat{\boldsymbol{\theta}}_n)\right\} d\boldsymbol{\theta} \\
 & = \left(\frac{2\pi}{\underline{\eta}_n^* n}\right)^{p/2} \mathbb{P}\left[\chi_p^2 \geq \underline{\eta}_n^* n \gamma_n^2\right] \\
 & = \left(\frac{2\pi}{\underline{\eta}_n^* n}\right)^{p/2} \mathbb{P}\left[\chi_p^2/p \geq 1 + \zeta_n\right],
 \end{aligned}$$

where $\zeta_n = \gamma^2 \log(n) \underline{\eta}_n^*/p - 1$. Then, by Lemma 3 in Fan and Lv (2008),

$$\begin{aligned}
 \mathbb{P}\left[\chi_p^2/p \geq 1 + \zeta_n\right] & \leq \exp\left\{\frac{p}{2}[\log(1 + \zeta_n) - \zeta_n]\right\} \\
 & = \exp\left\{\frac{p}{2}\left[\log\left(\frac{\gamma^2 \log(n) \underline{\eta}_n^*}{p}\right) - \frac{\gamma^2 \log(n) \underline{\eta}_n^*}{p} + 1\right]\right\} \\
 & \leq \exp\left\{\frac{p}{2}\left[-\frac{\gamma^2 \log(n) \underline{\eta}_n^*}{2p} + 1\right]\right\} \\
 & = e^{p/2} n^{-\gamma^2 \underline{\eta}_n^*/4},
 \end{aligned}$$

where we have used that $\log(x) < x/2$ for all $x > 0$.

Thus,

$$\begin{aligned}
 & \int_{[B_{\hat{\boldsymbol{\theta}}_n}^p(\gamma_n)]^c \cap B_{\boldsymbol{\theta}^*}^p(\delta)} \exp\{\ell_n^\pi(\boldsymbol{\theta}) - \ell_n^\pi(\hat{\boldsymbol{\theta}}_n)\} d\boldsymbol{\theta} \\
 & \leq \left(\frac{2\pi e}{\underline{\eta}_n^*}\right)^{p/2} n^{-\gamma^2 \underline{\eta}_n^*/4 - p/2}.
 \end{aligned}$$

By Assumption 4, we have $\lim_{n \rightarrow \infty} \mathbb{P}_n^*[\hat{\boldsymbol{\theta}}_n \in B_{\boldsymbol{\theta}^*}^p(\gamma_n)] = 1$, and by Assumption 2 we have $\lim_{n \rightarrow \infty} \mathbb{P}_n^*[\underline{\eta}_n^* \geq \underline{\eta}] = 1$, giving the statement of the lemma. \square

B.3. Proof of Lemma 3

For all $\mathbf{z} \in \mathcal{Q}$, a third order Taylor expansion of the posterior around $\hat{\boldsymbol{\theta}}_n$ gives

$$\begin{aligned}
 \frac{\pi(\hat{\mathbf{L}}_n \mathbf{z} + \hat{\boldsymbol{\theta}}_n, \mathbf{Y}^{(n)})}{\pi(\hat{\boldsymbol{\theta}}_n, \mathbf{Y}^{(n)})} & = \exp\left\{-\frac{1}{2}(\hat{\mathbf{L}}_n \mathbf{z})^\top \mathbf{H}_n(\hat{\boldsymbol{\theta}}_n)(\hat{\mathbf{L}}_n \mathbf{z}) + \frac{1}{6}(\hat{\mathbf{L}}_n \mathbf{z})_{i_1 i_2 i_3} \partial^{i_1 i_2 i_3} \ell_n^\pi(\boldsymbol{\vartheta}_n \hat{\mathbf{L}}_n \mathbf{z} + \hat{\boldsymbol{\theta}}_n)\right\} \\
 & = \exp\left\{-\frac{1}{2} \mathbf{z}^\top \mathbf{z} + \frac{1}{6}(\hat{\mathbf{L}}_n \mathbf{z})_{i_1 i_2 i_3} \partial^{i_1 i_2 i_3} \ell_n^\pi(\boldsymbol{\vartheta}_n \hat{\mathbf{L}}_n \mathbf{z} + \hat{\boldsymbol{\theta}}_n)\right\},
 \end{aligned}$$

where $\boldsymbol{\vartheta}_n^{\widehat{\mathbf{L}}_n \mathbf{z} + \widehat{\boldsymbol{\theta}}_n} = \tau_z(\widehat{\mathbf{L}}_n \mathbf{z} + \widehat{\boldsymbol{\theta}}_n) + (1 - \tau_z)\widehat{\boldsymbol{\theta}}_n$ for some $\tau_z \in [0, 1]$. If $\widehat{\boldsymbol{\theta}}_n \in B_{\boldsymbol{\theta}^*}^p(\delta/2)$ and $\underline{\eta}_n \geq \underline{\eta}$, then

$$\begin{aligned} \left\| \boldsymbol{\vartheta}_n^{\widehat{\mathbf{L}}_n \mathbf{z} + \widehat{\boldsymbol{\theta}}_n} - \boldsymbol{\theta}^* \right\|_2 &= \left\| \tau_z(\widehat{\mathbf{L}}_n \mathbf{z} + \widehat{\boldsymbol{\theta}}_n) + (1 - \tau_z)\widehat{\boldsymbol{\theta}}_n - \tau_z \boldsymbol{\theta}^* - (1 - \tau_z)\boldsymbol{\theta}^* \right\|_2 \\ &\leq \left\| \widehat{\mathbf{L}}_n \mathbf{z} \right\|_2 + \left\| \widehat{\boldsymbol{\theta}}_n - \boldsymbol{\theta}^* \right\|_2 \\ &\leq [\lambda_p(\mathbf{H}_n(\widehat{\boldsymbol{\theta}}_n))]^{-1/2} \bar{z} + \delta/2 \\ &\leq (\underline{\eta}_n n)^{-1/2} \bar{z} + \delta/2 \\ &\leq (\underline{\eta} n)^{-1/2} \bar{z} + \delta/2. \end{aligned}$$

That is, under these conditions, for large enough n we have $\boldsymbol{\vartheta}_n^{\widehat{\mathbf{L}}_n \mathbf{z} + \widehat{\boldsymbol{\theta}}_n} \in B_{\boldsymbol{\theta}^*}^p(\delta)$. Further, these conditions imply

$$\begin{aligned} \frac{1}{6} \left| (\widehat{\mathbf{L}}_n \mathbf{z})_{i_1 i_2 i_3} \partial^{i_1 i_2 i_3} \ell_n^\pi(\boldsymbol{\vartheta}_n^{\widehat{\mathbf{L}}_n \mathbf{z} + \widehat{\boldsymbol{\theta}}_n}) \right| &\leq \frac{1}{6} p^3 \max_{\mathbf{z} \in \mathcal{Q}} \left\| \widehat{\mathbf{L}}_n \mathbf{z} \right\|_2^3 \max_{\mathbf{z} \in \mathcal{Q}, (i_1, i_2, i_3) \in [p]} \left| \partial^{i_1 i_2 i_3} \ell_n^\pi(\boldsymbol{\vartheta}_n^{\widehat{\mathbf{L}}_n \mathbf{z} + \widehat{\boldsymbol{\theta}}_n}) \right| \\ &\leq \frac{1}{6} p^3 (\underline{\eta} n)^{-3/2} \bar{z} \max_{\mathbf{z} \in \mathcal{Q}, (i_1, i_2, i_3) \in [p]} \left| \partial^{i_1 i_2 i_3} \ell_n^\pi(\boldsymbol{\vartheta}_n^{\widehat{\mathbf{L}}_n \mathbf{z} + \widehat{\boldsymbol{\theta}}_n}) \right| := B(n). \end{aligned}$$

Thus, using the crude bound $e^x \geq 1 - x$,

$$\begin{aligned} \frac{\tilde{\pi}_{(\mathcal{Q}, \boldsymbol{\omega})}^A(\mathbf{Y}^{(n)})}{\pi(\mathbf{Y}^{(n)} | \widehat{\boldsymbol{\theta}}_n)} &= \pi(\widehat{\boldsymbol{\theta}}_n) |\widehat{\mathbf{L}}_n| \sum_{\mathbf{z} \in \mathcal{Q}} \boldsymbol{\omega}(\mathbf{z}) \frac{\pi(\widehat{\mathbf{L}}_n \mathbf{z} + \widehat{\boldsymbol{\theta}}_n, \mathbf{Y}^{(n)})}{\pi(\widehat{\boldsymbol{\theta}}_n, \mathbf{Y}^{(n)})} \\ &= \pi(\widehat{\boldsymbol{\theta}}_n) |\widehat{\mathbf{L}}_n| \sum_{\mathbf{z} \in \mathcal{Q}} \boldsymbol{\omega}(\mathbf{z}) \exp \left\{ -\frac{1}{2} \mathbf{z}^\top \mathbf{z} + \frac{1}{6} (\widehat{\mathbf{L}}_n \mathbf{z})_{i_1 i_2 i_3} \partial^{i_1 i_2 i_3} \ell_n^\pi(\boldsymbol{\vartheta}_n^{\widehat{\mathbf{L}}_n \mathbf{z} + \widehat{\boldsymbol{\theta}}_n}) \right\} \\ &\geq \pi(\widehat{\boldsymbol{\theta}}_n) |\widehat{\mathbf{L}}_n| \sum_{\mathbf{z} \in \mathcal{Q}} \boldsymbol{\omega}(\mathbf{z}) \exp \left\{ -\frac{1}{2} \mathbf{z}^\top \mathbf{z} \right\} [1 - B(n)] \\ &\geq \pi(\widehat{\boldsymbol{\theta}}_n) |\widehat{\mathbf{L}}_n| \left[\sum_{\mathbf{z} \in \mathcal{Q}} \boldsymbol{\omega}(\mathbf{z}) \exp \left\{ -\frac{1}{2} \mathbf{z}^\top \mathbf{z} \right\} - B(n) \sum_{\mathbf{z} \in \mathcal{Q}} |\boldsymbol{\omega}(\mathbf{z})| \right] \\ &= \pi(\widehat{\boldsymbol{\theta}}_n) |\widehat{\mathbf{L}}_n| \left[(2\pi)^{p/2} - B(n) \sum_{\mathbf{z} \in \mathcal{Q}} |\boldsymbol{\omega}(\mathbf{z})| \right], \end{aligned} \tag{14}$$

where the last step uses $\mathcal{P}(k, p)$.

Note we also have, if $\bar{\eta}_n \leq \bar{\eta}$,

$$|\widehat{\mathbf{L}}_n| = \sqrt{\left| [\mathbf{H}_n(\widehat{\boldsymbol{\theta}}_n)]^{-1} \right|} = \left| \mathbf{H}_n(\widehat{\boldsymbol{\theta}}_n) \right|^{-1/2} \geq \left[\lambda_1(\mathbf{H}_n(\widehat{\boldsymbol{\theta}}_n)) \right]^{-p/2} = (\bar{\eta}_n n)^{-p/2} \geq (\bar{\eta} n)^{-p/2}.$$

Under these conditions, $B(n) \rightarrow 0$ and $\sum_{\mathbf{z} \in \mathcal{Q}} |\boldsymbol{\omega}(\mathbf{z})|$ is bounded by some constant. Thus, for large enough n , Eq. (14) gives that if $\widehat{\boldsymbol{\theta}}_n \in B_{\boldsymbol{\theta}^*}^p(\delta/2)$, $\underline{\eta}_n \geq \underline{\eta}$, $\bar{\eta}_n^* \leq \bar{\eta}$, and $\bar{\eta}_n \leq \bar{\eta}$, then

$$\frac{\tilde{\pi}_{(\mathcal{Q}, \boldsymbol{\omega})}^A(\mathbf{Y}^{(n)})}{\pi(\mathbf{Y}^{(n)} | \widehat{\boldsymbol{\theta}}_n)} \geq c_1 (\bar{\eta} n)^{-p/2} \left[(2\pi)^{p/2} - B(n) \sum_{\mathbf{z} \in \mathcal{Q}} |\boldsymbol{\omega}(\mathbf{z})| \right] \geq C' n^{-p/2},$$

where $C' > 0$ is some constant. The statement of the lemma then follows from Assumptions 2, 4, and 5, as well as Lemma 5. \square

C. Proof of Lemma 4

We first state the argument for $k \geq 2$, and then address the slight modifications that must be made when $k = 1$ in Appendix C.9. For all $\boldsymbol{\theta} \in \Theta$, the $2k$ th order Taylor expansion of ℓ_n^π around $\widehat{\boldsymbol{\theta}}_n$ gives

$$\begin{aligned} & \exp \left\{ \ell_n^\pi(\boldsymbol{\theta}) - \ell_n^\pi(\widehat{\boldsymbol{\theta}}_n) \right\} \\ &= \exp \left\{ \frac{1}{2}(\boldsymbol{\theta} - \widehat{\boldsymbol{\theta}}_n)_{i_1 i_2} \partial^{i_1 i_2} \ell_n^\pi(\widehat{\boldsymbol{\theta}}_n) \right\} \times \\ & \quad \exp \left\{ \sum_{j=3}^{2k-1} (\boldsymbol{\theta} - \widehat{\boldsymbol{\theta}}_n)_{[i_1 \dots i_j]} \partial^{i_1 \dots i_j} \ell_n^\pi(\widehat{\boldsymbol{\theta}}_n) + (\boldsymbol{\theta} - \widehat{\boldsymbol{\theta}}_n)_{[i_1 \dots i_{2k}]} \partial^{i_1 \dots i_{2k}} \ell_n^\pi(\widehat{\boldsymbol{\theta}}_n^\theta) \right\}, \end{aligned} \quad (15)$$

where $\widehat{\boldsymbol{\theta}}_n^\theta = \widehat{\tau}_{\boldsymbol{\theta}, n} \widehat{\boldsymbol{\theta}}_n + (1 - \widehat{\tau}_{\boldsymbol{\theta}, n}) \boldsymbol{\theta}$ for some $\widehat{\tau}_{\boldsymbol{\theta}, n} \in [0, 1]$. Further,

$$\begin{aligned} \exp \left\{ \frac{1}{2}(\boldsymbol{\theta} - \widehat{\boldsymbol{\theta}}_n)_{i_1 i_2} \partial^{i_1 i_2} \ell_n^\pi(\widehat{\boldsymbol{\theta}}_n) \right\} &= \exp \left\{ -\frac{1}{2}(\boldsymbol{\theta} - \widehat{\boldsymbol{\theta}}_n)^\top [\mathbf{H}_n(\widehat{\boldsymbol{\theta}}_n)] (\boldsymbol{\theta} - \widehat{\boldsymbol{\theta}}_n) \right\} \\ &= (2\pi)^{p/2} \left| [\mathbf{H}_n(\widehat{\boldsymbol{\theta}}_n)]^{-1} \right|^{1/2} \phi(\boldsymbol{\theta}; \widehat{\boldsymbol{\theta}}_n, [\mathbf{H}_n(\widehat{\boldsymbol{\theta}}_n)]^{-1}) \\ &= (2\pi)^{p/2} |\widehat{\mathbf{L}}_n| \phi(\boldsymbol{\theta}; \widehat{\boldsymbol{\theta}}_n, [\mathbf{H}_n(\widehat{\boldsymbol{\theta}}_n)]^{-1}), \end{aligned} \quad (16)$$

For notational simplicity, we define

$$A_n(\boldsymbol{\theta}) = \sum_{s=3}^{2k-1} (\boldsymbol{\theta} - \widehat{\boldsymbol{\theta}}_n)_{[i_1 \dots i_s]} \partial^{i_1 \dots i_s} \ell_n^\pi(\widehat{\boldsymbol{\theta}}_n) + (\boldsymbol{\theta} - \widehat{\boldsymbol{\theta}}_n)_{[i_1 \dots i_{2k}]} \partial^{i_1 \dots i_{2k}} \ell_n^\pi(\widehat{\boldsymbol{\theta}}_n^\theta).$$

Substituting Eqs. (15) and (16) into the difference of interest, we obtain

$$\begin{aligned}
 & \left| \int_{B_{\hat{\boldsymbol{\theta}}_n}^p(\gamma_n)} \exp \left\{ \ell_n^\pi(\boldsymbol{\theta}) - \ell_n^\pi(\hat{\boldsymbol{\theta}}_n) \right\} d\boldsymbol{\theta} - |\hat{\mathbf{L}}_n| \sum_{\mathbf{z} \in \mathcal{Q}} \boldsymbol{\omega}(\mathbf{z}) \exp \left\{ \ell_n^\pi(\hat{\mathbf{L}}_n \mathbf{z} + \hat{\boldsymbol{\theta}}_n) - \ell_n^\pi(\hat{\boldsymbol{\theta}}_n) \right\} \right| \\
 &= (2\pi)^{p/2} |\hat{\mathbf{L}}_n| \\
 & \quad \times \left| \int_{B_{\hat{\boldsymbol{\theta}}_n}^p(\gamma_n)} \phi(\boldsymbol{\theta}; \hat{\boldsymbol{\theta}}_n, [\mathbf{H}_n(\hat{\boldsymbol{\theta}}_n)]^{-1}) \exp \{A_n(\boldsymbol{\theta})\} d\boldsymbol{\theta} \right. \\
 & \quad \left. - |\hat{\mathbf{L}}_n| \sum_{\mathbf{z} \in \mathcal{Q}} \boldsymbol{\omega}(\mathbf{z}) \phi(\hat{\mathbf{L}}_n \mathbf{z} + \hat{\boldsymbol{\theta}}_n; \hat{\boldsymbol{\theta}}_n, [\mathbf{H}_n(\hat{\boldsymbol{\theta}}_n)]^{-1}) \exp \left\{ A_n(\hat{\mathbf{L}}_n \mathbf{z} + \hat{\boldsymbol{\theta}}_n) \right\} \right| \quad (17) \\
 &= (2\pi)^{p/2} |\hat{\mathbf{L}}_n| \\
 & \quad \times \left| \int_{B_{\hat{\boldsymbol{\theta}}_n}^p(\gamma_n)} \phi(\boldsymbol{\theta}; \hat{\boldsymbol{\theta}}_n, [\mathbf{H}_n(\hat{\boldsymbol{\theta}}_n)]^{-1}) \exp \{A_n(\boldsymbol{\theta})\} d\boldsymbol{\theta} \right. \\
 & \quad \left. - \sum_{\mathbf{z} \in \mathcal{Q}} \boldsymbol{\omega}(\mathbf{z}) \phi(\mathbf{z}; 0, \mathbf{I}_p) \exp \left\{ A_n(\hat{\mathbf{L}}_n \mathbf{z} + \hat{\boldsymbol{\theta}}_n) \right\} \right|.
 \end{aligned}$$

Now, evaluating the $(\kappa + 2)$ th order Taylor expansion of e^x around zero at $A_n(\boldsymbol{\theta})$ gives

$$\exp\{A_n(\boldsymbol{\theta})\} = \sum_{j=0}^{\kappa+1} \frac{A_n(\boldsymbol{\theta})^j}{j!} + \frac{A_n(\boldsymbol{\theta})^{(\kappa+2)}}{(\kappa+2)!} \exp\{\overline{A}_n(\boldsymbol{\theta})\},$$

where $\overline{A}_n(\boldsymbol{\theta}) = \tau_n A_n(\boldsymbol{\theta})$ for some $\tau_n \in [0, 1]$. For each $j \leq \kappa$ and $\mathbf{t} = (t_3, \dots, t_{2k})$ satisfying $\sum_{s=3}^{2k} t_s = j$, denote the multinomial coefficient by

$$\mathbb{M}_{j, \mathbf{t}} = \binom{j}{t_3, \dots, t_{2k}}.$$

This simplifies notation, so we can write $A_n(\boldsymbol{\theta})^j$ as

$$\sum_{\mathbf{t}: t_3 + \dots + t_{2k} = j} \mathbb{M}_{j, \mathbf{t}} \left\{ \left(\prod_{s=3}^{2k-1} [(\boldsymbol{\theta} - \hat{\boldsymbol{\theta}}_n)_{[i_1 \dots i_s]}! \partial^{i_1 \dots i_s} \ell_n^\pi(\hat{\boldsymbol{\theta}}_n)]^{t_s} \right) [(\boldsymbol{\theta} - \hat{\boldsymbol{\theta}}_n)_{[i_1 \dots i_{2k}]}! \partial^{i_1 \dots i_{2k}} \ell_n^\pi(\hat{\boldsymbol{\theta}}_n)]^{t_{2k}} \right\}.$$

For each $s \in \{3, \dots, 2k-1\}$, note that $(\boldsymbol{\theta} - \hat{\boldsymbol{\theta}}_n)_{[i_1 \dots i_s]}! \partial^{i_1 \dots i_s} \ell_n^\pi(\hat{\boldsymbol{\theta}}_n)$ is a polynomial in $\boldsymbol{\theta}$ of total order s . Thus, $A_n(\boldsymbol{\theta})^j$ is actually equal to

$$\begin{aligned}
 & \sum_{\mathbf{t} \in \tau_{<2k}^{(j)}} \mathbb{M}_{j, \mathbf{t}} \left\{ \left(\prod_{s=3}^{2k-1} [(\boldsymbol{\theta} - \hat{\boldsymbol{\theta}}_n)_{[i_1 \dots i_s]}! \partial^{i_1 \dots i_s} \ell_n^\pi(\hat{\boldsymbol{\theta}}_n)]^{t_s} \right) [(\boldsymbol{\theta} - \hat{\boldsymbol{\theta}}_n)_{[i_1 \dots i_{2k}]}! \partial^{i_1 \dots i_{2k}} \ell_n^\pi(\hat{\boldsymbol{\theta}}_n)]^{t_{2k}} \right\} \\
 & + \sum_{\mathbf{t} \in \tau_{\geq 2k}^{(j)}} \mathbb{M}_{j, \mathbf{t}} \left\{ \left(\prod_{s=3}^{2k-1} [(\boldsymbol{\theta} - \hat{\boldsymbol{\theta}}_n)_{[i_1 \dots i_s]}! \partial^{i_1 \dots i_s} \ell_n^\pi(\hat{\boldsymbol{\theta}}_n)]^{t_s} \right) [(\boldsymbol{\theta} - \hat{\boldsymbol{\theta}}_n)_{[i_1 \dots i_{2k}]}! \partial^{i_1 \dots i_{2k}} \ell_n^\pi(\hat{\boldsymbol{\theta}}_n)]^{t_{2k}} \right\}.
 \end{aligned}$$

In summary, we have broken $A_n(\boldsymbol{\theta})^j$ up into two cases: the terms in the first sum are polynomials in $\boldsymbol{\theta}$ of total order at most $2k - 1$, while all polynomials in $\boldsymbol{\theta}$ contained in the terms of the second sum have degree at least $2k$. Importantly, for any j , all $\mathbf{t} \in \tau_{<2k}^{(j)}$ satisfy $t_{2k} = 0$ necessarily, which means there is no dependence of $\widehat{\boldsymbol{\vartheta}}_n^\theta$ in these polynomials. Since $\mathfrak{R}(\mathcal{Q}, \boldsymbol{\omega})$ satisfies $\mathcal{P}(k, p)$,

$$\begin{aligned}
 & \sum_{\mathbf{z} \in \mathcal{Q}} \boldsymbol{\omega}(\mathbf{z}) \phi(\mathbf{z}; 0, \mathbf{I}_p) \exp \left\{ A_n \left(\widehat{\mathbf{L}}_n \mathbf{z} + \widehat{\boldsymbol{\theta}}_n \right) \right\} \\
 &= \sum_{j=0}^{\kappa} \int_{\Theta} \phi(\boldsymbol{\theta}; 0, \mathbf{I}_p) \sum_{\mathbf{t} \in \tau_{<2k}^{(j)}} \mathbb{M}_{j, \mathbf{t}} \prod_{s=3}^{2k-1} \left[(\widehat{\mathbf{L}}_n \boldsymbol{\theta})_{[i_1 \dots i_s]}! \partial^{i_1 \dots i_s} \ell_n^\pi(\widehat{\boldsymbol{\theta}}_n) \right]^{t_s} d\boldsymbol{\theta} \\
 & \quad + \sum_{j=1}^{\kappa} \sum_{\mathbf{z} \in \mathcal{Q}} \boldsymbol{\omega}(\mathbf{z}) \phi(\mathbf{z}; 0, \mathbf{I}_p) \sum_{\mathbf{t} \in \tau_{\geq 2k}^{(j)}} \mathbb{M}_{j, \mathbf{t}} \left\{ \left(\prod_{s=3}^{2k-1} \left[(\widehat{\mathbf{L}}_n \mathbf{z})_{[i_1 \dots i_s]}! \partial^{i_1 \dots i_s} \ell_n^\pi(\widehat{\boldsymbol{\theta}}_n) \right]^{t_s} \right) \right. \\
 & \quad \quad \quad \left. \left[(\widehat{\mathbf{L}}_n \mathbf{z})_{[i_1 \dots i_{2k}]}! \partial^{i_1 \dots i_{2k}} \ell_n^\pi(\widehat{\boldsymbol{\vartheta}}_n^{\widehat{\mathbf{L}}_n \mathbf{z} + \widehat{\boldsymbol{\theta}}_n}) \right]^{t_{2k}} \right\} \\
 & \quad + \sum_{\mathbf{z} \in \mathcal{Q}} \boldsymbol{\omega}(\mathbf{z}) \phi(\mathbf{z}; 0, \mathbf{I}_p) \frac{A_n(\widehat{\mathbf{L}}_n \mathbf{z} + \widehat{\boldsymbol{\theta}}_n)^{(\kappa+1)}}{(\kappa+1)!} \\
 & \quad + \sum_{\mathbf{z} \in \mathcal{Q}} \boldsymbol{\omega}(\mathbf{z}) \phi(\mathbf{z}; 0, \mathbf{I}_p) \frac{A_n(\widehat{\mathbf{L}}_n \mathbf{z} + \widehat{\boldsymbol{\theta}}_n)^{(\kappa+2)}}{(\kappa+2)!} \exp \{ \overline{A}_n(\widehat{\mathbf{L}}_n \mathbf{z} + \widehat{\boldsymbol{\theta}}_n) \}.
 \end{aligned}$$

Note that we have deliberately treated the $\kappa + 1$ and $\kappa + 2$ powers of $A_n(\boldsymbol{\theta})$ separately, which is crucial to obtain the correct rate and to handle the remainder term $\exp \{ \overline{A}_n(\widehat{\mathbf{L}}_n \mathbf{z} + \widehat{\boldsymbol{\theta}}_n) \}$. Applying a change of variable, splitting up Θ , and recalling that the quadrature process applied to polynomials of total order $2k - 1$ is exactly the same as the integral of this polynomial then

gives

$$\begin{aligned}
 & \sum_{z \in \mathcal{Q}} \omega(z) \phi(z; 0, \mathbf{I}_p) \exp \left\{ A_n \left(\widehat{\mathbf{L}}_n z + \widehat{\boldsymbol{\theta}}_n \right) \right\} \\
 &= \sum_{j=0}^{\kappa} \int_{B_{\widehat{\boldsymbol{\theta}}_n}^p(\gamma_n)} \phi(\boldsymbol{\theta}; \widehat{\boldsymbol{\theta}}_n, [\mathbf{H}_n(\widehat{\boldsymbol{\theta}}_n)]^{-1}) \sum_{t \in \tau_{<2k}^{(j)}} \mathbb{M}_{j,t} \prod_{s=3}^{2k-1} \left[(\boldsymbol{\theta} - \widehat{\boldsymbol{\theta}}_n)_{[i_1 \dots i_s]}! \partial^{i_1 \dots i_s} \ell_n^\pi(\widehat{\boldsymbol{\theta}}_n) \right]^{t_s} d\boldsymbol{\theta} \\
 & \quad + \sum_{j=0}^{\kappa} \int_{[B_{\widehat{\boldsymbol{\theta}}_n}^p(\gamma_n)]^c} \phi(\boldsymbol{\theta}; \widehat{\boldsymbol{\theta}}_n, [\mathbf{H}_n(\widehat{\boldsymbol{\theta}}_n)]^{-1}) \sum_{t \in \tau_{<2k}^{(j)}} \mathbb{M}_{j,t} \prod_{s=3}^{2k-1} \left[(\boldsymbol{\theta} - \widehat{\boldsymbol{\theta}}_n)_{[i_1 \dots i_s]}! \partial^{i_1 \dots i_s} \ell_n^\pi(\widehat{\boldsymbol{\theta}}_n) \right]^{t_s} d\boldsymbol{\theta} \\
 & \quad + \sum_{j=1}^{\kappa} \sum_{z \in \mathcal{Q}} \omega(z) \phi(z; 0, \mathbf{I}_p) \sum_{t \in \tau_{\geq 2k}^{(j)}} \mathbb{M}_{j,t} \left\{ \left(\prod_{s=3}^{2k-1} \left[(\widehat{\mathbf{L}}_n z)_{[i_1 \dots i_s]}! \partial^{i_1 \dots i_s} \ell_n^\pi(\widehat{\boldsymbol{\theta}}_n) \right]^{t_s} \right) \right. \\
 & \quad \quad \quad \left. \left[(\widehat{\mathbf{L}}_n z)_{[i_1 \dots i_{2k}]}! \partial^{i_1 \dots i_{2k}} \ell_n^\pi(\widehat{\boldsymbol{\theta}}_n \widehat{\mathbf{L}}_n z + \widehat{\boldsymbol{\theta}}_n) \right]^{t_{2k}} \right\} \\
 & \quad + \sum_{z \in \mathcal{Q}} \omega(z) \phi(z; 0, \mathbf{I}_p) \frac{A_n(\widehat{\mathbf{L}}_n z + \widehat{\boldsymbol{\theta}}_n)^{(\kappa+1)}}{(\kappa+1)!} \\
 & \quad + \sum_{z \in \mathcal{Q}} \omega(z) \phi(z; 0, \mathbf{I}_p) \frac{A_n(\widehat{\mathbf{L}}_n z + \widehat{\boldsymbol{\theta}}_n)^{(\kappa+2)}}{(\kappa+2)!} \exp\{\overline{A}_n(\widehat{\mathbf{L}}_n z + \widehat{\boldsymbol{\theta}}_n)\}.
 \end{aligned} \tag{18}$$

Similarly,

$$\begin{aligned}
 & \int_{B_{\widehat{\boldsymbol{\theta}}_n}^p(\gamma_n)} \phi(\boldsymbol{\theta}; \widehat{\boldsymbol{\theta}}_n, [\mathbf{H}_n(\widehat{\boldsymbol{\theta}}_n)]^{-1}) \exp \{ A_n(\boldsymbol{\theta}) \} d\boldsymbol{\theta} \\
 &= \sum_{j=0}^{\kappa} \int_{B_{\widehat{\boldsymbol{\theta}}_n}^p(\gamma_n)} \phi(\boldsymbol{\theta}; \widehat{\boldsymbol{\theta}}_n, [\mathbf{H}_n(\widehat{\boldsymbol{\theta}}_n)]^{-1}) \sum_{t \in \tau_{<2k}^{(j)}} \mathbb{M}_{j,t} \prod_{s=3}^{2k-1} \left[(\boldsymbol{\theta} - \widehat{\boldsymbol{\theta}}_n)_{[i_1 \dots i_s]}! \partial^{i_1 \dots i_s} \ell_n^\pi(\widehat{\boldsymbol{\theta}}_n) \right]^{t_s} d\boldsymbol{\theta} \\
 & \quad + \sum_{j=1}^{\kappa} \int_{B_{\widehat{\boldsymbol{\theta}}_n}^p(\gamma_n)} \phi(\boldsymbol{\theta}; \widehat{\boldsymbol{\theta}}_n, [\mathbf{H}_n(\widehat{\boldsymbol{\theta}}_n)]^{-1}) \sum_{t \in \tau_{\geq 2k}^{(j)}} \mathbb{M}_{j,t} \left\{ \left(\prod_{s=3}^{2k-1} \left[(\boldsymbol{\theta} - \widehat{\boldsymbol{\theta}}_n)_{[i_1 \dots i_s]}! \partial^{i_1 \dots i_s} \ell_n^\pi(\widehat{\boldsymbol{\theta}}_n) \right]^{t_s} \right) \right. \\
 & \quad \quad \quad \left. \left[(\boldsymbol{\theta} - \widehat{\boldsymbol{\theta}}_n)_{[i_1 \dots i_{2k}]}! \partial^{i_1 \dots i_{2k}} \ell_n^\pi(\widehat{\boldsymbol{\theta}}_n) \right]^{t_{2k}} \right\} d\boldsymbol{\theta} \\
 & \quad + \int_{B_{\widehat{\boldsymbol{\theta}}_n}^p(\gamma_n)} \phi(\boldsymbol{\theta}; \widehat{\boldsymbol{\theta}}_n, [\mathbf{H}_n(\widehat{\boldsymbol{\theta}}_n)]^{-1}) \frac{A_n(\boldsymbol{\theta})^{(\kappa+1)}}{(\kappa+1)!} d\boldsymbol{\theta} \\
 & \quad + \int_{B_{\widehat{\boldsymbol{\theta}}_n}^p(\gamma_n)} \phi(\boldsymbol{\theta}; \widehat{\boldsymbol{\theta}}_n, [\mathbf{H}_n(\widehat{\boldsymbol{\theta}}_n)]^{-1}) \frac{A_n(\boldsymbol{\theta})^{(\kappa+2)}}{(\kappa+2)!} \exp\{\overline{A}_n(\boldsymbol{\theta})\} d\boldsymbol{\theta}.
 \end{aligned} \tag{19}$$

Substituting Eqs. (18) and (19) into the absolute difference in Eq. (17) and applying triangle

inequality gives

$$\begin{aligned}
 & \left| \int_{B_{\hat{\boldsymbol{\theta}}_n}^p(\gamma_n)} \phi(\boldsymbol{\theta}; \hat{\boldsymbol{\theta}}_n, [\mathbf{H}_n(\hat{\boldsymbol{\theta}}_n)]^{-1}) \exp\{A_n(\boldsymbol{\theta})\} d\boldsymbol{\theta} \right. \\
 & \quad \left. - \sum_{\mathbf{z} \in \mathcal{Q}} \boldsymbol{\omega}(\mathbf{z}) \phi(\mathbf{z}; 0, \mathbf{I}_p) \exp\left\{A_n(\hat{\mathbf{L}}_n \mathbf{z} + \hat{\boldsymbol{\theta}}_n)\right\} \right| \\
 & \leq \sum_{j=1}^{\kappa} \int_{B_{\hat{\boldsymbol{\theta}}_n}^p(\gamma_n)} \phi(\boldsymbol{\theta}; \hat{\boldsymbol{\theta}}_n, [\mathbf{H}_n(\hat{\boldsymbol{\theta}}_n)]^{-1}) \sum_{\mathbf{t} \in \tau_{\geq 2k}^{(j)}} \mathbb{M}_{j,t} \left\{ \left(\prod_{s=3}^{2k-1} |(\boldsymbol{\theta} - \hat{\boldsymbol{\theta}}_n)_{[i_1 \dots i_s]}| \partial^{i_1 \dots i_s} \ell_n^\pi(\hat{\boldsymbol{\theta}}_n) \right)^{t_s} \right. \\
 & \quad \left. |(\boldsymbol{\theta} - \hat{\boldsymbol{\theta}}_n)_{[i_1 \dots i_{2k}]}| \partial^{i_1 \dots i_{2k}} \ell_n^\pi(\hat{\boldsymbol{\theta}}_n) \right\}^{t_{2k}} d\boldsymbol{\theta} \\
 & + \left| \int_{B_{\hat{\boldsymbol{\theta}}_n}^p(\gamma_n)} \phi(\boldsymbol{\theta}; \hat{\boldsymbol{\theta}}_n, [\mathbf{H}_n(\hat{\boldsymbol{\theta}}_n)]^{-1}) \frac{A_n(\boldsymbol{\theta})^{(\kappa+1)}}{(\kappa+1)!} d\boldsymbol{\theta} \right| \\
 & + \int_{B_{\hat{\boldsymbol{\theta}}_n}^p(\gamma_n)} \phi(\boldsymbol{\theta}; \hat{\boldsymbol{\theta}}_n, [\mathbf{H}_n(\hat{\boldsymbol{\theta}}_n)]^{-1}) \left| \frac{A_n(\boldsymbol{\theta})^{(\kappa+2)}}{(\kappa+2)!} \right| \exp\{\overline{A}_n(\boldsymbol{\theta})\} d\boldsymbol{\theta} \\
 & + \sum_{j=0}^{\kappa} \int_{[B_{\hat{\boldsymbol{\theta}}_n}^p(\gamma_n)]^c} \phi(\boldsymbol{\theta}; \hat{\boldsymbol{\theta}}_n, [\mathbf{H}_n(\hat{\boldsymbol{\theta}}_n)]^{-1}) \sum_{\mathbf{t} \in \tau_{< 2k}^{(j)}} \mathbb{M}_{j,t} \prod_{s=3}^{2k-1} |(\boldsymbol{\theta} - \hat{\boldsymbol{\theta}}_n)_{[i_1 \dots i_s]}| \partial^{i_1 \dots i_s} \ell_n^\pi(\hat{\boldsymbol{\theta}}_n) \Big|^{t_s} d\boldsymbol{\theta} \\
 & + \sum_{j=1}^{\kappa} \sum_{\mathbf{z} \in \mathcal{Q}} \boldsymbol{\omega}(\mathbf{z}) \phi(\mathbf{z}; 0, \mathbf{I}_p) \sum_{\mathbf{t} \in \tau_{\geq 2k}^{(j)}} \mathbb{M}_{j,t} \left\{ \left(\prod_{s=3}^{2k-1} |(\hat{\mathbf{L}}_n \mathbf{z})_{[i_1 \dots i_s]}| \partial^{i_1 \dots i_s} \ell_n^\pi(\hat{\boldsymbol{\theta}}_n) \right)^{t_s} \right. \\
 & \quad \left. |(\hat{\mathbf{L}}_n \mathbf{z})_{[i_1 \dots i_{2k}]}| \partial^{i_1 \dots i_{2k}} \ell_n^\pi(\hat{\boldsymbol{\theta}}_n) \right\}^{t_{2k}} \\
 & + \left| \sum_{\mathbf{z} \in \mathcal{Q}} \boldsymbol{\omega}(\mathbf{z}) \phi(\mathbf{z}; 0, \mathbf{I}_p) \frac{A_n(\hat{\mathbf{L}}_n \mathbf{z} + \hat{\boldsymbol{\theta}}_n)^{(\kappa+1)}}{(\kappa+1)!} \right| \\
 & + \sum_{\mathbf{z} \in \mathcal{Q}} \boldsymbol{\omega}(\mathbf{z}) \phi(\mathbf{z}; 0, \mathbf{I}_p) \left| \frac{A_n(\hat{\mathbf{L}}_n \mathbf{z} + \hat{\boldsymbol{\theta}}_n)^{(\kappa+1)}}{(\kappa+1)!} \right| \exp\{\overline{A}_n(\hat{\mathbf{L}}_n \mathbf{z} + \hat{\boldsymbol{\theta}}_n)\}.
 \end{aligned}$$

Next, observe that $\overline{A}_n(\boldsymbol{\theta}) \leq |A_n(\boldsymbol{\theta})|$ and $\overline{A}_n(\hat{\mathbf{L}}_n \mathbf{z} + \hat{\boldsymbol{\theta}}_n) \leq |A_n(\hat{\mathbf{L}}_n \mathbf{z} + \hat{\boldsymbol{\theta}}_n)|$. Additionally, by definition of the radius for which \widehat{M}_n is a bound on the derivatives, it holds that $|\partial^\alpha \ell_n^\pi(\hat{\boldsymbol{\theta}}_n)| \leq \widehat{M}_n$, $|\partial^\alpha \ell_n^\pi(\hat{\boldsymbol{\theta}}_n)| \leq \widehat{M}_n$, and $|\partial^\alpha \ell_n^\pi(\hat{\boldsymbol{\theta}}_n)| \leq \widehat{M}_n$ for any α , $\mathbf{z} \in \mathcal{Q}$, and $\boldsymbol{\theta} \in B_{\hat{\boldsymbol{\theta}}_n}^p(\gamma_n)$. Thus,

we have

$$\begin{aligned}
 & \left| \int_{B_{\hat{\boldsymbol{\theta}}_n}^p(\gamma_n)} \phi(\boldsymbol{\theta}; \hat{\boldsymbol{\theta}}_n, [\mathbf{H}_n(\hat{\boldsymbol{\theta}}_n)]^{-1}) \exp \{A_n(\boldsymbol{\theta})\} d\boldsymbol{\theta} \right. \\
 & \quad \left. - \sum_{\mathbf{z} \in \mathcal{Q}} \boldsymbol{\omega}(\mathbf{z}) \phi(\mathbf{z}; 0, \mathbf{I}_p) \exp \left\{ A_n(\hat{\mathbf{L}}_n \mathbf{z} + \hat{\boldsymbol{\theta}}_n) \right\} \right| \\
 & \leq \sum_{j=1}^{\kappa} (\widehat{M}_n)^j \int_{B_{\hat{\boldsymbol{\theta}}_n}^p(\gamma_n)} \phi(\boldsymbol{\theta}; \hat{\boldsymbol{\theta}}_n, [\mathbf{H}_n(\hat{\boldsymbol{\theta}}_n)]^{-1}) \sum_{\mathbf{t} \in \tau_{\geq 2k}^{(j)}} \mathbb{M}_{j,\mathbf{t}} \prod_{s=3}^{2k} \left| \sum_{i_1, \dots, i_s \in [p]} \prod_{\ell=1}^s (\boldsymbol{\theta} - \hat{\boldsymbol{\theta}}_n)_{i_\ell} \right|^{t_s} d\boldsymbol{\theta} \\
 & \quad + \left| \int_{B_{\hat{\boldsymbol{\theta}}_n}^p(\gamma_n)} \phi(\boldsymbol{\theta}; \hat{\boldsymbol{\theta}}_n, [\mathbf{H}_n(\hat{\boldsymbol{\theta}}_n)]^{-1}) \frac{A_n(\boldsymbol{\theta})^{(\kappa+1)}}{(\kappa+1)!} d\boldsymbol{\theta} \right| \\
 & \quad + \int_{B_{\hat{\boldsymbol{\theta}}_n}^p(\gamma_n)} \phi(\boldsymbol{\theta}; \hat{\boldsymbol{\theta}}_n, [\mathbf{H}_n(\hat{\boldsymbol{\theta}}_n)]^{-1}) \left| \frac{A_n(\boldsymbol{\theta})^{(\kappa+2)}}{(\kappa+2)!} \right| \exp \left\{ |A_n(\boldsymbol{\theta})| \right\} d\boldsymbol{\theta} \\
 & \quad + \sum_{j=0}^{\kappa} (\widehat{M}_n)^j \int_{[B_{\hat{\boldsymbol{\theta}}_n}^p(\gamma_n)]^c} \phi(\boldsymbol{\theta}; \hat{\boldsymbol{\theta}}_n, [\mathbf{H}_n(\hat{\boldsymbol{\theta}}_n)]^{-1}) \sum_{\mathbf{t} \in \tau_{< 2k}^{(j)}} \mathbb{M}_{j,\mathbf{t}} \prod_{s=3}^{2k-1} \left| \sum_{i_1, \dots, i_s \in [p]} \prod_{\ell=1}^s (\boldsymbol{\theta} - \hat{\boldsymbol{\theta}}_n)_{i_\ell} \right|^{t_s} d\boldsymbol{\theta} \\
 & \quad + \sum_{j=1}^{\kappa} (\widehat{M}_n)^j \sum_{\mathbf{z} \in \mathcal{Q}} \boldsymbol{\omega}(\mathbf{z}) \phi(\mathbf{z}; 0, \mathbf{I}_p) \sum_{\mathbf{t} \in \tau_{\geq 2k}^{(j)}} \mathbb{M}_{j,\mathbf{t}} \prod_{s=3}^{2k} \left| \sum_{i_1, \dots, i_s \in [p]} \prod_{\ell=1}^s (\hat{\mathbf{L}}_n \mathbf{z})_{i_\ell} \right|^{t_s} \\
 & \quad + \left| \sum_{\mathbf{z} \in \mathcal{Q}} \boldsymbol{\omega}(\mathbf{z}) \phi(\mathbf{z}; 0, \mathbf{I}_p) \frac{A_n(\hat{\mathbf{L}}_n \mathbf{z} + \hat{\boldsymbol{\theta}}_n)^{(\kappa+1)}}{(\kappa+1)!} \right| \\
 & \quad + \sum_{\mathbf{z} \in \mathcal{Q}} \boldsymbol{\omega}(\mathbf{z}) \phi(\mathbf{z}; 0, \mathbf{I}_p) \left| \frac{A_n(\hat{\mathbf{L}}_n \mathbf{z} + \hat{\boldsymbol{\theta}}_n)^{(\kappa+2)}}{(\kappa+2)!} \right| \exp \left\{ |A_n(\hat{\mathbf{L}}_n \mathbf{z} + \hat{\boldsymbol{\theta}}_n)| \right\}.
 \end{aligned} \tag{20}$$

Our next step is to simplify the dependence on $\mathbf{H}_n(\hat{\boldsymbol{\theta}}_n)$ for some terms. In particular, for every $\boldsymbol{\theta} \in \Theta$,

$$\begin{aligned}
 \phi(\boldsymbol{\theta}; \hat{\boldsymbol{\theta}}_n, [\mathbf{H}_n(\hat{\boldsymbol{\theta}}_n)]^{-1}) &= \frac{1}{|\hat{\mathbf{L}}_n| (2\pi)^{p/2}} \exp \left\{ -\frac{1}{2} (\boldsymbol{\theta} - \hat{\boldsymbol{\theta}}_n)^\top \mathbf{H}_n(\hat{\boldsymbol{\theta}}_n) (\boldsymbol{\theta} - \hat{\boldsymbol{\theta}}_n) \right\} \\
 &\leq \frac{[\lambda_1(\mathbf{H}_n(\hat{\boldsymbol{\theta}}_n))]^{p/2}}{(2\pi)^{p/2}} \exp \left\{ -\frac{1}{2} \lambda_p(\mathbf{H}_n(\hat{\boldsymbol{\theta}}_n)) (\boldsymbol{\theta} - \hat{\boldsymbol{\theta}}_n)^\top (\boldsymbol{\theta} - \hat{\boldsymbol{\theta}}_n) \right\} \\
 &= \frac{[\lambda_1(\mathbf{H}_n(\hat{\boldsymbol{\theta}}_n))]^{p/2}}{[\lambda_p(\mathbf{H}_n(\hat{\boldsymbol{\theta}}_n))]^{p/2}} \phi(\boldsymbol{\theta}; \hat{\boldsymbol{\theta}}_n, [\lambda_p(\mathbf{H}_n(\hat{\boldsymbol{\theta}}_n))]^{-1} \mathbf{I}_p).
 \end{aligned}$$

Finally, for each $j \leq \kappa$, \mathbf{t} such that $\sum_{s=3}^{2k} t_s = j$, and $\boldsymbol{\theta}' \in \Theta$, it holds that

$$\prod_{s=3}^{2k} \left(\sum_{i_1, \dots, i_s \in [p]} \prod_{\ell=1}^s |(\boldsymbol{\theta}')_{i_\ell}| \right)^{t_s} \leq \sum_{i_1, \dots, i_{\tau(\mathbf{t})} \in [p]} \prod_{\ell=1}^{\tau(\mathbf{t})} |(\boldsymbol{\theta}')_{i_\ell}| \leq \sum_{i_1, \dots, i_{\tau(\mathbf{t})} \in [p]} \frac{1}{\tau(\mathbf{t})} \sum_{\ell=1}^{\tau(\mathbf{t})} |(\boldsymbol{\theta}')_{i_\ell}|^{\tau(\mathbf{t})},$$

where the first inequality is because all permutations that show up on the LHS must appear in the sum on the RHS by definition, and the second inequality is by the AM-GM inequality. We will further control $1/\tau(\mathbf{t})$ using that if $\mathbf{t} \in \tau_{\geq 2k}^{(j)}$ then $\tau(\mathbf{t}) \geq 2k$, and $\tau(\mathbf{t}) \leq 2kj \leq 2k\kappa$ for all \mathbf{t} .

Applying this simplification of both $\phi(\boldsymbol{\theta}; \widehat{\boldsymbol{\theta}}_n, [\mathbf{H}_n(\widehat{\boldsymbol{\theta}}_n)]^{-1})$ and the polynomial terms, we get, informally,

$$\begin{aligned} & \left| \int_{B_{\widehat{\boldsymbol{\theta}}_n}^p(\gamma_n)} \phi(\boldsymbol{\theta}; \widehat{\boldsymbol{\theta}}_n, [\mathbf{H}_n(\widehat{\boldsymbol{\theta}}_n)]^{-1}) \exp \{A_n(\boldsymbol{\theta})\} d\boldsymbol{\theta} - \sum_{\mathbf{z} \in \mathcal{Q}} \omega(\mathbf{z}) \phi(\mathbf{z}; 0, \mathbf{I}_p) \exp \left\{ A_n \left(\widehat{\mathbf{L}}_n \mathbf{z} + \widehat{\boldsymbol{\theta}}_n \right) \right\} \right| \\ & \leq \text{High-degree polynomial remainder} + \text{Low-degree polynomial remainder} \\ & \quad + \text{True posterior remainder} + \text{Approximate posterior remainder.} \end{aligned} \tag{21}$$

Each of these terms are precisely quantified as follows, and broken up into Terms 1 through 7.

High-degree polynomial remainder:

$$\begin{aligned} & = \left(\frac{\overline{\eta}_n}{\eta_n} \right)^{p/2} \sum_{j=1}^{\kappa} (\widehat{M}_n)^j \sum_{\mathbf{t} \in \tau_{\geq 2k}^{(j)}} \frac{\mathbb{M}_{j,\mathbf{t}}}{2k} \sum_{i_1, \dots, i_{\tau(\mathbf{t})} \in [p]} \sum_{\iota=1}^{\tau(\mathbf{t})} \\ & \quad \times \underbrace{\int_{B_{\widehat{\boldsymbol{\theta}}_n}^p(\gamma_n)} \phi(\boldsymbol{\theta}; \widehat{\boldsymbol{\theta}}_n, [\lambda_p(\mathbf{H}_n(\widehat{\boldsymbol{\theta}}_n))]^{-1} \mathbf{I}_p) \left| (\boldsymbol{\theta} - \widehat{\boldsymbol{\theta}}_n)_{i_\iota} \right|^{\tau(\mathbf{t})} d\boldsymbol{\theta}}_{\text{Term 1}} \\ & \quad + \underbrace{\sum_{j=1}^{\kappa} (\widehat{M}_n)^j \sum_{\mathbf{t} \in \tau_{\geq 2k}^{(j)}} \frac{\mathbb{M}_{j,\mathbf{t}}}{2k} \sum_{i_1, \dots, i_{\tau(\mathbf{t})} \in [p]} \sum_{\iota=1}^{\tau(\mathbf{t})} \sum_{\mathbf{z} \in \mathcal{Q}} \omega(\mathbf{z}) \phi(\mathbf{z}; 0, \mathbf{I}_p) \left| (\widehat{\mathbf{L}}_n \mathbf{z})_{i_\iota} \right|^{\tau(\mathbf{t})}}_{\text{Term 2}}. \end{aligned}$$

These terms involve terms that are the higher order polynomial terms that are cancelled out by the quadrature process.

Low-degree polynomial remainder:

$$\begin{aligned} & = \left(\frac{\overline{\eta}_n}{\eta_n} \right)^{p/2} \sum_{j=0}^{\kappa} (\widehat{M}_n)^j \sum_{\mathbf{t} \in \tau_{< 2k}^{(j)}} \frac{\mathbb{M}_{j,\mathbf{t}}}{\tau(\mathbf{t})} \sum_{i_1, \dots, i_{\tau(\mathbf{t})} \in [p]} \sum_{\iota=1}^{\tau(\mathbf{t})} \\ & \quad \times \underbrace{\int_{[B_{\widehat{\boldsymbol{\theta}}_n}^p(\gamma_n)]^c} \phi(\boldsymbol{\theta}; \widehat{\boldsymbol{\theta}}_n, [\lambda_p(\mathbf{H}_n(\widehat{\boldsymbol{\theta}}_n))]^{-1} \mathbf{I}_p) \left| (\boldsymbol{\theta} - \widehat{\boldsymbol{\theta}}_n)_{i_\iota} \right|^{\tau(\mathbf{t})} d\boldsymbol{\theta}}_{\text{Term 3}}. \end{aligned}$$

These terms involve the tails integrals of the lower order polynomial terms that are not cancelled out by the quadrature process due to our truncation argument.

True posterior remainder:

$$\begin{aligned}
 &= \underbrace{\left(\frac{\overline{\eta}_n}{\underline{\eta}_n}\right)^{p/2} \int_{B_{\widehat{\boldsymbol{\theta}}_n}^p(\gamma_n)} \phi(\boldsymbol{\theta}; \widehat{\boldsymbol{\theta}}_n, [\lambda_p(\mathbf{H}_n(\widehat{\boldsymbol{\theta}}_n))]^{-1} \mathbf{I}_p) |A_n(\boldsymbol{\theta})|^{(\kappa+2)} \exp\{|A_n(\boldsymbol{\theta})|\} d\boldsymbol{\theta}}_{\text{Term 4}} \\
 &\quad + \underbrace{\left| \int_{B_{\widehat{\boldsymbol{\theta}}_n}^p(\gamma_n)} \phi(\boldsymbol{\theta}; \widehat{\boldsymbol{\theta}}_n, [\mathbf{H}_n(\widehat{\boldsymbol{\theta}}_n)]^{-1}) A_n(\boldsymbol{\theta})^{(\kappa+1)} d\boldsymbol{\theta} \right|}_{\text{Term 5}}.
 \end{aligned}$$

These correspond to the integral of higher order terms that are not cancelled out by the quadrature process, but also have some peculiarities that we need to exploit or address within the proof. Term 4 contains an exponential term that needs to be bounded, and the behaviour of Term 5 changes depending on the value of κ .

Approximate posterior remainder:

$$\begin{aligned}
 &= \underbrace{\sum_{z \in \mathcal{Q}} \omega(z) \phi(z; 0, \mathbf{I}_p) |A_n(\widehat{\mathbf{L}}_n z + \widehat{\boldsymbol{\theta}}_n)|^{(\kappa+2)} \exp\{|A_n(\widehat{\mathbf{L}}_n z + \widehat{\boldsymbol{\theta}}_n)|\}}_{\text{Term 6}} \\
 &\quad + \underbrace{\left| \sum_{z \in \mathcal{Q}} \omega(z) \phi(z; 0, \mathbf{I}_p) \frac{A_n(\widehat{\mathbf{L}}_n z + \widehat{\boldsymbol{\theta}}_n)^{(\kappa+1)}}{(\kappa+1)!} \right|}_{\text{Term 7}}.
 \end{aligned}$$

These correspond to the numerical summation of the higher order terms that are not cancelled by the quadrature process, but also have some peculiarities that we need to exploit or address within the proof, similar to the ‘‘true posterior terms’’. Term 6 contains an exponential term that needs to be bounded, and the behaviour of Term 7 changes depending on the value of κ . We now handle each of these terms separately.

C.1. Bounding Term 1 of Eq. (21)

For any $i \in [p]$, $j \in [\kappa]$, and $\mathbf{t} \in \tau_{\geq 2k}^{(j)}$,

$$\int_{B_{\widehat{\boldsymbol{\theta}}_n}^p(\gamma_n)} \phi(\boldsymbol{\theta}; \widehat{\boldsymbol{\theta}}_n, [\lambda_p(\mathbf{H}_n(\widehat{\boldsymbol{\theta}}_n))]^{-1} \mathbf{I}_p) |(\boldsymbol{\theta} - \widehat{\boldsymbol{\theta}}_n)_i|^{\tau(\mathbf{t})} d\boldsymbol{\theta} \leq \int_0^{\gamma_n} \phi(\theta; 0, [\lambda_p(\mathbf{H}_n(\widehat{\boldsymbol{\theta}}_n))]^{-1}) |\theta|^{\tau(\mathbf{t})} d\theta.$$

This can be bounded by standard results on the moments of Gaussians. In particular, Eq. (18) of Winkelbauer (2012) gives

$$\begin{aligned}
 & \int_{B_{\hat{\boldsymbol{\theta}}_n}^p(\gamma_n)} \phi(\boldsymbol{\theta}; \hat{\boldsymbol{\theta}}_n, [\lambda_p(\mathbf{H}_n(\hat{\boldsymbol{\theta}}_n))]^{-1} \mathbf{I}_p) |(\boldsymbol{\theta} - \hat{\boldsymbol{\theta}}_n)_i|^{\tau(\mathbf{t})} d\boldsymbol{\theta} \\
 & \leq 2^{\tau(\mathbf{t})/2} \Gamma\left(\frac{\tau(\mathbf{t})+1}{2}\right) [\lambda_p(\mathbf{H}_n(\hat{\boldsymbol{\theta}}_n))]^{-\frac{1}{2}\tau(\mathbf{t})} \\
 & = 2^{\tau(\mathbf{t})/2} \Gamma\left(\frac{\tau(\mathbf{t})+1}{2}\right) (\underline{\eta}_n n)^{-\tau(\mathbf{t})/2} \\
 & \leq 2^{k\kappa} \Gamma\left(\frac{2k\kappa+1}{2}\right) (\underline{\eta}_n n)^{-\tau(\mathbf{t})/2}
 \end{aligned}$$

C.2. Bounding Term 2 of Eq. (21)

For any $i \in [p]$, $j \in [\kappa]$, $\mathbf{t} \in \tau_{\geq 2k}^{(j)}$, and $\mathbf{z} \in \mathcal{Q}$,

$$\left| (\hat{\mathbf{L}}_n \mathbf{z})_i \right|^{\tau(\mathbf{t})} \leq \left[\left\| \hat{\mathbf{L}}_n \right\|_{\text{Op}} \|\mathbf{z}\|_2 \right]^{\tau(\mathbf{t})} \leq \left[[\lambda_p(\mathbf{H}_n(\hat{\boldsymbol{\theta}}_n))]^{-1/2} \|\mathbf{z}\|_2 \right]^{\tau(\mathbf{t})} \leq (\underline{\eta}_n n)^{-\tau(\mathbf{t})/2} \bar{\mathbf{z}}^{\tau(\mathbf{t})}.$$

Thus, since $\sup_{\mathbf{z}} \phi(\mathbf{z}; 0, \mathbf{I}_p) \leq (2\pi)^{-p/2}$ and $|\mathcal{Q}| = k^p$,

$$\sum_{\mathbf{z} \in \mathcal{Q}} \boldsymbol{\omega}(\mathbf{z}) \phi(\mathbf{z}; 0, \mathbf{I}_p) \left| (\hat{\mathbf{L}}_n \mathbf{z})_i \right|^{\tau(\mathbf{t})} \leq (\underline{\eta}_n n)^{-\tau(\mathbf{t})/2} k^p (2\pi)^{-p/2} \bar{\mathbf{z}}^{2k\kappa}$$

C.3. Bounding Term 3 of Eq. (21)

For any $i \in [p]$, $j \in \{0\} \cup [\kappa]$, and $\mathbf{t} \in \tau_{< 2k}^{(j)}$,

$$\begin{aligned}
 & \int_{[B_{\hat{\boldsymbol{\theta}}_n}^p(\gamma_n)]^c} \phi(\boldsymbol{\theta}; \hat{\boldsymbol{\theta}}_n, [\lambda_p(\mathbf{H}_n(\hat{\boldsymbol{\theta}}_n))]^{-1} \mathbf{I}_p) |(\boldsymbol{\theta} - \hat{\boldsymbol{\theta}}_n)_i|^{\tau(\mathbf{t})} d\boldsymbol{\theta} \\
 & = \int_{\gamma_n}^{\infty} \phi(\theta; 0, [\lambda_p(\mathbf{H}_n(\hat{\boldsymbol{\theta}}_n))]^{-1}) |\theta|^{\tau(\mathbf{t})} d\theta \\
 & = [\lambda_p(\mathbf{H}_n(\hat{\boldsymbol{\theta}}_n))]^{-1/2} \int_{\gamma_n \sqrt{\lambda_p(\mathbf{H}_n(\hat{\boldsymbol{\theta}}_n))}}^{\infty} \frac{1}{\sqrt{2\pi}} e^{-v^2/2} |v|^{\tau(\mathbf{t})} dv,
 \end{aligned}$$

where the last step uses the transformation $v = \theta \sqrt{\lambda_p(\mathbf{H}_n(\hat{\boldsymbol{\theta}}_n))}$.

Then, using the further transformation $x = v^2$,

$$\begin{aligned}
 & \int_{\gamma_n \sqrt{\lambda_p(\mathbf{H}_n(\hat{\boldsymbol{\theta}}_n))}}^{\infty} \frac{1}{\sqrt{2\pi}} e^{-v^2/2} |v|^{\tau(\mathbf{t})} dv \\
 & = \int_{\gamma \sqrt{\log(n)\underline{\eta}_n}}^{\infty} \frac{1}{\sqrt{2\pi}} e^{-v^2/2} (v^2)^{\tau(\mathbf{t})/2} dv \\
 & = \frac{1}{2} \int_{\gamma^2 \log(n)\underline{\eta}_n}^{\infty} \frac{x^{-1/2}}{\sqrt{2\pi}} e^{-x/2} x^{\tau(\mathbf{t})/2} dx \\
 & = \frac{\Gamma\left(\frac{\tau(\mathbf{t})+1}{2}\right) 2^{\frac{\tau(\mathbf{t})+1}{2}}}{2\sqrt{2\pi}} \int_{\gamma^2 \log(n)\underline{\eta}_n}^{\infty} \frac{1}{\Gamma\left(\frac{\tau(\mathbf{t})+1}{2}\right) 2^{\frac{\tau(\mathbf{t})+1}{2}}} x^{\frac{\tau(\mathbf{t})+1}{2}-1} e^{-x/2} dx.
 \end{aligned}$$

This integral is just the tail of a chi-square distribution, which we bound using Lemma 3 of Fan and Lv (2008). In particular, for any $\nu \in \mathbb{N}$,

$$\mathbb{P}[\chi_\nu^2 \geq \gamma^2 \log(n) \underline{\eta}_n] = \mathbb{P}\left[\frac{\chi_\nu^2}{\nu} > 1 + \zeta_n\right] \leq \exp\{\nu(\log(1 + \zeta_n) - \zeta_n)/2\},$$

where $\zeta_n = \gamma^2 \log(n) \underline{\eta}_n / \nu - 1$. Substituting in $\nu = \tau(\mathbf{t}) + 1$, observe that

$$\begin{aligned} & \exp\{\nu(\log(1 + \zeta_n) - \zeta_n)/2\} \\ &= \exp\left\{\frac{(\tau(\mathbf{t}) + 1)}{2} \left[\log\left(\frac{\gamma^2 \log(n) \underline{\eta}_n}{\tau(\mathbf{t}) + 1}\right) - \frac{\gamma^2 \log(n) \underline{\eta}_n}{\tau(\mathbf{t}) + 1} + 1\right]\right\} \\ &\leq \exp\left\{\frac{(\tau(\mathbf{t}) + 1)}{2} \left[-\frac{\gamma^2 \log(n) \underline{\eta}_n}{2(\tau(\mathbf{t}) + 1)} + 1\right]\right\} \\ &= e^{(\tau(\mathbf{t})+1)/2} n^{-\gamma^2 \underline{\eta}_n/4}, \end{aligned}$$

where we have used that $\log(x) < x/2$ for all $x > 0$.

Thus,

$$\begin{aligned} & \int_{[B_{\hat{\boldsymbol{\theta}}_n}^p(\gamma_n)]^c} \phi(\boldsymbol{\theta}; \hat{\boldsymbol{\theta}}_n, [\lambda_p(\mathbf{H}_n(\hat{\boldsymbol{\theta}}_n))]^{-1} \mathbf{I}_p) |(\boldsymbol{\theta} - \hat{\boldsymbol{\theta}}_n)_i|^{\tau(\mathbf{t})} d\boldsymbol{\theta} \\ &\leq [\lambda_p(\mathbf{H}_n(\hat{\boldsymbol{\theta}}_n))]^{-1/2} \frac{\Gamma\left(\frac{\tau(\mathbf{t})+1}{2}\right) 2^{\frac{\tau(\mathbf{t})+1}{2}}}{2\sqrt{2\pi}} e^{(d+1)/2} n^{-\gamma^2 \underline{\eta}_n/4} \\ &\leq \frac{\Gamma\left(\frac{2k+1}{2}\right) (2e)^{\frac{2k+1}{2}}}{2\sqrt{2\pi \underline{\eta}_n}} n^{-\frac{\gamma^2 \underline{\eta}_n + 2}{4}}. \end{aligned}$$

C.4. Bounding Term 4 of Eq. (21)

First, we can control $\exp\{|A_n(\boldsymbol{\theta})|\}$ by observing that for any $\boldsymbol{\theta} \in B_{\hat{\boldsymbol{\theta}}_n}^p(\gamma_n)$, the AM-GM inequality gives

$$\begin{aligned} |A_n(\boldsymbol{\theta})| &\leq \sum_{s=3}^{2k-1} \left| (\boldsymbol{\theta} - \hat{\boldsymbol{\theta}}_n)_{[i_1 \dots i_s]}! \partial^{i_1 \dots i_s} \ell_n^\pi(\hat{\boldsymbol{\theta}}_n) \right| + \left| (\boldsymbol{\theta} - \hat{\boldsymbol{\theta}}_n)_{[i_1 \dots i_{2k}]}! \partial^{i_1 \dots i_{2k}} \ell_n^\pi(\hat{\boldsymbol{\theta}}_n) \right| \\ &\leq \widehat{M}_n \sum_{s=3}^{2k} \sum_{i_1, \dots, i_s \in [p]} \prod_{\ell=1}^s |(\boldsymbol{\theta} - \hat{\boldsymbol{\theta}}_n)_{i_\ell}| \\ &\leq \widehat{M}_n \sum_{s=3}^{2k} \sum_{i_1, \dots, i_s \in [p]} \frac{1}{s} \sum_{\ell=1}^s |(\boldsymbol{\theta} - \hat{\boldsymbol{\theta}}_n)_{i_\ell}|^s \\ &\leq \widehat{M}_n p^{2k} \sum_{s=3}^{2k} \gamma_n^s \\ &= \widehat{M}_n p^{2k} \sum_{s=3}^{2k} \gamma^s \left(\frac{\log(n)}{n}\right)^{s/2} \\ &\leq (2k) p^{2k} \max\{1, \gamma^{2k}\} \widehat{M}_n \left(\frac{\log(n)}{n}\right)^{3/2}. \end{aligned}$$

Then, for any $\boldsymbol{\theta} \in B_{\hat{\boldsymbol{\theta}}_n}^p(\gamma_n)$, $|A_n(\boldsymbol{\theta})|^{(\kappa+2)}$ can be written as

$$\begin{aligned} & \sum_{\mathbf{t} \in \tau_{<2k}^{(\kappa+2)}} \mathbb{M}_{\kappa+2, \mathbf{t}} \left\{ \left(\prod_{s=3}^{2k-1} |(\boldsymbol{\theta} - \hat{\boldsymbol{\theta}}_n)_{[i_1 \dots i_s]}! \partial^{i_1 \dots i_s} \ell_n^\pi(\hat{\boldsymbol{\theta}}_n)|^{t_s} \right) |(\boldsymbol{\theta} - \hat{\boldsymbol{\theta}}_n)_{[i_1 \dots i_{2k}]!} \partial^{i_1 \dots i_{2k}} \ell_n^\pi(\hat{\boldsymbol{\theta}}_n^\theta)|^{t_{2k}} \right\} \\ & + \sum_{\mathbf{t} \in \tau_{\geq 2k}^{(\kappa+2)}} \mathbb{M}_{\kappa+2, \mathbf{t}} \left\{ \left(\prod_{s=3}^{2k-1} |(\boldsymbol{\theta} - \hat{\boldsymbol{\theta}}_n)_{[i_1 \dots i_s]}! \partial^{i_1 \dots i_s} \ell_n^\pi(\hat{\boldsymbol{\theta}}_n)|^{t_s} \right) |(\boldsymbol{\theta} - \hat{\boldsymbol{\theta}}_n)_{[i_1 \dots i_{2k}]!} \partial^{i_1 \dots i_{2k}} \ell_n^\pi(\hat{\boldsymbol{\theta}}_n^\theta)|^{t_{2k}} \right\}. \end{aligned}$$

By definition $\sum_{s=3}^{2k} t_s = \kappa + 2$, so it holds that $\sum_{s=3}^{2k} s t_s \geq 3(\kappa + 2)$. Thus, $|A_n(\boldsymbol{\theta})|^{(\kappa+2)}$ can further be written as

$$\sum_{\mathbf{t} \in \tau_{\geq 3(\kappa+2)}^{(\kappa+2)}} \mathbb{M}_{\kappa+2, \mathbf{t}} \left\{ \left(\prod_{s=3}^{2k-1} |(\boldsymbol{\theta} - \hat{\boldsymbol{\theta}}_n)_{[i_1 \dots i_s]}! \partial^{i_1 \dots i_s} \ell_n^\pi(\hat{\boldsymbol{\theta}}_n)|^{t_s} \right) |(\boldsymbol{\theta} - \hat{\boldsymbol{\theta}}_n)_{[i_1 \dots i_{2k}]!} \partial^{i_1 \dots i_{2k}} \ell_n^\pi(\hat{\boldsymbol{\theta}}_n^\theta)|^{t_{2k}} \right\}.$$

As before, since $\boldsymbol{\theta} \in B_{\hat{\boldsymbol{\theta}}_n}^p(\gamma_n)$ all derivatives of ℓ_n^π are bounded by \widehat{M}_n . Similarly, the resulting polynomial in $\boldsymbol{\theta}$ can be bounded again using the AM-GM inequality, so

$$\begin{aligned} & \int_{B_{\hat{\boldsymbol{\theta}}_n}^p(\gamma_n)} \phi(\boldsymbol{\theta}; \hat{\boldsymbol{\theta}}_n, [\lambda_p(\mathbf{H}_n(\hat{\boldsymbol{\theta}}_n))]^{-1} \mathbf{I}_p) |A_n(\boldsymbol{\theta})|^{(\kappa+2)} d\boldsymbol{\theta} \\ & \leq (\widehat{M}_n)^{\kappa+2} \sum_{\mathbf{t} \in \tau_{\geq 3(\kappa+2)}^{(\kappa+2)}} \frac{\mathbb{M}_{\kappa+2, \mathbf{t}}}{3(\kappa+2)} \sum_{i_1, \dots, i_{\tau(\mathbf{t})} \in [p]} \sum_{\ell=1}^{\tau(\mathbf{t})} \int_{B_{\hat{\boldsymbol{\theta}}_n}^p(\gamma_n)} \phi(\boldsymbol{\theta}; \hat{\boldsymbol{\theta}}_n, [\lambda_p(\mathbf{H}_n(\hat{\boldsymbol{\theta}}_n))]^{-1} \mathbf{I}_p) |(\boldsymbol{\theta} - \hat{\boldsymbol{\theta}}_n)_i|^{\tau(\mathbf{t})} d\boldsymbol{\theta} \\ & \leq (\widehat{M}_n)^{\kappa+2} \sum_{\mathbf{t} \in \tau_{\geq 3(\kappa+2)}^{(\kappa+2)}} \frac{\mathbb{M}_{\kappa+2, \mathbf{t}}}{3(\kappa+2)} \sum_{i_1, \dots, i_{\tau(\mathbf{t})} \in [p]} \sum_{\ell=1}^{\tau(\mathbf{t})} 2^{\tau(\mathbf{t})/2} \Gamma\left(\frac{\tau(\mathbf{t})+1}{2}\right) (\underline{\eta}_n n)^{-\tau(\mathbf{t})/2} \\ & \leq (\widehat{M}_n)^{\kappa+2} \sum_{\mathbf{t} \in \tau_{\geq 3(\kappa+2)}^{(\kappa+2)}} \frac{\mathbb{M}_{\kappa+2, \mathbf{t}}}{3(\kappa+2)} p^{2k\kappa} (2k\kappa) 2^{k\kappa} \Gamma\left(\frac{2k\kappa+1}{2}\right) (\underline{\eta}_n n)^{-\tau(\mathbf{t})/2}, \end{aligned}$$

where we have again used Eq. (18) of Winkelbauer (2012).

C.5. Bounding Term 5 of Eq. (21)

In the case that $2k \not\equiv 2 \pmod{3}$, this term can be treated in the same manner as in Appendix C.4. In particular,

$$\begin{aligned} & \left| \int_{B_{\hat{\boldsymbol{\theta}}_n}^p(\gamma_n)} \phi(\boldsymbol{\theta}; \hat{\boldsymbol{\theta}}_n, [\mathbf{H}_n(\hat{\boldsymbol{\theta}}_n)]^{-1}) A_n(\boldsymbol{\theta})^{(\kappa+1)} d\boldsymbol{\theta} \right| \\ & \leq \left(\frac{\overline{\eta}_n}{\underline{\eta}_n} \right)^{p/2} (\widehat{M}_n)^{\kappa+1} \sum_{\mathbf{t} \in \tau_{\geq 3(\kappa+1)}^{(\kappa+1)}} \frac{\mathbb{M}_{\kappa+1, \mathbf{t}}}{3(\kappa+1)} p^{2k\kappa} (2k\kappa) 2^{k\kappa} \Gamma\left(\frac{2k\kappa+1}{2}\right) (\underline{\eta}_n n)^{-\tau(\mathbf{t})/2}. \end{aligned}$$

However, in the case that $2k = 2 \pmod{3}$, $3(\kappa + 1) = 2k + 1$, and we write $A_n(\boldsymbol{\theta})^{(\kappa+1)}$ as

$$\begin{aligned} & \sum_{\mathbf{t} \in \tau_{=3(\kappa+1)}^{(\kappa+1)}} \mathbb{M}_{\kappa+1, \mathbf{t}} \left\{ \left(\prod_{s=3}^{2k-1} \left((\boldsymbol{\theta} - \widehat{\boldsymbol{\theta}}_n)_{[i_1 \dots i_s]}! \partial^{i_1 \dots i_s} \ell_n^\pi(\widehat{\boldsymbol{\theta}}_n) \right)^{t_s} \right) \left((\boldsymbol{\theta} - \widehat{\boldsymbol{\theta}}_n)_{[i_1 \dots i_{2k}]}! \partial^{i_1 \dots i_{2k}} \ell_n^\pi(\widehat{\boldsymbol{\theta}}_n) \right)^{t_{2k}} \right\} \\ & + \sum_{\mathbf{t} \in \tau_{\geq 3(\kappa+1)+1}^{(\kappa+1)}} \mathbb{M}_{\kappa+1, \mathbf{t}} \left\{ \left(\prod_{s=3}^{2k-1} \left((\boldsymbol{\theta} - \widehat{\boldsymbol{\theta}}_n)_{[i_1 \dots i_s]}! \partial^{i_1 \dots i_s} \ell_n^\pi(\widehat{\boldsymbol{\theta}}_n) \right)^{t_s} \right) \left((\boldsymbol{\theta} - \widehat{\boldsymbol{\theta}}_n)_{[i_1 \dots i_{2k}]}! \partial^{i_1 \dots i_{2k}} \ell_n^\pi(\widehat{\boldsymbol{\theta}}_n) \right)^{t_{2k}} \right\}. \end{aligned} \quad (22)$$

For the first of these terms, note that since $2k = 3(\kappa + 1) - 1 > \kappa + 1$, $t_{2k} = 0$. Further, by the symmetry of the multivariate normal distribution and the fact that $3(\kappa + 1)$ is odd,

$$\int_{B_{\widehat{\boldsymbol{\theta}}_n}^p(\gamma_n)} \phi(\boldsymbol{\theta}; \widehat{\boldsymbol{\theta}}_n, [\mathbf{H}_n(\widehat{\boldsymbol{\theta}}_n)]^{-1}) \sum_{\mathbf{t} \in \tau_{=3(\kappa+1)}^{(\kappa+1)}} \mathbb{M}_{\kappa+1, \mathbf{t}} \left(\prod_{s=3}^{2k-1} \left((\boldsymbol{\theta} - \widehat{\boldsymbol{\theta}}_n)_{[i_1 \dots i_s]}! \partial^{i_1 \dots i_s} \ell_n^\pi(\widehat{\boldsymbol{\theta}}_n) \right)^{t_s} \right) d\boldsymbol{\theta} = 0.$$

Thus, in this case the magnitude of Term 5 can be instead bounded by the second term in Eq. (22), giving

$$\begin{aligned} & \left| \int_{B_{\widehat{\boldsymbol{\theta}}_n}^p(\gamma_n)} \phi(\boldsymbol{\theta}; \widehat{\boldsymbol{\theta}}_n, [\mathbf{H}_n(\widehat{\boldsymbol{\theta}}_n)]^{-1}) A_n(\boldsymbol{\theta})^{(\kappa+1)} d\boldsymbol{\theta} \right| \\ & \leq \left(\frac{\underline{\eta}_n}{\overline{\eta}_n} \right)^{p/2} (\widehat{M}_n)^{\kappa+1} \sum_{\mathbf{t} \in \tau_{\geq 3(\kappa+1)+1}^{(\kappa+1)}} \frac{\mathbb{M}_{\kappa+1, \mathbf{t}}}{3(\kappa + 1) + 1} p^{2k\kappa} (2k\kappa) 2^{k\kappa} \Gamma\left(\frac{2k\kappa + 1}{2}\right) (\underline{\eta}_n n)^{-\tau(\mathbf{t})/2}, \end{aligned}$$

where we have once again applied the same argument as in Appendix C.4.

C.6. Bounding Term 6 of Eq. (21)

By the same argument for bounding $\exp\{|A_n(\boldsymbol{\theta})|\}$ that we used in Appendix C.4, for all $\mathbf{z} \in \mathcal{Q}$ it holds that

$$\begin{aligned} \left| A_n(\widehat{\mathbf{L}}_n \mathbf{z} + \widehat{\boldsymbol{\theta}}_n) \right| & \leq \widehat{M}_n \sum_{s=3}^{2k} \sum_{i_1, \dots, i_s \in [p]} \frac{1}{s} \sum_{\iota=1}^s \left| (\widehat{\mathbf{L}}_n \mathbf{z})_{i_\iota} \right|^s \\ & \leq \widehat{M}_n p^{2k} \sum_{s=3}^{2k} (\underline{\eta}_n n)^{-s/2} \overline{\mathbf{z}}^s \\ & \leq (2k) p^{2k} \max\{1, \overline{\mathbf{z}}^{2k}\} \widehat{M}_n \max\{(\underline{\eta}_n n)^{-3/2}, (\underline{\eta}_n n)^{-k}\}. \end{aligned}$$

Similarly, by the same argument for bounding $|A_n(\boldsymbol{\theta})|^{\kappa+2}$ that we used in Appendix C.4,

$$\begin{aligned}
 & \sum_{\mathbf{z} \in \mathcal{Q}} \boldsymbol{\omega}(\mathbf{z}) \phi(\mathbf{z}; 0, \mathbf{I}_p) \left| A_n(\widehat{\mathbf{L}}_n \mathbf{z} + \widehat{\boldsymbol{\theta}}_n) \right|^{\kappa+2} \\
 & \leq (\widehat{M}_n)^{\kappa+2} \sum_{t \in \tau_{\geq 3(\kappa+2)}^{(\kappa+2)}} \frac{\mathbb{M}_{\kappa+2,t}}{3(\kappa+2)} \sum_{i_1, \dots, i_{\tau(t)} \in [p]} \sum_{\ell=1}^{\tau(t)} \sum_{\mathbf{z} \in \mathcal{Q}} \boldsymbol{\omega}(\mathbf{z}) \phi(\mathbf{z}; 0, \mathbf{I}_p) \left| (\widehat{\mathbf{L}}_n \mathbf{z})_{i_\ell} \right|^{\tau(t)} \\
 & \leq (\widehat{M}_n)^{\kappa+2} \sum_{t \in \tau_{\geq 3(\kappa+2)}^{(\kappa+2)}} \frac{\mathbb{M}_{\kappa+2,t}}{3(\kappa+2)} p^{2k\kappa} (2k\kappa) (\underline{\eta}_n n)^{-\tau(t)/2} k^p (2\pi)^{-p/2} \bar{\mathbf{z}}^{2k\kappa},
 \end{aligned}$$

where the last step uses the bound of Appendix C.2.

C.7. Bounding Term 7 of Eq. (21)

We handle this term using a similar logical argument to Appendix C.5. In the case that $2k \not\equiv 2 \pmod{3}$, this term can be treated in the same manner as Appendix C.6, giving

$$\begin{aligned}
 & \left| \sum_{\mathbf{z} \in \mathcal{Q}} \boldsymbol{\omega}(\mathbf{z}) \phi(\mathbf{z}; 0, \mathbf{I}_p) \frac{A_n(\widehat{\mathbf{L}}_n \mathbf{z} + \widehat{\boldsymbol{\theta}}_n)^{(\kappa+1)}}{(\kappa+1)!} \right| \\
 & \leq (\widehat{M}_n)^{\kappa+1} \sum_{t \in \tau_{\geq 3(\kappa+1)}^{(\kappa+1)}} \frac{\mathbb{M}_{\kappa+1,t}}{3(\kappa+1)} p^{2k\kappa} (2k\kappa) (\underline{\eta}_n n)^{-\tau(t)/2} k^p (2\pi)^{-p/2} \bar{\mathbf{z}}^{2k\kappa}.
 \end{aligned}$$

However, in the case that $2k \equiv 2 \pmod{3}$, we split $A_n(\widehat{\mathbf{L}}_n \mathbf{z} + \widehat{\boldsymbol{\theta}}_n)^{(\kappa+1)}$ in the same manner as in Eq. (22). Namely, since $\mathfrak{R}(\mathcal{Q}, \boldsymbol{\omega})$ is symmetric, $\phi(\mathbf{z}; 0, \mathbf{I}_p)$ is symmetric around zero, and $3(\kappa+1)$ is odd,

$$\sum_{\mathbf{z} \in \mathcal{Q}} \boldsymbol{\omega}(\mathbf{z}) \phi(\mathbf{z}; 0, \mathbf{I}_p) \sum_{t \in \tau_{=3(\kappa+1)}^{(\kappa+1)}} \mathbb{M}_{\kappa+1,t} \left(\prod_{s=3}^{2k-1} \left((\widehat{\mathbf{L}}_n \mathbf{z})_{[i_1 \dots i_s]} \partial^{i_1 \dots i_s} \rho_n^\pi(\widehat{\boldsymbol{\theta}}_n) \right)^{t_s} \right) = 0.$$

That is, in this case

$$\begin{aligned}
 & \left| \sum_{\mathbf{z} \in \mathcal{Q}} \boldsymbol{\omega}(\mathbf{z}) \phi(\mathbf{z}; 0, \mathbf{I}_p) \frac{A_n(\widehat{\mathbf{L}}_n \mathbf{z} + \widehat{\boldsymbol{\theta}}_n)^{(\kappa+1)}}{(\kappa+1)!} \right| \\
 & \leq (\widehat{M}_n)^{\kappa+1} \sum_{t \in \tau_{\geq 3(\kappa+1)+1}^{(\kappa+1)}} \frac{\mathbb{M}_{\kappa+1,t}}{3(\kappa+1)+1} p^{2k\kappa} (2k\kappa) (\underline{\eta}_n n)^{-\tau(t)/2} k^p (2\pi)^{-p/2} \bar{\mathbf{z}}^{2k\kappa}.
 \end{aligned}$$

C.8. Combining the Bounds on Eq. (21)

We now combine the results of Appendices C.1 to C.7 and apply them to Eq. (21). We group the terms slightly more compactly than in Eq. (21) to summarize this, grouping them by bounds on the summation or integration of high-degree polynomials, bounds on the tails of low-degree

polynomials, and bounds on the summation or integration of high-degree polynomials involving a remainder of the expansion of the exponential function. Consider,

Term 1 + Term 2 + Term 5 + Term 7

$$\begin{aligned}
 &= \left(\frac{\overline{\eta}_n}{\underline{\eta}_n}\right)^{p/2} \sum_{j=1}^{\kappa} (\widehat{M}_n)^j \sum_{t \in \tau_{\geq 2k}^{(j)}} \frac{\mathbb{M}_{j,t}}{2k} p^{2k\kappa} (2k\kappa) 2^{k\kappa} \Gamma\left(\frac{2k\kappa+1}{2}\right) (\underline{\eta}_n n)^{-\tau(t)/2} \\
 &\quad + \left(\frac{\overline{\eta}_n}{\underline{\eta}_n}\right)^{p/2} (\widehat{M}_n)^{\kappa+1} \sum_{t \in \tau_{\geq 3(\kappa+1)+\mathbb{I}\{2k=2 \pmod{3}\}}^{(\kappa+1)}} \frac{\mathbb{M}_{\kappa+1,t}}{3(\kappa+1)} p^{2k\kappa} (2k\kappa) 2^{k\kappa} \Gamma\left(\frac{2k\kappa+1}{2}\right) (\underline{\eta}_n n)^{-\tau(t)/2} \\
 &\quad + \sum_{j=1}^{\kappa} (\widehat{M}_n)^j \sum_{t \in \tau_{\geq 2k}^{(j)}} \frac{\mathbb{M}_{j,t}}{2k} p^{2k\kappa} (2k\kappa) (\underline{\eta}_n n)^{-\tau(t)/2} k^p (2\pi)^{-p/2} \underline{z}^{2k\kappa} \\
 &\quad + (\widehat{M}_n)^{\kappa+1} \sum_{t \in \tau_{\geq 3(\kappa+1)+\mathbb{I}\{2k=2 \pmod{3}\}}^{(\kappa+1)}} \frac{\mathbb{M}_{\kappa+1,t}}{3(\kappa+1)} p^{2k\kappa} (2k\kappa) (\underline{\eta}_n n)^{-\tau(t)/2} k^p (2\pi)^{-p/2} \underline{z}^{2k\kappa},
 \end{aligned}$$

which can be upper bounded by:

$$\begin{aligned}
 &\leq p^{2k\kappa} \kappa \left[\left(\frac{\overline{\eta}_n}{\underline{\eta}_n}\right)^{p/2} 2^{k\kappa} \Gamma\left(\frac{2k\kappa+1}{2}\right) + k^p (2\pi)^{-p/2} \underline{z}^{2k\kappa} \right] \\
 &\quad \times \left[\sum_{j=1}^{\kappa} (\widehat{M}_n)^j \sum_{t \in \tau_{\geq 2k}^{(j)}} \mathbb{M}_{j,t} (\underline{\eta}_n n)^{-\tau(t)/2} + (\widehat{M}_n)^{\kappa+1} \sum_{t \in \tau_{\geq 3(\kappa+1)+\mathbb{I}\{2k=2 \pmod{3}\}}^{(\kappa+1)}} \mathbb{M}_{\kappa+1,t} (\underline{\eta}_n n)^{-\tau(t)/2} \right].
 \end{aligned} \tag{23}$$

Additionally

$$\text{Term 3} = \left(\frac{\overline{\eta}_n}{\underline{\eta}_n}\right)^{p/2} \sum_{j=0}^{\kappa} (\widehat{M}_n)^j \sum_{t \in \tau_{< 2k}^{(j)}} \mathbb{M}_{j,t} p^{2k\kappa} (2k\kappa) \frac{\Gamma\left(\frac{2k+1}{2}\right) (2e)^{\frac{2k+1}{2}}}{2\sqrt{2\pi\eta_n}} n^{-\frac{\gamma^2 \eta_n + 2}{4}}. \tag{24}$$

Finally,

Term 4 + Term 6

$$\begin{aligned}
 &= \left(\frac{\overline{\eta}_n}{\underline{\eta}_n}\right)^{p/2} \exp \left\{ (2k) p^{2k} \max\{1, \gamma^{2k}\} \widehat{M}_n \left(\frac{\log(n)}{n}\right)^{3/2} \right\} \\
 &\quad \times (\widehat{M}_n)^{\kappa+2} \sum_{t \in \tau_{\geq 3(\kappa+2)}^{(\kappa+2)}} \frac{\mathbb{M}_{\kappa+2,t}}{3(\kappa+2)} p^{2k\kappa} (2k\kappa) 2^{k\kappa} \Gamma\left(\frac{2k\kappa+1}{2}\right) (\underline{\eta}_n n)^{-\tau(t)/2} \\
 &\quad + \exp \left\{ (2k) p^{2k} \max\{1, \underline{z}^{2k}\} \widehat{M}_n \max\{(\underline{\eta}_n n)^{-3/2}, (\underline{\eta}_n n)^{-k}\} \right\} \\
 &\quad \times (\widehat{M}_n)^{\kappa+2} \sum_{t \in \tau_{\geq 3(\kappa+2)}^{(\kappa+2)}} \frac{\mathbb{M}_{\kappa+2,t}}{3(\kappa+2)} p^{2k\kappa} (2k\kappa) (\underline{\eta}_n n)^{-\tau(t)/2} k^p (2\pi)^{-p/2} \underline{z}^{2k\kappa},
 \end{aligned}$$

which can be upper bounded by:

$$\begin{aligned} &\leq \left[\left(\frac{\overline{\eta}_n}{\underline{\eta}_n} \right)^{p/2} 2^{k\kappa} \Gamma \left(\frac{2k\kappa + 1}{2} \right) \exp \left\{ (2k) p^{2k} \max\{1, \gamma^{2k}\} \widehat{M}_n \left(\frac{\log(n)}{n} \right)^{3/2} \right\} \right. \\ &\quad \left. + k^p (2\pi)^{-p/2} \overline{\mathbf{z}}^{2k\kappa} \exp \left\{ (2k) p^{2k} \max\{1, \overline{\mathbf{z}}^{2k}\} \widehat{M}_n \max \left\{ (\underline{\eta}_n n)^{-3/2}, (\underline{\eta}_n n)^{-k} \right\} \right\} \right] \quad (25) \\ &\times (\widehat{M}_n)^{\kappa+2} \sum_{\substack{t \in \tau_{\geq 3(\kappa+2)}^{(\kappa+2)}}} \mathbb{M}_{\kappa+2,t} p^{2k\kappa} \kappa (\underline{\eta}_n n)^{-\tau(t)/2}. \end{aligned}$$

Combining Eqs. (23) to (25), we obtain the final inequality

$$\begin{aligned} &\left| \int_{B_{\widehat{\boldsymbol{\theta}}_n}^p(\gamma_n)} \phi(\boldsymbol{\theta}; \widehat{\boldsymbol{\theta}}_n, [\mathbf{H}_n(\widehat{\boldsymbol{\theta}}_n)]^{-1}) \exp \{A_n(\boldsymbol{\theta})\} d\boldsymbol{\theta} - \sum_{\mathbf{z} \in \mathcal{Q}} \omega(\mathbf{z}) \phi(\mathbf{z}; 0, \mathbf{I}_p) \exp \left\{ A_n \left(\widehat{\mathbf{L}}_n \mathbf{z} + \widehat{\boldsymbol{\theta}}_n \right) \right\} \right| \\ &\leq p^{2k\kappa} \kappa \left[\left(\frac{\overline{\eta}_n}{\underline{\eta}_n} \right)^{p/2} 2^{k\kappa} \Gamma \left(\frac{2k\kappa + 1}{2} \right) + k^p (2\pi)^{-p/2} \overline{\mathbf{z}}^{2k\kappa} \right] \\ &\quad \times \left[\sum_{j=1}^{\kappa} (\widehat{M}_n)^j \sum_{t \in \tau_{\geq 2k}^{(j)}} \mathbb{M}_{j,t} (\underline{\eta}_n n)^{-\tau(t)/2} + (\widehat{M}_n)^{\kappa+1} \sum_{t \in \tau_{\geq 3(\kappa+1)+\mathbb{I}\{2k=2 \pmod{3}\}}^{(\kappa+1)}} \mathbb{M}_{\kappa+1,t} (\underline{\eta}_n n)^{-\tau(t)/2} \right] \\ &\quad + \left(\frac{\overline{\eta}_n}{\underline{\eta}_n} \right)^{p/2} \sum_{j=0}^{\kappa} (\widehat{M}_n)^j \sum_{t \in \tau_{< 2k}^{(j)}} \mathbb{M}_{j,t} p^{2k\kappa} (2k\kappa) \frac{\Gamma \left(\frac{2k+1}{2} \right) (2e)^{\frac{2k+1}{2}}}{2\sqrt{2\pi\underline{\eta}_n}} n^{-\frac{\gamma^2 \underline{\eta}_n + 2}{4}} \\ &\quad + \left[\left(\frac{\overline{\eta}_n}{\underline{\eta}_n} \right)^{p/2} 2^{k\kappa} \Gamma \left(\frac{2k\kappa + 1}{2} \right) \exp \left\{ (2k) p^{2k} \max\{1, \gamma^{2k}\} \widehat{M}_n \left(\frac{\log(n)}{n} \right)^{3/2} \right\} \right. \\ &\quad \left. + k^p (2\pi)^{-p/2} \overline{\mathbf{z}}^{2k\kappa} \exp \left\{ (2k) p^{2k} \max\{1, \overline{\mathbf{z}}^{2k}\} \widehat{M}_n \max \left\{ (\underline{\eta}_n n)^{-3/2}, (\underline{\eta}_n n)^{-k} \right\} \right\} \right] \\ &\quad \times (\widehat{M}_n)^{\kappa+2} \sum_{\substack{t \in \tau_{\geq 3(\kappa+2)}^{(\kappa+2)}}} \mathbb{M}_{\kappa+2,t} p^{2k\kappa} \kappa (\underline{\eta}_n n)^{-\tau(t)/2}. \end{aligned}$$

The statement of the lemma then follows by taking the worst-case choices of the sum indices for the constants, which all depend combinatorially on only p and k . Additionally, the statement of the lemma includes the dependence on $|\widehat{\mathbf{L}}_n| \leq [\lambda_p(\mathbf{H}_n(\widehat{\boldsymbol{\theta}}_n))]^{-p/2} = (\underline{\eta}_n n)^{-p/2}$ that was dropped after Eq. (17).

C.9. Laplace Approximation Proof ($k = 1$)

When $k = 1$ the argument follows nearly identically. The primary difference is that for Eq. (11) we use a fourth-order rather than second-order initial Taylor expansion. The proof then follows through as though $k = 2$ for the expansions, although the terms of Eq. (21) are slightly different. By definition, $\kappa = 0$, so Terms 1 and 2 no longer appear. Further, the only valid t for Term

3 is all zeros since $j = 0$, and the empty sum cancels with $1/\tau(\mathbf{t})$, leaving only the tail of a multivariate Normal. The bound used to control this in Appendix C.3 then still applies, recalling that while we have expanded as though $k = 2$, we still actually have $k = 1$. Terms 4, 5, 6, and 7 are treated in exactly the same way. \square

D. Proofs of Convergence Rates for Approximate Posterior Summaries

D.1. Proofs for Exact Integration of Approximate Posterior

As mentioned in Section 3, in the idealized situation where one can exactly integrate the approximate posterior, the convergence rate of Theorem 1 is preserved without additional assumptions. We now describe summary statistics of interest and prove this is the case. Of particular interest is credible set coverage and quantiles, since these require integration over a subset of the parameter space, and consequently the results of Section 3.2 do not apply. For details on how these quantities are computed in practice (for which it remains open to prove convergence rates), see Appendix E.

First, letting $\mathcal{B}(\mathbb{R}^p)$ denote the Borel sets on \mathbb{R}^p , a *credible function* is any function $\mathcal{K} : \mathbb{R}^{n \times d} \times [0, 1] \rightarrow \mathcal{B}(\mathbb{R}^p)$ such that for all datasets $\mathbf{Y}^{(n)}$ and $\alpha \in [0, 1]$,

$$\int_{\mathcal{K}(\mathbf{Y}^{(n)}, \alpha)} \pi(\boldsymbol{\theta} \mid \mathbf{Y}^{(n)}) d\boldsymbol{\theta} = \alpha.$$

When $\mathbf{Y}^{(n)}$ is clear, we denote $\mathcal{K}(\mathbf{Y}^{(n)}, \alpha)$ by $\mathcal{K}_n(\alpha)$, and call the output an α -*credible set*. Beyond generic credible sets, we are also interested in the *marginal posterior quantiles*. For $j \in [p] = \{1, \dots, p\}$, the *marginal posterior* evaluated at $\theta \in \mathbb{R}$ is

$$\pi^{(j)}(\theta \mid \mathbf{Y}^{(n)}) = \int_{\mathbb{R}^{p-1}} \pi(\theta_1, \dots, \theta_{j-1}, \theta, \theta_{j+1}, \dots, \theta_p \mid \mathbf{Y}^{(n)}) d\boldsymbol{\theta}_{-j},$$

and we denote its CDF by $F_n^{(j)}(x)$. Further, the *pseudo-inverse* of the marginal posterior CDF is defined in the usual way for $y \in [0, 1]$ by

$$[F_n^{(j)}]^{-1}(y) = \inf \{x \in \mathbb{R} \mid F_n^{(j)}(x) \geq y\}.$$

Then, for any $j \in [p]$ and $\alpha \in [0, 1]$, the marginal posterior quantile is $q_n^{(j)}(\alpha) = [F_n^{(j)}]^{-1}(\alpha)$. The posterior median $q_n^{(j)}(0.5)$ is often used as a point estimate of θ_j^* , and the 95% posterior credible interval $(q_n^{(j)}(0.025), q_n^{(j)}(0.975))$ is often used as a measure of uncertainty for this estimate. In addition to credible intervals, it is of interest to compute posterior moments, defined for any measurable function $g : \Theta \rightarrow \mathbb{R}$ by $\mathbb{E}[g(\boldsymbol{\theta}) \mid \mathbf{Y}^{(n)}] = \int_{\Theta} g(\boldsymbol{\theta}) \pi(\boldsymbol{\theta} \mid \mathbf{Y}^{(n)}) d\boldsymbol{\theta}$.

Using the accent \checkmark to denote exact integration of any approximate posterior $\tilde{\pi}(\boldsymbol{\theta} \mid \mathbf{Y}^{(n)})$, an *approximate credible function* $\check{\mathcal{K}}$ is analogous to a credible function that satisfies

$$\int_{\check{\mathcal{K}}(\mathbf{Y}^{(n)}, \alpha)} \tilde{\pi}(\boldsymbol{\theta} \mid \mathbf{Y}^{(n)}) d\boldsymbol{\theta} = \alpha.$$

Similarly,

$$\check{\pi}^{(j)}(\boldsymbol{\theta} | \mathbf{Y}^{(n)}) = \int_{\mathbb{R}^{p-1}} \tilde{\pi}(\theta_1, \dots, \theta_{j-1}, \theta, \theta_{j+1}, \dots, \theta_p | \mathbf{Y}^{(n)}) d\boldsymbol{\theta}_{-j},$$

and $\check{F}_n^{(j)}(\cdot)$, $[\check{F}_n^{(j)}]^{-1}(\cdot)$, and $\check{q}_n^{(j)}(\cdot)$ are defined using $\check{\pi}^{(j)}(\cdot | \mathbf{Y}^{(n)})$. Finally, define $\check{\mathbb{E}}[g(\boldsymbol{\theta}) | \mathbf{Y}^{(n)}] = \int_{\Theta} g(\boldsymbol{\theta}) \tilde{\pi}(\boldsymbol{\theta} | \mathbf{Y}^{(n)}) d\boldsymbol{\theta}$.

Corollary 4. *If $\tilde{\pi}(\boldsymbol{\theta} | \mathbf{Y}^{(n)})$ satisfies the conditions of Theorem 1,*

i) *For any $\check{\mathcal{K}}$,*

$$\lim_{n \rightarrow \infty} \mathbb{P}_n^* \left(\sup_{\alpha \in [0,1]} \left| \int_{\check{\mathcal{K}}_n(\alpha)} \pi(\boldsymbol{\theta} | \mathbf{Y}^{(n)}) d\boldsymbol{\theta} - \alpha \right| \leq C n^{-\lfloor \frac{k+2}{3} \rfloor} \right) = 1.$$

ii) *For all $L > 0$,*

$$\lim_{n \rightarrow \infty} \mathbb{P}_n^* \left(\sup_{j \in [p], \alpha \in [0,1]} \left\{ \left| \check{q}_n^{(j)}(\alpha) - q_n^{(j)}(\alpha) \right| \text{ s.t. } \pi^{(j)}(q_n^{(j)}(\alpha) | \mathbf{Y}^{(n)}) \geq L \right\} \leq \frac{2C}{L} n^{-\lfloor \frac{k+2}{3} \rfloor} \right) = 1.$$

iii) *For all measurable $g : \Theta \rightarrow \mathbb{R}$ with $\mathbb{E}[g(\boldsymbol{\theta}) | \mathbf{Y}^{(n)}] < \infty$ a.s.,*

$$\lim_{n \rightarrow \infty} \mathbb{P}_n^* \left(\left| \frac{\mathbb{E}[g(\boldsymbol{\theta}) | \mathbf{Y}^{(n)}]}{\check{\mathbb{E}}[g(\boldsymbol{\theta}) | \mathbf{Y}^{(n)}]} - 1 \right| \leq C n^{-\lfloor \frac{k+2}{3} \rfloor} \right) = 1.$$

Remark 6. *Corollary 4 ii) quantifies the notion that approximating quantiles in regions where the posterior cumulative distribution function is very flat is more difficult than regions where it is steep, which is seen in typical applications. \triangleleft*

Proof of Corollary 4. i) For each n ,

$$\begin{aligned} & \mathbb{P}_n^* \left(\sup_{\alpha \in [0,1]} \left| \int_{\check{\mathcal{K}}_n(\alpha)} \pi(\boldsymbol{\theta} | \mathbf{Y}^{(n)}) d\boldsymbol{\theta} - \alpha \right| \leq C n^{-\lfloor \frac{k+2}{3} \rfloor} \right) \\ & \geq \mathbb{P}_n^* \left(\sup_{\alpha \in [0,1]} \sup_{\boldsymbol{\theta}' \in \Theta} \left| \frac{\pi(\boldsymbol{\theta}' | \mathbf{Y}^{(n)})}{\tilde{\pi}_{(\mathcal{Q}, \boldsymbol{\omega})}^{\mathcal{A}}(\boldsymbol{\theta}' | \mathbf{Y}^{(n)})} \int_{\check{\mathcal{K}}_n(\alpha)} \tilde{\pi}_{(\mathcal{Q}, \boldsymbol{\omega})}^{\mathcal{A}}(\boldsymbol{\theta} | \mathbf{Y}^{(n)}) d\boldsymbol{\theta} - \alpha \right| \leq C n^{-\lfloor \frac{k+2}{3} \rfloor} \right) \\ & = \mathbb{P}_n^* \left(\sup_{\alpha \in [0,1]} \alpha \sup_{\boldsymbol{\theta}' \in \Theta} \left| \frac{\pi(\boldsymbol{\theta}' | \mathbf{Y}^{(n)})}{\tilde{\pi}_{(\mathcal{Q}, \boldsymbol{\omega})}^{\mathcal{A}}(\boldsymbol{\theta}' | \mathbf{Y}^{(n)})} - 1 \right| \leq C n^{-\lfloor \frac{k+2}{3} \rfloor} \right) \\ & = \mathbb{P}_n^* \left(\sup_{\boldsymbol{\theta}' \in \Theta} \left| \frac{\pi(\boldsymbol{\theta}' | \mathbf{Y}^{(n)})}{\tilde{\pi}_{(\mathcal{Q}, \boldsymbol{\omega})}^{\mathcal{A}}(\boldsymbol{\theta}' | \mathbf{Y}^{(n)})} - 1 \right| \leq C n^{-\lfloor \frac{k+2}{3} \rfloor} \right). \end{aligned}$$

The results follows since the RHS tends to 1 as $n \rightarrow \infty$ by applying Lemma 1 to Corollary 1.

ii) Fix n , and let $B_{n,k} = C n^{-\lfloor \frac{k+2}{3} \rfloor}$, where C is the constant from Theorem 1. Suppose that $\left\| \pi(\cdot | \mathbf{Y}^{(n)}) - \tilde{\pi}_{(\mathcal{Q}, \boldsymbol{\omega})}^{\mathcal{A}}(\cdot | \mathbf{Y}^{(n)}) \right\|_{\text{TV}} \leq B_{n,k}$. By smoothness conditions, $\frac{d}{dq} F_n^{(j)}(q) = \pi^{(j)}(q | \mathbf{Y}^{(n)})$ for every $j \in [p]$. Consider $j \in [p]$ and $\alpha \in [0, 1]$ such that

$$\pi^{(j)}(q_n^{(j)}(\alpha) | \mathbf{Y}^{(n)}) \geq L.$$

This implies that

$$\frac{d}{dy}[F_n^{(j)}]^{-1}(y)\Big|_{\alpha} \leq 1/L,$$

so

$$[F_n^{(j)}]^{-1}(\alpha) - [F_n^{(j)}]^{-1}(\alpha - B_{n,k}) \leq B_{n,k}/L.$$

Choose an arbitrary y (which we have just guaranteed exists) such that $[F_n^{(j)}]^{-1}(\alpha) - 2B_{n,k}/L < y < [F_n^{(j)}]^{-1}(\alpha - B_{n,k})$. This implies that $F_n^{(j)}(y) < \alpha - B_{n,k}$, which implies that $\check{F}_n^{(j)}(y) < \alpha$, and thus $[\check{F}_n^{(j)}]^{-1}(\alpha) \geq y$. That is, $[F_n^{(j)}]^{-1}(\alpha) - [\check{F}_n^{(j)}]^{-1}(\alpha) \leq 2B_{n,k}/L$. The reverse direction follows by exactly the same logic, giving $|q_n^{(j)}(\alpha) - \check{q}_n^{(j)}(\alpha)| = |[F_n^{(j)}]^{-1}(\alpha) - [\check{F}_n^{(j)}]^{-1}(\alpha)| \leq 2B_{n,k}/L$.

Putting this together gives

$$\begin{aligned} & \lim_{n \rightarrow \infty} \mathbb{P}_n^* \left(\sup_{j \in [p], \alpha \in [0,1]} \left\{ \left| \check{q}_n^{(j)}(\alpha) - q_n^{(j)}(\alpha) \right| \text{ s.t. } \pi^{(j)}(q_n^{(j)}(\alpha) \mid \mathbf{Y}^{(n)}) \geq L \right\} \leq 2B_{n,k}/L \right) \\ & \geq \lim_{n \rightarrow \infty} \mathbb{P}_n^* \left(\left\| \pi(\cdot \mid \mathbf{Y}^{(n)}) - \tilde{\pi}_{(\mathcal{Q}, \omega)}^A(\cdot \mid \mathbf{Y}^{(n)}) \right\|_{\text{TV}} \leq C n^{-\lfloor \frac{k+2}{3} \rfloor} \right) \\ & = 1. \end{aligned}$$

iii) Rearranging and then applying Theorem 1 gives

$$\begin{aligned} & \lim_{n \rightarrow \infty} \mathbb{P}_n^* \left(\left| \check{\mathbb{E}}[f(\boldsymbol{\theta}) \mid \mathbf{Y}^{(n)}] - \mathbb{E}[f(\boldsymbol{\theta}) \mid \mathbf{Y}^{(n)}] \right| \leq C \mathbb{E}[f(\boldsymbol{\theta}) \mid \mathbf{Y}^{(n)}] n^{-\lfloor \frac{k+2}{3} \rfloor} \right) \\ & = \lim_{n \rightarrow \infty} \mathbb{P}_n^* \left(\left| \int_{\Theta} f(\boldsymbol{\theta}) \left[\tilde{\pi}_{(\mathcal{Q}, \omega)}^A(\boldsymbol{\theta} \mid \mathbf{Y}^{(n)}) - \pi(\boldsymbol{\theta} \mid \mathbf{Y}^{(n)}) \right] d\boldsymbol{\theta} \right| \leq C \mathbb{E}[f(\boldsymbol{\theta}) \mid \mathbf{Y}^{(n)}] n^{-\lfloor \frac{k+2}{3} \rfloor} \right) \\ & = \lim_{n \rightarrow \infty} \mathbb{P}_n^* \left(\left| \int_{\Theta} f(\boldsymbol{\theta}) \left[\frac{\pi(\boldsymbol{\theta}, \mathbf{Y}^{(n)})}{\tilde{\pi}_{(\mathcal{Q}, \omega)}^A(\mathbf{Y}^{(n)})} - \frac{\pi(\boldsymbol{\theta}, \mathbf{Y}^{(n)})}{\pi(\mathbf{Y}^{(n)})} \right] d\boldsymbol{\theta} \right| \leq C \mathbb{E}[f(\boldsymbol{\theta}) \mid \mathbf{Y}^{(n)}] n^{-\lfloor \frac{k+2}{3} \rfloor} \right) \\ & = \lim_{n \rightarrow \infty} \mathbb{P}_n^* \left(\left| \frac{1}{\tilde{\pi}_{(\mathcal{Q}, \omega)}^A(\mathbf{Y}^{(n)})} - \frac{1}{\pi(\mathbf{Y}^{(n)})} \right| \pi(\mathbf{Y}^{(n)}) \left| \int_{\Theta} f(\boldsymbol{\theta}) \pi(\boldsymbol{\theta} \mid \mathbf{Y}^{(n)}) d\boldsymbol{\theta} \right| \leq C \mathbb{E}[f(\boldsymbol{\theta}) \mid \mathbf{Y}^{(n)}] n^{-\lfloor \frac{k+2}{3} \rfloor} \right) \\ & = \lim_{n \rightarrow \infty} \mathbb{P}_n^* \left(\left| \frac{\pi(\mathbf{Y}^{(n)})}{\tilde{\pi}_{(\mathcal{Q}, \omega)}^A(\mathbf{Y}^{(n)})} - 1 \right| \mathbb{E}[f(\boldsymbol{\theta}) \mid \mathbf{Y}^{(n)}] \leq C \mathbb{E}[f(\boldsymbol{\theta}) \mid \mathbf{Y}^{(n)}] n^{-\lfloor \frac{k+2}{3} \rfloor} \right) \\ & = 1. \end{aligned}$$

The result then follows from Lemma 1. □

D.2. Proofs for Approximating Marginal Posterior Density

Recall Corollary 2, which states that the convergence rate is preserved for marginal posterior approximations for values of ψ_0 that satisfy certain conditions.

Corollary 2. Fix the value of ψ_0 . Suppose the conditions in Theorem 1 are satisfied when replacing all instances of θ with (ψ_0, λ) , θ^* with some constant $\theta_{\psi_0}^* = (\psi_0, \lambda_{\psi_0}^*)$, \mathbf{H}_n with $\mathbf{H}_n^{\psi_0}$ and $B_{\theta^*}^p(\cdot)$ with $B_{\lambda_{\psi_0}^*}^{p-q}(\cdot)$. Then

$$\lim_{n \rightarrow \infty} \mathbb{P}_n^* \left(\left| \frac{\pi(\psi_0 | \mathbf{Y}^{(n)})}{\tilde{\pi}(\psi_0 | \mathbf{Y}^{(n)})} - 1 \right| \leq C n^{-\lfloor \frac{k+2}{3} \rfloor} \right) = 1.$$

We now provide sufficient conditions for Corollary 2 to apply.

Proposition 1. Letting $\hat{\theta}_n = (\hat{\psi}_n, \hat{\lambda}_n)$ be the decomposition of the unrestricted mode, for all C' there exists C such that under Assumptions 1 to 5

$$\lim_{n \rightarrow \infty} \mathbb{P}_n^* \left(\sup_{\psi_0 \in B_{\hat{\psi}_n}^q(C' n^{-1/2})} \left| \frac{\pi(\psi_0 | \mathbf{Y}^{(n)})}{\tilde{\pi}(\psi_0 | \mathbf{Y}^{(n)})} - 1 \right| \leq C n^{-\lfloor \frac{k+2}{3} \rfloor} \right) = 1.$$

Remark 7. Proposition 1 states that the posterior marginal density can be accurately approximated in a $n^{-1/2}$ -neighbourhood of the unrestricted posterior mode without any additional assumptions. By the proof of Theorem 1, the posterior is sufficiently small outside of this neighbourhood such that for large enough n the marginal posterior density is well-approximated everywhere. \triangleleft

Proof of Proposition 1. For any ψ_0 , let $\pi^{\psi_0}(\mathbf{Y}^{(n)}) = \int \pi(\psi_0, \lambda, \mathbf{Y}^{(n)}) d\lambda$ and

$$\tilde{\pi}^{\psi_0}(\mathbf{Y}^{(n)}) = |\hat{\mathbf{L}}_n^{\psi_0}| \sum_{z' \in \mathcal{Q}'} \pi \left((0, \hat{\mathbf{L}}_n^{\psi_0} z'^{\top})^{\top} + \hat{\theta}_n^{\psi_0}, \mathbf{Y}^{(n)} \right) \omega'(z'),$$

using the quantities defined in Section 2.4. Recall that

$$\pi(\psi_0 | \mathbf{Y}^{(n)}) = \frac{\pi^{\psi_0}(\mathbf{Y}^{(n)})}{\pi(\mathbf{Y}^{(n)})},$$

so since the conditions of Theorem 1 hold, it remains to show that

$$\lim_{n \rightarrow \infty} \mathbb{P}_n^* \left(\sup_{\psi_0 \in B_{\hat{\psi}_n}^q(C' n^{-1/2})} \left| \frac{\pi^{\psi_0}(\mathbf{Y}^{(n)})}{\tilde{\pi}^{\psi_0}(\mathbf{Y}^{(n)})} - 1 \right| \leq C n^{-\lfloor \frac{k+2}{3} \rfloor} \right) = 1.$$

In particular, this amounts to a variant of Theorem 1 that (a) applies to the constrained likelihood and (b) holds uniformly over a shrinking ball of values of ψ_0 .

First, observe that for every ψ_0 , Lemma 4 will hold almost surely with the quantities adjusted appropriately to depend on $\tilde{\pi}^{\psi_0}$, $\hat{\theta}_n^{\psi_0}$, and $\hat{\mathbf{L}}_n^{\psi_0}$. We now focus on verifying that the other lemmas in the proof of Theorem 1 can be appropriately applied in supremum over $\psi_0 \in B_{\hat{\psi}_n}^q(C' n^{-1/2})$.

The key observation is that Assumptions 1 to 3 and 5 all hold uniformly in a fixed ball around θ^* , and Assumptions 2 and 3 imply that in limiting probability the unconstrained likelihood is strictly convex inside this ball and exponentially small outside of this ball respectively.

By continuity of the likelihood, and hence continuity of $\widehat{\boldsymbol{\theta}}_n^{\psi_0}$ as a function of ψ_0 , these assumptions also imply

$$\lim_{n \rightarrow \infty} \mathbb{P}_n^* \left[\left\{ \widehat{\boldsymbol{\theta}}_n^{\psi_0} : \psi_0 \in B_{\widehat{\psi}_n}^q (C' n^{-1/2}) \right\} \subseteq B_{\boldsymbol{\theta}^*}^p(\delta) \right] = 1.$$

This implies that the uniform analogues of Assumptions 1 to 3 and 5 all hold with respect to $B_{\widehat{\psi}_n}^q (C' n^{-1/2})$, and more specifically this implies the constants appearing in these bounds have no dependence on ψ_0 .

We now show that Assumption 4 holds with the constrained mode. Following the second derivative notation and the proof of Lemma 1 in Tang and Reid (2020), the derivative of $\widehat{\boldsymbol{\theta}}_n^{\psi_0}$ is

$$\frac{\partial \widehat{\boldsymbol{\theta}}_n^{\psi_0}}{\partial \psi_0} = [\mathbf{H}_n^{\lambda\lambda}(\widehat{\boldsymbol{\theta}}_n^{\psi_0})]^{-1} \mathbf{H}_n^{\psi\lambda}(\widehat{\boldsymbol{\theta}}_n^{\psi_0}),$$

where

$$\mathbf{H}_n(\boldsymbol{\theta}) = \begin{pmatrix} \mathbf{H}_n^{\psi\psi}(\boldsymbol{\theta}) & \mathbf{H}_n^{\psi\lambda}(\boldsymbol{\theta}) \\ \mathbf{H}_n^{\lambda\psi}(\boldsymbol{\theta}) & \mathbf{H}_n^{\lambda\lambda}(\boldsymbol{\theta}) \end{pmatrix}.$$

By the uniform analogues of Assumptions 1 and 2 on $B_{\widehat{\psi}_n}^q (C' n^{-1/2})$, we have that the $\widehat{\boldsymbol{\theta}}_n^{\psi_0}$ is a Lipschitz function in this ball when viewed as a function of ψ_0 , which then implies the uniform version of Assumption 4. Thus, the random coefficients appearing in the constrained variant of Lemma 4 can then be upper bounded uniformly using Lemma 5, since the uniform variants of Assumptions 1 to 5 have no dependence on the value of ψ_0 .

To finish the proof, it remains to observe that the uniform analogues of Lemmas 6 and 7 follow from the uniform analogues of the assumptions, and hence the uniform variants of Lemmas 2 and 3 hold. \square

D.3. Proofs for Approximating Marginal Posterior Expectation

We require the following assumptions on g in order to prove convergence rates for marginal poster expectations computed using further applications of AGHQ.

(M1) There exists $M > 0$ such that for all $\boldsymbol{\alpha} \subseteq \mathbb{N}^p$ with $0 \leq |\boldsymbol{\alpha}| \leq m$

$$\sup_{\boldsymbol{\theta} \in B_{\boldsymbol{\theta}^*}^p(\delta)} |\partial^{\boldsymbol{\alpha}} \log g(\boldsymbol{\theta})| < M.$$

(M2) There exists $-\infty < \underline{\eta}^g \leq \bar{\eta}^g < \infty$ such that

$$\underline{\eta}^g \leq \inf_{\boldsymbol{\theta} \in B_{\boldsymbol{\theta}^*}^p(\delta)} \lambda_p(\partial^2[-\log g(\boldsymbol{\theta})]) \leq \sup_{\boldsymbol{\theta} \in B_{\boldsymbol{\theta}^*}^p(\delta)} \lambda_1(\partial^2[-\log g(\boldsymbol{\theta})]) \leq \bar{\eta}^g.$$

(M3) There exist $0 < c_1 < c_2 < \infty$ such that

$$c_1 \leq \inf_{\boldsymbol{\theta} \in B_{\boldsymbol{\theta}^*}^p(\delta)} g(\boldsymbol{\theta}) \leq \sup_{\boldsymbol{\theta} \in B_{\boldsymbol{\theta}^*}^p(\delta)} g(\boldsymbol{\theta}) \leq c_2.$$

We restate Corollary 3 here for convenience.

Corollary 3. *Suppose $g : \Theta \rightarrow \mathbb{R}_+$ satisfies assumptions (M1) through (M3) from Appendix D.3. Then, if the conditions of Theorem 1 also hold,*

$$\lim_{n \rightarrow \infty} \mathbb{P}_n^* \left(\left| \frac{\mathbb{E}[g(\boldsymbol{\theta}) \mid \mathbf{Y}^{(n)}]}{\widetilde{\mathbb{E}}[g(\boldsymbol{\theta}) \mid \mathbf{Y}^{(n)}]} - 1 \right| \leq C n^{-\lfloor \frac{k+2}{3} \rfloor} \right) = 1.$$

Proof of Corollary 3. We want to verify that the assumptions of Appendix A hold for the new ‘‘prior’’ $\pi^g(\boldsymbol{\theta})$. Under (M1), Assumption 1 holds since by product rule,

$$\begin{aligned} \left| \partial^\alpha \log \pi^g(\mathbf{Y}^{(n)}, \boldsymbol{\theta}) \right| &= \frac{|\partial^\alpha \log \pi^g(\mathbf{Y}^{(n)}, \boldsymbol{\theta})|}{\pi^g(\mathbf{Y}^{(n)}, \boldsymbol{\theta})} \\ &= \frac{|\partial^\alpha \pi(\mathbf{Y}^{(n)}, \boldsymbol{\theta})| g(\boldsymbol{\theta}) + \pi(\mathbf{Y}^{(n)}, \boldsymbol{\theta}) |\partial^\alpha g(\boldsymbol{\theta})|}{\pi(\mathbf{Y}^{(n)}, \boldsymbol{\theta}) g(\boldsymbol{\theta})} \\ &= |\partial^\alpha \log \pi(\mathbf{Y}^{(n)}, \boldsymbol{\theta})| + |\partial^\alpha \log g(\boldsymbol{\theta})|. \end{aligned}$$

Under (M2), it holds almost surely that

$$\begin{aligned} \underline{\eta}^g + \inf_{\boldsymbol{\theta} \in B_{\boldsymbol{\theta}^*}^p(\delta)} \lambda_p(\mathbf{H}_n(\boldsymbol{\theta})) &\leq \inf_{\boldsymbol{\theta} \in B_{\boldsymbol{\theta}^*}^p(\delta)} \lambda_p(\partial^2[-\log g(\boldsymbol{\theta})]) + \inf_{\boldsymbol{\theta} \in B_{\boldsymbol{\theta}^*}^p(\delta)} \lambda_p(\mathbf{H}_n(\boldsymbol{\theta})) \\ &\leq \inf_{\boldsymbol{\theta} \in B_{\boldsymbol{\theta}^*}^p(\delta)} \lambda_p(\mathbf{H}_n^g(\boldsymbol{\theta})) \\ &\leq \sup_{\boldsymbol{\theta} \in B_{\boldsymbol{\theta}^*}^p(\delta)} \lambda_1(\mathbf{H}_n^g(\boldsymbol{\theta})) \\ &\leq \sup_{\boldsymbol{\theta} \in B_{\boldsymbol{\theta}^*}^p(\delta)} \lambda_1(\partial^2[-\log g(\boldsymbol{\theta})]) + \sup_{\boldsymbol{\theta} \in B_{\boldsymbol{\theta}^*}^p(\delta)} \lambda_1(\mathbf{H}_n(\boldsymbol{\theta})) \\ &\leq \bar{\eta}^g + \sup_{\boldsymbol{\theta} \in B_{\boldsymbol{\theta}^*}^p(\delta)} \lambda_1(\mathbf{H}_n(\boldsymbol{\theta})). \end{aligned}$$

Thus, if Assumption 2 holds for the prior π , we also have

$$\lim_{n \rightarrow \infty} \mathbb{P}_n^* \left[n\underline{\eta}/2 \leq \inf_{\boldsymbol{\theta} \in B_{\boldsymbol{\theta}^*}^p(\delta)} \lambda_p(\mathbf{H}_n^g(\boldsymbol{\theta})) \leq \sup_{\boldsymbol{\theta} \in B_{\boldsymbol{\theta}^*}^p(\delta)} \lambda_1(\mathbf{H}_n^g(\boldsymbol{\theta})) \leq 2n\bar{\eta} \right] = 1,$$

since for large enough n , $\underline{\eta}^g > -n\underline{\eta}/2$ and $\bar{\eta}^g < n\bar{\eta}$. In particular, Assumption 2 holds for π^g with the constants $\underline{\eta}/2$ and $2\bar{\eta}$, and so \mathbf{H}_n^g is locally positive definite at $\boldsymbol{\theta}^*$ (and hence $\widehat{\mathbf{L}}_n^g$ exists) with probability tending to one.

Assumption 3 is implied by (M3) and the positivity of g . Finally, Assumption 4 is implied by (M3) and the usual consistency argument, while Assumption 5 is trivially implied by (M3).

Having verified these conditions, we also note that for $x \in (0, 1/2)$,

$$\frac{1+x}{1-x} \leq 1+4x \quad \text{and} \quad \frac{1-x}{1+x} \geq 1-2x.$$

Thus, the statement follows from the following three facts:

$$\lim_{n \rightarrow \infty} \mathbb{P}_n^* \left(\left| \frac{\int \pi^g(\boldsymbol{\theta}, \mathbf{Y}^{(n)}) d\boldsymbol{\theta}}{|\widehat{\mathbf{L}}_n^g| \sum_{\mathbf{z} \in \mathcal{Q}} \pi^g(\widehat{\mathbf{L}}_n^g \mathbf{z} + \widehat{\boldsymbol{\theta}}_n^g, \mathbf{Y}^{(n)}) \boldsymbol{\omega}(\mathbf{z})} - 1 \right| \leq C n^{-\lfloor \frac{k+2}{3} \rfloor} \right) = 1,$$

$$\lim_{n \rightarrow \infty} \mathbb{P}_n^* \left(\left| \frac{\int \pi(\boldsymbol{\theta}, \mathbf{Y}^{(n)}) d\boldsymbol{\theta}}{|\widehat{\mathbf{L}}_n| \sum_{\mathbf{z} \in \mathcal{Q}} \pi(\widehat{\mathbf{L}}_n \mathbf{z} + \widehat{\boldsymbol{\theta}}_n, \mathbf{Y}^{(n)}) \omega(\mathbf{z})} - 1 \right| \leq C n^{-\lfloor \frac{k+2}{3} \rfloor} \right) = 1,$$

and

$$\mathbb{E}[g(\boldsymbol{\theta}) \mid \mathbf{Y}^{(n)}] = \frac{\int \pi^g(\boldsymbol{\theta}, \mathbf{Y}^{(n)}) d\boldsymbol{\theta}}{\int \pi(\boldsymbol{\theta}, \mathbf{Y}^{(n)}) d\boldsymbol{\theta}},$$

as $0 < C n^{-\lfloor \frac{k+2}{3} \rfloor} < 1/2$ eventually for large n , leading to the desired limiting statement. \square

The most relevant application of Corollary 3 is to compute the marginal posterior moments, which we now show satisfies the conditions of Corollary 3.

Proposition 2. *For every $j \in [p]$ and $i \in \mathbb{N}$, if $g(\boldsymbol{\theta}) = (\theta_j)^i$, Assumptions (M1) through (M3) from Appendix D.3 are satisfied for g^+ when $\theta_j^* > 0$ and g^- when $\theta_j^* < 0$.*

Remark 8. *For odd moments, when the parameter is negative the integral cannot be approximated using the techniques of this paper, but by posterior concentration this contribution to the integral is tending to zero and can be discarded (see Appendix E.2 for computational details).* \triangleleft

Proof of Proposition 2. Without loss of generality, suppose $\theta_j^* > 0$; when $\theta_j^* < 0$ the argument is identical swapping g^+ and g^- . Thus, there exists $\delta > 0$ small enough such that for all $\boldsymbol{\theta} \in B_{\boldsymbol{\theta}^*}^p(\delta)$, $\theta_j \in (a_1, a_2)$ for some $0 < a_1 < a_2$. Since i will only change the scaling of $\log g(\boldsymbol{\theta})$, it suffices to verify (M1) through (M3) for $i = 1$.

For any $\boldsymbol{\theta} \in B_{\boldsymbol{\theta}^*}^p(\delta)$ and $\alpha_j \in [m]$, $\boldsymbol{\alpha} = (0, \dots, \alpha_j, 0, \dots, 0)$ satisfies

$$\partial^\alpha [-\log g^+(\boldsymbol{\theta})] = (-1)^{\alpha_j} (\alpha_j - 1)! \theta_j^{-\alpha_j},$$

and for every $\boldsymbol{\alpha} \in \mathbb{N}^p$ not of this form, $\partial^\alpha \log g^+(\boldsymbol{\theta}) = 0$. Thus, by boundedness of θ_j , (M1) holds for g^+ .

For (M2), the Hessian satisfies $\partial^2 [-\log g(\boldsymbol{\theta})]_{jj} = \theta_j^{-2}$ and $\partial^2 [-\log g(\boldsymbol{\theta})]_{ij} = 0$ otherwise. Thus, by boundedness of θ_j in $B_{\boldsymbol{\theta}^*}^p(\delta)$, the eigenvalues are all nonnegative and bounded above as required.

(M3) holds trivially since $\theta_j \in (a_1, a_2)$. \square

E. Computational Considerations

In this section we describe the necessary computational and implementation details for applying AGHQ to models of the type we consider in Sections 4 and 5.

E.1. The aghq Package

All of the computations described in this paper are implemented in the R package aghq, current version 0.4.0, on CRAN. The user only needs to provide an unnormalized log-posterior and two derivatives (which can be obtain automatically, see Appendix E.4). From this input the aghq

package performs all subsequent computations automatically, including: optimization and approximate normalization; approximate moments; and marginal densities, distribution functions, and quantiles. This section gives the details on how the package performs these computations automatically without requiring any additional user input.

The AGHQ procedure employed in Section 4 (i.e., for low-dimensional models) is implemented as follows. The user provides a list `ff` containing the following elements, each of which are functions of $\boldsymbol{\theta}$,

$$\begin{aligned} \text{fn} &: \log \pi(\boldsymbol{\theta}, \mathbf{Y}^{(n)}), \\ \text{gr} &: \partial_{\boldsymbol{\theta}} \log \pi(\boldsymbol{\theta}, \mathbf{Y}^{(n)}), \\ \text{he} &: \partial_{\boldsymbol{\theta}}^2 \log \pi(\boldsymbol{\theta}, \mathbf{Y}^{(n)}). \end{aligned}$$

In all of our examples, `ff` is obtained via a call to `TMB::MakeADFun` (see Appendix E.4), and the user therefore only has to construct a TMB template implementing $\log \pi(\boldsymbol{\theta}, \mathbf{Y}^{(n)})$. This construction is problem-specific.

Given `ff`, a numeric number of (one-dimensional) quadrature points `k`, and a numeric vector of length $p = \dim(\boldsymbol{\theta})$ of starting values for the optimization `start`, the command

```
quad <- aghq(ff,k,start)
```

calculates $\log \tilde{\pi}^{\text{AGHQ}}(\mathbf{Y}^{(n)})$ using product GHQ as the base grid (other grids satisfying $\mathcal{P}(k, p)$ are also supported). The command `get_log_normconst(quad)` returns the $\log \tilde{\pi}^{\text{AGHQ}}(\mathbf{Y}^{(n)})$ prescribed by Theorem 1.

The object `quad` has class `aghq`, and the commands

```
summary(quad)
plot(aghq)
```

will compute and print or plot univariate marginal densities according to Eq. (8) and approximate moments according to Eq. (9), which are exactly the quantities for which the theoretical guarantees of Corollaries 2 and 3 apply. Also computed are approximate quantiles and cumulative distribution functions, which are not covered by the theoretical guarantees of the present work.

As of version 0.4.0, the user must set

```
control = default_control(method_summaries='correct')
```

to turn on the computation of moments and marginals according to Eqs. (8) and (9). This was done for backwards compatibility, and the correct computation will be made the default setting in the eventual 1.0.0 version release of `aghq`.

The use of parameter transformations is ubiquitous and convenient in Bayesian models. While Theorem 1 does not require any transformation to be made (only the assumptions of Appendix A to hold), Naylor and Smith (1982) point out that often a simple transformation,

like `log` or `logit`, can yield a transformed parameter whose posterior is closer to being log-quadratic than that of the parameter of inferential interest, and that this can improve the finite-sample accuracy of the quadrature and/or the speed and stability of the optimization.

The `aghq` package provides an interface for parameter transformations. Suppose inferential interest is in parameter ϕ , but the user implements `ff` to depend on a transformed parameter $\theta = h(\phi)$ where $h : \mathbb{R} \rightarrow \mathbb{R}$ is monotonic and invertible. It is desirable for the quadrature to be done on the θ scale, but all summary methods to return results for $\phi = h^{-1}(\theta)$. The user creates a transformation object of class `aghqtrans` using the command

```
trans <- make_transformation(totheta = h,fromtheta = hinv),
```

where `h = h` and `hinv = h-1`. These functions are passed through `match.fun` internally.

The quadrature

```
quad <- aghq(ff,k,start,transformation = trans)
```

is then performed in exactly the same way, but the `summary` and `plot` commands will now return inferences for $\phi = h^{-1}(\theta)$. When $p > 1$, h is interpreted as a vectorized scalar-to-scalar function; fully multivariate transformations are not yet supported.

As a concrete example, suppose `ff` is a template implementing $\log \pi(\boldsymbol{\theta}, \mathbf{Y}^{(n)})$ for the infectious disease model of Section 4. Recall the parameters of interest are (α, β) , but the quadrature was done on the posterior of the transformed parameters $\theta_1 = \log \alpha$ and $\theta_2 = \log \beta$. The full code to implement one instance of this example is

```
quad <- aghq(ff,7,c(0,0),
  make_transformation('log','exp'),
  control = default_control(method_summaries='correct'))
summary(quad); plot(quad).
```

In Section 5, we describe the use of AGHQ within a more complicated framework for making approximate Bayesian inferences. This full framework is also implemented within the `aghq` package. The simplest way, which we describe here, is for the user to implement a TMB template computing $-\log \pi(\boldsymbol{w}, \boldsymbol{\theta}, \mathbf{Y}^{(n)})$ and set `random = w`. This provides a list `ff` containing elements (again functions of $\boldsymbol{\theta}$):

$$\begin{aligned} \text{fn} &: -\log \tilde{\pi}_{\text{LA}}(\boldsymbol{\theta}, \mathbf{Y}^{(n)}), \\ \text{gr} &: -\partial_{\boldsymbol{\theta}} \log \tilde{\pi}_{\text{LA}}(\boldsymbol{\theta}, \mathbf{Y}^{(n)}). \end{aligned}$$

The requirement to implement the *negative* log-posterior is for compatibility with TMB and its automatic Laplace approximation. This is handled internally by `aghq`.

The command

```
quad <- marginal_laplace_tmb(ff,k,start)
```

performs the computations necessary to use $\tilde{\pi}(\mathbf{w} \mid \mathbf{Y}^{(n)})$ (Eq. (10)). The `summary` and `plot` methods provide inferences for $\boldsymbol{\theta}$ based on the AGHQ-normalized marginal Laplace approximation $\log \tilde{\pi}_{\text{LA}}(\boldsymbol{\theta} \mid \mathbf{Y}^{(n)})$, providing an implementation of the method of Tierney and Kadane (1986). The user obtains M samples from the mixture of Gaussians $\tilde{\pi}(\mathbf{w} \mid \mathbf{Y}^{(n)})$ using the command

```
sample_marginal(quad,M).
```

This can be done automatically within `summary`, by setting the `max_print` option to be greater than $\dim(\mathbf{w})$, in which case `summary` will compute and return sample-based summary statistics of \mathbf{w} . By default, `max_print` is set to 30, and summaries are computed using 1000 samples, but these can be easily changed by the user.

E.2. Computing Posterior Summaries

The `marginal_posterior`, `compute_moment`, `compute_pdf_and_cdf`, and `compute_quantiles` functions are all automatically called within `aghq` and the `summary` and `plot` methods for `aghq` objects, and automatically handle any parameter transformations provided using `make_transformation`. They are also exported directly so that the user has further control over the computation of summary statistics.

The `compute_moment` function computes the approximate moment $\tilde{\mathbb{E}}[g(\boldsymbol{\theta}) \mid \mathbf{Y}^{(n)}]$ of a function $g : \mathbb{R}^p \rightarrow \mathbb{R}^+$ according to Eq. (9). The user provides a list `gg` containing the following elements, each of which are functions of $\boldsymbol{\theta}$,

```
fn : log g(θ),
gr : ∂θ log g(θ),
he : ∂θ2 log g(θ).
```

The `make_moment_function` helper helps to automate this process. The user calls

```
make_moment_function(g),
```

where $g = g$, and `make_moment_function` creates the appropriate list, using numeric derivatives. Other, more detailed options are described in the package documentation.

The `marginal_posterior` function computes the approximate marginal posterior $\tilde{\pi}(\boldsymbol{\psi}_0 \mid \mathbf{Y}^{(n)})$ at any point $\mathbf{q} \in \mathbb{R}$ according to Eq. (8). If unspecified by the user (the default), the evaluation points \mathbf{q} are chosen automatically, using a default based on a one-dimensional adapted GHQ rule.

For computing raw and central moments, the user may instead pass a numeric scalar `nn` to `compute_moment`, as well as `type = 'raw'` or `type = 'central'`. In this case, `compute_moment` automatically constructs an appropriate input list for the function $g(\boldsymbol{\theta}) = \theta_j^{\text{nn}}$ (`type='raw'`) or $g(\boldsymbol{\theta}) = (\theta_j - \tilde{\mathbb{E}}(\theta_j \mid \mathbf{Y}^{(n)}))^{\text{nn}}$ (`type='central'`), for $j \in [p]$, and returns the corresponding vector of approximate moments. To ensure positivity (which is required both theoretically for Corollary 3 and computationally for AGHQ to be applicable), the function automatically detects whether $\min_{\mathbf{z} \in \mathcal{Q}}(\widehat{\mathbf{L}}_n \mathbf{z} + \widehat{\boldsymbol{\theta}}_n)_j^{\text{nn}} < 0$, adds a buffer value $a > -\min_{\mathbf{z} \in \mathcal{Q}}(\widehat{\mathbf{L}}_n \mathbf{z} + \widehat{\boldsymbol{\theta}}_n)_j^{\text{nn}}$, and outputs $\tilde{\mathbb{E}}(\theta_j^{\text{nn}} - a \mid \mathbf{Y}^{(n)}) + a$.

Data suitable for creating plots of the approximate probability density and cumulative distribution functions are computed using `compute_pdf_and_cdf`. Unlike `marginal_posterior` and `compute_moment`, the output of these functions are not covered by Corollaries 2 and 3. For any $\psi \in \mathbb{R}$, denote the Lagrange polynomial interpolant of $\log \tilde{\pi}_j^{\text{AGHQ}}(\psi \mid \mathbf{Y}^{(n)})$ by $\mathcal{P}_j(\psi)$ and define

$$\tilde{\pi}_j^{\text{POLY}}(\psi \mid \mathbf{Y}^{(n)}) = \exp \{ \mathcal{P}_j(\psi) \}.$$

The marginal CDF is defined by

$$F_j(\psi \mid \mathbf{Y}^{(n)}) = \int_{-\infty}^{\psi} \pi_j(\psi' \mid \mathbf{Y}^{(n)}) d\psi',$$

and approximated by choosing a fine grid x_1, \dots, x_L for some large $L \in \mathbb{N}$ and computing

$$\tilde{F}_j^{\text{POLY}}(\psi \mid \mathbf{Y}^{(n)}) = \sum_{l: x_l \leq \psi} \tilde{\pi}_j^{\text{POLY}}(x_l \mid \mathbf{Y}^{(n)})(x_{l+1} - x_l).$$

The choice of grid is again handled internally by `compute_pdf_and_cdf`, with no input required by the user.

Finally, marginal quantiles are computed by `compute_quantiles`. For any level $\alpha \in (0, 1)$, `compute_quantile` outputs:

$$\tilde{q}_j^{\text{POLY}}(\alpha) = \min \left\{ x \in \{x_1, \dots, x_L\} \mid \tilde{F}_j^{\text{POLY}}(x \mid \mathbf{Y}^{(n)}) \geq \alpha \right\}.$$

We reiterate that all of the quantities described in this section are computed and displayed to the user automatically by `summary.aghq`.

E.3. Software Package Versions

For AGHQ, we use CRAN version 0.4.0 of the `aghq` package, which may be installed using the command `install.packages('aghq')`. For MCMC, we use the `tmbstan` package (Monnahan and Kristensen 2018), version 1.0.2 from CRAN, which implements the state-of-the-art No-U-Turn sampler (Hoffman and Gelman 2014), the self-tuning version of Hamiltonian Monte Carlo that is the default in the popular STAN language (Carpenter et al. 2017).

E.4. Automatic Differentiation

Approximate computation of $\tilde{\pi}^{\text{AGHQ}}(\mathbf{Y}^{(n)})$ requires two derivatives of $\log \pi(\boldsymbol{\theta}, \mathbf{Y}^{(n)})$, and this is often too burdensome to be done by hand or numerically. Automatic Differentiation (AD) (Kristensen et al. 2016; Carpenter et al. 2017; Duvenaud and Adams 2015; Margossian et al. 2020; Falbel and Luraschi 2020; Yao et al. 2020) provides exact derivatives of any differentiable function that can be represented by a computer. Other prominent methods for Bayesian inference, including Hamiltonian Monte Carlo (Carpenter et al. 2017) and Stochastic Variational Inference (Duvenaud and Adams 2015), also require differentiation of complicated (and in the latter case, intractable) objective functions, and the cited implementations of these methods use AD for this purpose. In our examples, we use TMB (Kristensen et al. 2016), but as described

in Appendix E.1, any manner by which the derivatives are obtained is compatible with the `aghq` package. Because of the wide availability of AD software, including in R (see Carpenter et al. 2017; Falbel and Luraschi 2020), the requirement of two derivatives of $\log \pi(\boldsymbol{\theta}, \mathbf{Y}^{(n)})$ is computationally benign.

E.5. Optimization Software

Computing $\tilde{\pi}^{\text{AGHQ}}(\mathbf{Y}^{(n)})$ requires computing $\hat{\boldsymbol{\theta}}_n = \arg \max_{\boldsymbol{\theta}} \log \pi(\boldsymbol{\theta}, \mathbf{Y}^{(n)})$, and this requires numerical optimization. By Assumption 2, $\log \pi(\boldsymbol{\theta}, \mathbf{Y}^{(n)})$ is locally convex for sufficiently large n , and we therefore use convex optimization techniques. When $\Theta = \mathbb{R}^p$, we use trust region optimization as implemented in the `trustOptim` (Braun 2014) or `trust` (Geyer 2020) packages. Box parameter constraints can be removed via parameter transformations (Sections 4.1 and 4.2 and Appendix E.1) or handled using more advanced optimization tools. General constraints, including box and non-linear constraints, are accommodated by using the IPOPT package (Wachter and Biegler 2006) for constrained optimization (Section 4.2).

A referee pointed out that the concentration behaviour of the log-likelihood implied by Assumptions 1 to 5 may make optimization challenging for large n . If any such difficulty is encountered, we recommend dividing the objective function by n when computing $\hat{\boldsymbol{\theta}}_n$. By Assumption 1, the log-likelihood is bounded in probability when scaled by n , and this precise knowledge of the scaling behaviour of the objective function is a useful feature of models satisfying these assumptions. However, such adjustments were not necessary to obtain stable results in the optimization step for any of the examples we considered.

F. Simulations

The results of Section 3 provide guarantees on the accuracy of approximating posterior distributions and posterior summary statistics using AGHQ. Naturally, such results require certain assumptions (see Appendix A) about the model, and are all statements about guarantees as the sample size tends to infinity. Additionally, all of these guarantees are upper bounds, and individual models may or may not achieve faster rates of convergence. Theorem 1 cannot be tight in all cases since, for example, if the posterior is a normal distribution then AGHQ will exactly approximate the density, resulting in zero error. However, we conjecture that for many models, AGHQ’s dependence on n and k is no better than in our upper bounds.

In the absence of theoretical lower bounds, we use simulation to show an example of a simple model in which the empirical error rate is not lower than our prescribed upper bound. For this simple model, we observe that the convergence rate given in Theorem 1 is realized at very small sample sizes ($n \ll 100$), empirically demonstrating the tightness of the upper bound. Further, in contrast to the existing literature, our results are stochastic in nature. We have designed our simulation to demonstrate this, as it is important that not only a single ideal realization of data achieves the desired rate, but that such datasets occur with high probability under the model.

We consider the following simple model:

$$\begin{aligned} \mathbf{Y}_i | \lambda &\overset{ind}{\sim} \text{Poisson}(\lambda), i \in [n], \\ \lambda &\sim \text{Exponential}(1), \end{aligned} \tag{26}$$

with posterior

$$\lambda | \mathbf{Y}^{(n)} \sim \text{Gamma}\left(1 + \sum_{i=1}^n \mathbf{Y}_i, n + 1\right).$$

We have chosen this conjugate model because the posterior and normalizing constant are known exactly, facilitating computation of error rates. In contrast, Jin and Andersson (2020) use an example in which their integral is not known exactly, and use AGHQ with a large number of quadrature points in place of the exact answer. Consequently, their simulation confirms that the variance of AGHQ diminishes with the number of quadrature points, but does not demonstrate anything about its bias.

If $\mathbb{E}_{\text{rel}}(\mathbf{Y}^{(n)}) \approx Cn^{-\lfloor \frac{k+2}{3} \rfloor}$ for some constant C , then $\log \mathbb{E}_{\text{rel}}(\mathbf{Y}^{(n)}) \approx \log(C) - \lfloor \frac{k+2}{3} \rfloor \log n$. Therefore, we compute $\log \mathbb{E}_{\text{rel}}(\mathbf{Y}^{(n)}) + \lfloor \frac{k+2}{3} \rfloor \log n$ for many simulated datasets and various values of n and k , and observe that there is no pattern in n in the resulting plots. The full details of this simulation procedure are described in Algorithm 1.

Figure 5 demonstrates the results over 1000 simulations with $\lambda = 5$. We consider n up to 100, and $k \in \{3, 5, 7, 11\}$, which correspond respectively to rates of $\mathcal{O}_P(n^{-1})$, $\mathcal{O}_P(n^{-2})$, $\mathcal{O}_P(n^{-3})$, and $\mathcal{O}_P(n^{-4})$ by Theorem 1. Each point represents a realization of $\log \mathbb{E}_{\text{rel}}(\mathbf{Y}^{(n)}) + \lfloor \frac{k+2}{3} \rfloor \log n$ for a dataset simulated from this model, which will equal $\log C$ for some constant $C > 0$ if the rate of Theorem 1 is achieved. The exact value of the vertical axis is of only secondary interest; the relevant observation is that there is no visible pattern with respect to n .

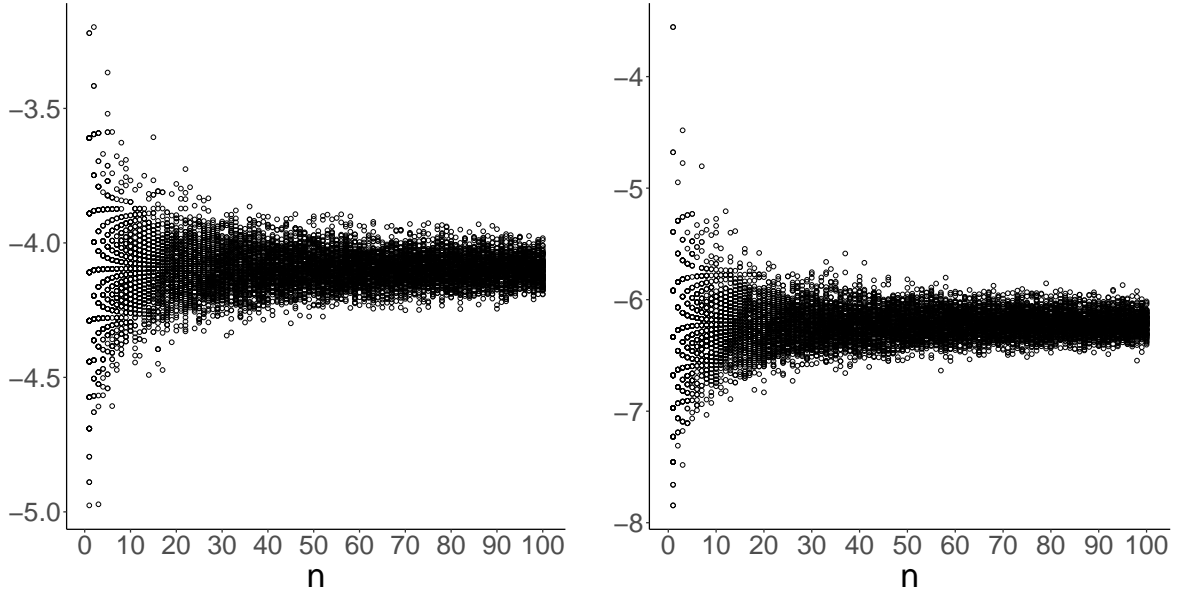
We observe no pattern in Fig. 5, implying that the rate of Theorem 1 is tight for this simple model. Computations are all done on the log scale for numerical stability, however due to the simplicity of the model we observed roundoff error when computing $\log \mathbb{E}_{\text{rel}}(\mathbf{Y}^{(n)})$ for some of the simulated datasets when $k = 11$ and $n > 80$, an artifact that appears in the lower right corner of Fig. 5 (d). This is due to roundoff error when computing $\log \mathbb{E}_{\text{rel}}(\mathbf{Y}^{(n)})$, and is not related to the properties of the AGHQ procedure.

G. Further detail for Section 5.2

In this section we discuss the results of running MCMC for the zero-inflated binomial geostatistical regression from Section 5.2 and include a brief simulation study to assess the empirical accuracy of the adaptive quadrature-based approximations used in Section 5.1.

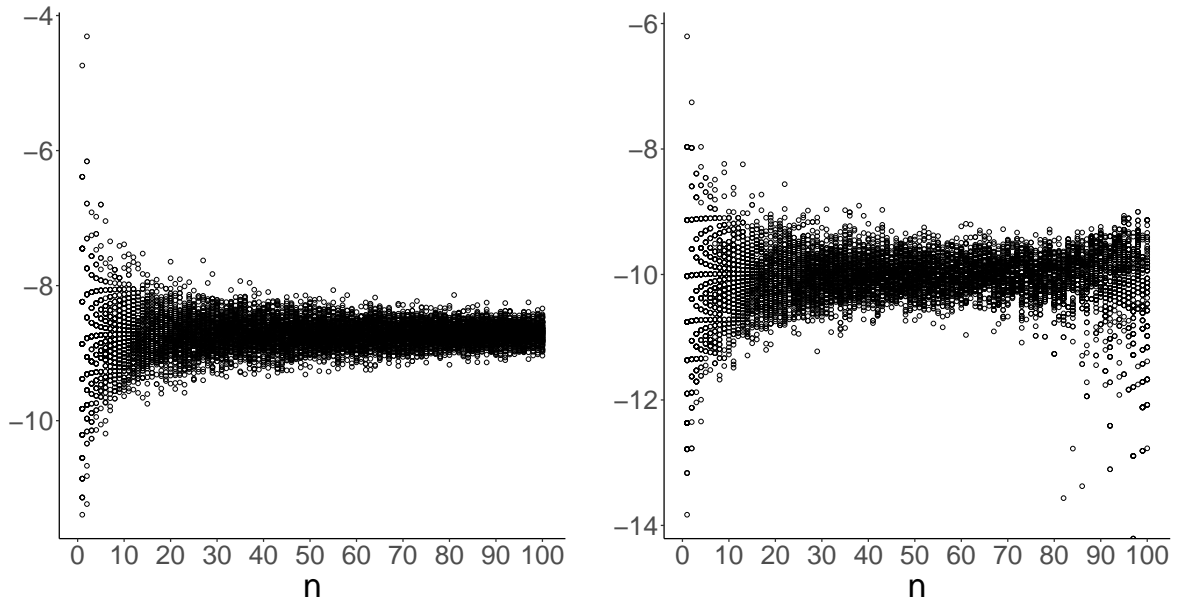
G.1. MCMC Results

We present the results of running the NUTS sampler through `tmbstan` using the default settings, with a computation time of 66 hours for running eight parallel chains of 10,000 iterations each, including a warmup of 1,000 iterations. We stress that we are confident an expert user of MCMC could tune the algorithm to produce favourable results, however the observed runtime



(a) $k = 3, \left| \frac{\pi(\mathbf{Y}^{(n)})}{\bar{\pi}_{\text{AGHQ}}(\mathbf{Y}^{(n)})} - 1 \right| = \mathcal{O}_P(n^{-1})$

(b) $k = 5, \left| \frac{\pi(\mathbf{Y}^{(n)})}{\bar{\pi}_{\text{AGHQ}}(\mathbf{Y}^{(n)})} - 1 \right| = \mathcal{O}_P(n^{-2})$



(c) $k = 7, \left| \frac{\pi(\mathbf{Y}^{(n)})}{\bar{\pi}_{\text{AGHQ}}(\mathbf{Y}^{(n)})} - 1 \right| = \mathcal{O}_P(n^{-3})$

(d) $k = 11, \left| \frac{\pi(\mathbf{Y}^{(n)})}{\bar{\pi}_{\text{AGHQ}}(\mathbf{Y}^{(n)})} - 1 \right| = \mathcal{O}_P(n^{-4})$

Figure 5: Realized de-trended error rates $\log E_{\text{rel}}(\mathbf{Y}^{(n)}) + \lfloor \frac{k+2}{3} \rfloor \log n$ for data generated from the model (see Eq. (26)), $k = 3, 5, 7, 11$, and $n < 100$.

of almost three days illustrates that doing so would be inconvenient and laborious even for such an expert. In contrast, the AGHQ strategy runs in approximately 90 seconds without problem-specific tuning, and if any tuning were required it could be done much more efficiently due to the short running time.

Fig. 6 shows the predicted suitability and incidence maps from the MCMC run, alongside those from AGHQ (Fig. 4) for comparison. While the predicted incidence probabilities are visually similar, the MCMC results appear to fail to identify the spatial pattern in suitability, which is the main practical reason to consider this model in the first place. Closer inspection reveals the problem is a failure to accurately sample from the posterior for β_{suit} , leading to inflated estimates of $\phi(\mathbf{s})$ at all locations. Fig. 7 shows pairs plots of the two intercepts from the `tmbstan` output, which illustrate the divergent transitions responsible for the inflated posterior of β_{suit} . Also shown are corresponding plots of posterior samples from the AGHQ fit for comparison; note the difference in scale for β_{suit} . Further explanation of the meaning of “divergent transition” and advice for tuning the sampler can be found in the STAN documentation at <https://mc-stan.org/misc/warnings.html#divergent-transitions-after-warmup> or in Gabry et al. (2019). In particular, Gabry et al. (2019) suggest that divergent transitions clustered in one region of the parameter space as is clearly seen in Fig. 7 indicates a serious problem with the ability of the sampler to adequately explore the posterior. The available advice amounts to either changing tuning parameters, which would lead to an increase in computational cost, or rewriting the model entirely. We reiterate that while an expert user may be able to tune MCMC in a problem-specific manner or implement a different type of sampler that would yield satisfactory results for this problem, tuning of this nature is extremely inconvenient due to the already astronomical computational cost of running MCMC in this example, and the complexity of the model. In contrast, the AGHQ-based approximation strategy of Section 5.1 runs in minutes without problem-specific tuning, and is hence a potentially appealing practical alternative, that would be made more appealing by the development of convergence theory for it.

G.2. MCMC Results with β Fixed

We re-ran the MCMC algorithm with the two intercept parameters fixed at their initial AGHQ estimates of $\beta_{\text{suit}} = 2.912111$ and $\beta_{\text{inc}} = -1.984655$. The wall time for 8 parallel chains of 10,000 iterations of each was 19.5 hours, compared to a wall time of 224 seconds for AGHQ with $k = 7$. AGHQ ran in the time taken for approximately 32 iterations of MCMC. Fig. 8 shows the estimated KS statistics between the $2n = 380$ marginal distributions of $u(\mathbf{s}_i)$ and $v(\mathbf{s}_i), i \in [n]$, for AGHQ and MCMC. The incidence spatial field $v(\mathbf{s})$ is more accurately estimated than the suitability field $u(\mathbf{s})$, and both show broad agreement with some villages having moderate disagreement.

G.3. Empirical Accuracy of AGHQ

In this section we present a brief simulation study to assess the accuracy of using AGHQ to fit the spatial model of Section 5.2. We observe that the empirical root-mean-square-error in the posterior mean of the parameter vector decreases with increased simulated sample size, sug-

Algorithm 1 Computing sample rates in the simulation study

Input: max sample size $N \in \mathbb{N}$, quadrature points parameter $k \in \mathbb{N}$, number of simulations $M \in \mathbb{N}$, mean response $\lambda \in \mathbb{R}$.

Let $r_k = \lfloor \frac{k+2}{3} \rfloor$.

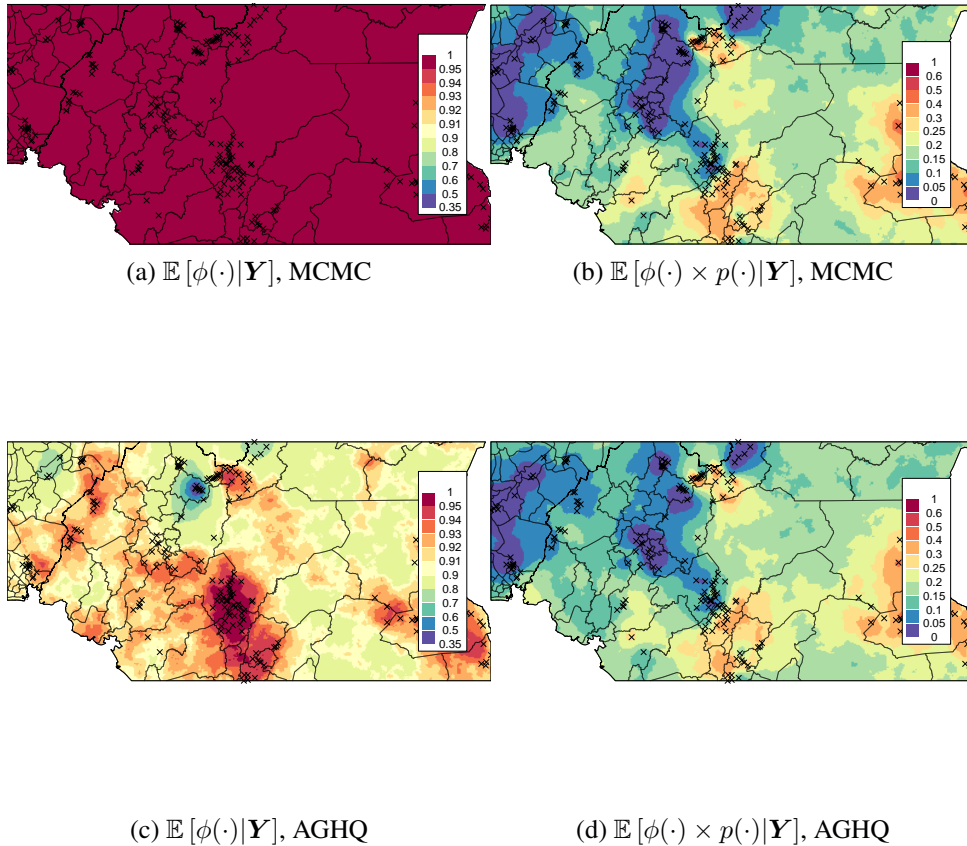
For $n = 1, \dots, N$ **do:**

• **For** $l = 1, \dots, M$, **do:**

1. Generate the l^{th} dataset of length n : $\mathbf{Y}_l^{(n)} = \mathbf{Y}_{1,l}, \dots, \mathbf{Y}_{n,l} \stackrel{iid}{\sim} \text{Poisson}(\lambda)$.
2. Compute the approximate normalizing constant: $\tilde{\pi}^{\text{AGHQ}}(\mathbf{Y}_l^{(n)})$ as in Eq. (7).
3. Compute the relative error: $E_{n,l} = \left| \frac{\pi(\mathbf{Y}_l^{(n)})}{\tilde{\pi}^{\text{AGHQ}}(\mathbf{Y}_l^{(n)})} - 1 \right|$.
4. Compute the *de-trended* log-relative error: $D_{n,l} = \log E_{n,l} + r_k \log n$.

Output: Sampled de-trended errors: $(D_{n,m})_{n \in [N], m \in [M]}$.

Figure 6: Estimated posterior mean (a,c) suitability probabilities and (b,d) incidence rates for the `loaloa` example of Section 5 using (a,b) MCMC and (c,d) AGHQ.



gesting empirical convergence to the true data-generating parameter. Performing a simulation of this nature is only feasible because of the favourable runtime of AGHQ in this example; running the 250 total simulations we ran would take approximately $(66 \cdot 250)/(24 \cdot 365) = 1.88$ years with MCMC based on the one run we completed, and only if we could tune that algorithm to produce satisfactory results.

The simulation procedure is described in Algorithm 2. We use sample sizes

$$\mathcal{N} = \{200, 500, 1000, 5000, 10000\}$$

with $M = 50$ simulated datasets for each size. To make the simulation as realistic as possible, we set the true parameter equal to the AGHQ estimated posterior mean of $\boldsymbol{w} = (\boldsymbol{U}, \beta_{\text{suit}}, \boldsymbol{V}, \beta_{\text{inc}})$ from Section 5.2. Fig. 9 shows the empirical RMSE and average coverage of quantile-based pointwise approximate 95% credible intervals for the parameter \boldsymbol{W} as well as the suitability probabilities $\phi(\cdot)$ and (conditional) incidence probabilities $p(\cdot)$ from each simulation. The RMSE for all three sets of parameters decreases on average with higher simulated sample size, with $p(\cdot)$ appearing especially accurately estimated and $\phi(\cdot)$ quite accurate as well. The credible intervals for \boldsymbol{W} and $\phi(\cdot)$ appear conservative—the less severe of the two types of possible inaccurate coverage—while those for $p(\cdot)$ appear to generally agree with their nominal level.

Algorithm 2 Simulations to assess empirical accuracy of AGHQ for Section 5.2

Input: size n_0 of original loa dataset, sample sizes $\mathcal{N} \subseteq \mathbb{N}_{\geq n_0}$ to simulate data for, number of simulations $M \in \mathbb{N}$ of each sample size to do, true parameters $\mathbf{w}_0 = (\mathbf{U}_0, \beta_{\text{suit},0}, \mathbf{V}_0, \beta_{\text{inc},0}) \in \mathbb{R}^m$.

For $n \in \mathcal{N}$ **do:**

- Choose village indices $\mathcal{J} \subseteq [n_0]$ uniformly and with replacement such that $|\mathcal{J}| = n$ and each $j \in [n_0]$ appears at minimum once in \mathcal{J} .

- **For** $l = 1, \dots, M$, **do:**

1. Generate the l^{th} dataset of length n , $\mathbf{Y}_l^{(n)} = \{Y_{l,i}, i \in [n]\}$ as follows.

For $i = 1, \dots, n$, **do:**

- (a) Let $p_i = [1 + \exp(-\beta_{\text{inc},0} - V_{\mathcal{J}_i})]^{-1}$ and $\phi_i = [1 + \exp(-\beta_{\text{suit},0} - U_{\mathcal{J}_i})]^{-1}$,
- (b) Generate $Z_i \sim \text{Binomial}(N_{\mathcal{J}_i}, p_i)$ and $X \sim \text{Unif}(0, 1)$,
- (c) If $X \leq \phi_i$ set $Y_{l,i} = Z_i$, else set $Y_{l,i} = 0$.

2. Fit the model (Section 5.2) using the AGHQ procedure (Section 5.1) to the data $\mathbf{Y}_l^{(n)}$.

3. Compute the estimates:

- Approximate posterior mean $\widehat{\mathbf{W}}_{l,n} = \widetilde{\mathbb{E}}(\mathbf{W} | \mathbf{Y}_l^{(n)})$,
- Approximate pointwise 95% credible interval:

$$\left(\mathbf{W}_{l,n}^{(\text{lower})}, \mathbf{W}_{l,n}^{(\text{upper})} \right) = \left\{ (\tilde{q}_n^{(j)}(.025), \tilde{q}_n^{(j)}(.975)) : j \in [m], \mathbf{Y}^{(n)} = \mathbf{Y}_l^{(n)} \right\},$$

- (similarly for $\phi(\cdot)$ and $p(\cdot)$).

4. Compute the metrics:

- Root-Mean-Square-Error $\text{RMSE}_{l,n} = \left[\frac{1}{m} \left(\widehat{\mathbf{W}}_{l,n} - \mathbf{W}_0 \right)^\top \left(\widehat{\mathbf{W}}_{l,n} - \mathbf{W}_0 \right) \right]^{1/2}$,
- Average coverage:

$$\text{COVR}_{l,n} = \frac{1}{m} \sum_{j=1}^m \mathbb{I} \left[\left(\mathbf{W}_{l,n}^{(\text{lower})} \right)_j \leq (\mathbf{W}_0)_j \right] \times \mathbb{I} \left[\left(\mathbf{W}_{l,n}^{(\text{upper})} \right)_j \geq (\mathbf{W}_0)_j \right],$$

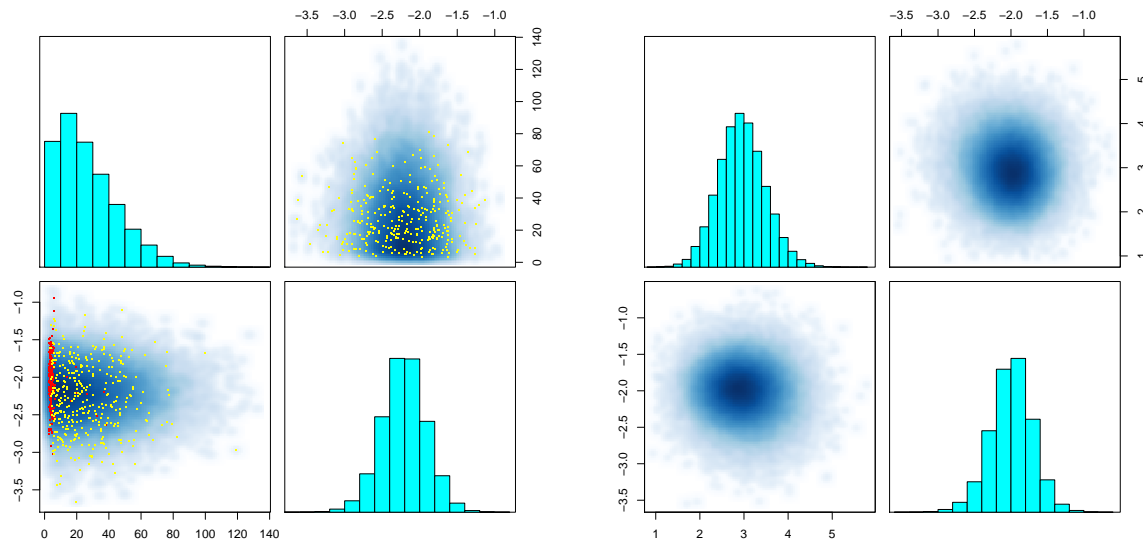
- (similarly for $\phi(\cdot)$ and $p(\cdot)$).

Output: Sampled RMSE and coverage values for \mathbf{W} , $\phi(\cdot)$ and $p(\cdot)$ for $(n, l) \in \mathcal{N} \times [M]$.

H. Glossary of Commonly Used Terms

Symbol	Mathematical Description	Verbal Description
$\boldsymbol{\theta}$	-	Model Parameter
$\mathbf{Y}^{(n)}$	-	Data vector
$\ell_n(\boldsymbol{\theta})$	$\log \pi(\mathbf{Y}^{(n)} \mid \boldsymbol{\theta})$	Log-likelihood function
$\pi(\mathbf{Y}^{(n)})$	-	Marginal likelihood
$\tilde{\pi}(\mathbf{Y}^{(n)})$	Eq. (7)	Approximate marginal likelihood
$\pi(\boldsymbol{\theta})$	-	Prior distribution on Θ
$\ell_n^\pi(\boldsymbol{\theta})$	$\ell_n(\boldsymbol{\theta}) + \log \pi(\boldsymbol{\theta})$	Unnormalized log-posterior
$\boldsymbol{\theta}^*$	-	Closest parameter to truth
$\boldsymbol{\theta}_n^{\text{MLE}}$	$\arg \max_{\boldsymbol{\theta} \in \Theta} \ell_n(\boldsymbol{\theta})$	Maximum likelihood estimator
$\hat{\boldsymbol{\theta}}_n$	$\arg \max_{\boldsymbol{\theta} \in \Theta} \ell_n^\pi(\boldsymbol{\theta})$	Posterior mode
$\mathbf{H}_n(\boldsymbol{\theta})$	$-\frac{\partial^2}{\partial \boldsymbol{\theta} \partial \boldsymbol{\theta}^\top} \ell_n^\pi(\boldsymbol{\theta})$	Negative Hessian of ℓ_n^π
$\hat{\mathbf{L}}_n$	$[\mathbf{H}_n(\hat{\boldsymbol{\theta}}_n)]^{-1} = \hat{\mathbf{L}}_n \hat{\mathbf{L}}_n^\top$	Lower Cholesky decomposition
k	-	Desired polynomial accuracy
\mathbf{z}	Section 2.2	Quadrature point ($\in \mathbb{R}^p$)
$\omega(\mathbf{z})$	Section 2.2	Quadrature weight assigned to \mathbf{z}
\mathcal{Q}	Section 2.2	Set of all quadrature points
\bar{z}_H	$\sup_{\mathbf{z} \in \mathcal{H}(k,p)} \ \mathbf{z}\ _2$	Max quadrature point norm
$\tau_{<b}^{(j)}$	$\{(t_3, \dots, t_{2k}) \in \mathbb{Z}_+^{2k-3} \mid \sum_{s=3}^{2k} t_s = j \text{ and } \sum_{s=3}^{2k} s t_s \leq b-1\}$	
$\tau_{\geq b}^{(j)}$	$\{(t_3, \dots, t_{2k}) \in \mathbb{Z}_+^{2k-3} \mid \sum_{s=3}^{2k} t_s = j \text{ and } \sum_{s=3}^{2k} s t_s \geq b\}$	
$\tau_{=b}^{(j)}$	$\{(t_3, \dots, t_{2k}) \in \mathbb{Z}_+^{2k-3} \mid \sum_{s=3}^{2k} t_s = j \text{ and } \sum_{s=3}^{2k} s t_s = b\}$	
$\tau(\mathbf{t})$	$\sum_{s=3}^a s t_s$ for any $\mathbf{t} = (t_3, \dots, t_a) \in \mathbb{Z}_+^{a-3}$ for $a \geq 3$	
$\mathbb{M}_{j,t}$	$\binom{j}{t_3, \dots, t_{2k}}$	Multinomial coefficients
$\bar{\eta}$	$\sup_{\boldsymbol{\theta} \in B_{\boldsymbol{\theta}^*}^p(\delta)} \lambda_1(\mathbf{H}_n(\boldsymbol{\theta})) \leq n\bar{\eta}$	Maximal Eigenvalue
$\bar{\eta}_n$	$\lambda_1(\mathbf{H}_n(\hat{\boldsymbol{\theta}}_n))/n$	Largest normalized Eigenvalue of the negative Hessian at the posterior mode
$\underline{\eta}$	$\inf_{\boldsymbol{\theta} \in B_{\boldsymbol{\theta}^*}^p(\delta)} \lambda_p(\mathbf{H}_n(\boldsymbol{\theta})) \geq n\underline{\eta}$	Minimal Eigenvalue
$\underline{\eta}_n$	$\lambda_p(\mathbf{H}_n(\hat{\boldsymbol{\theta}}_n))/n$	Smallest normalized Eigenvalue of the negative Hessian at the posterior mode
$F_n^{(j)}(x)$	Section 2.1	True j th marginal CDF of $\boldsymbol{\theta}$
$q_n^{(j)}(\alpha)$	$\inf\{x \mid F_n^{(j)}(x) \geq \alpha\}$	True α -quantile for the j th marginal of $\boldsymbol{\theta}$
$\tilde{F}_n^{(j)}(x)$	Section 2.4	Approx j th marginal CDF of $\boldsymbol{\theta}$
$\tilde{q}_n^{(j)}(\alpha)$	$\inf\{x \mid \tilde{F}_n^{(j)}(x) \geq \alpha\}$	Approx α -quantile for the j th marginal of $\boldsymbol{\theta}$
\widehat{M}_n	$\sup_{\alpha: \alpha \leq m} \sup_{\boldsymbol{\theta} \in B_{\hat{\boldsymbol{\theta}}_n}^p} (\bar{z}_H \ \hat{\mathbf{L}}_n\ \vee \gamma_n) \left \partial^\alpha \ell_n^\pi(\hat{\boldsymbol{\theta}}_n) \right $	

Figure 7: Pairs plots for (a) MCMC and (b) AGHQ posterior samples of β_{suit} (left) and β_{inc} (right). Divergent transitions (●) cause the MCMC algorithm to put non-negligible posterior mass on very large values of β_{suit} , causing the high estimated posterior mean for $\phi(\cdot)$ at all locations (Fig. 6). The clustering of these transitions indicates a potentially serious problem with the algorithm (Gabry et al. 2019).



(a) $\tilde{\pi}(\beta_{\text{suit}}, \beta_{\text{inc}} | \mathbf{Y}^{(n)})$, MCMC

(b) $\tilde{\pi}(\beta_{\text{suit}}, \beta_{\text{inc}} | \mathbf{Y}^{(n)})$, AGHQ

Figure 8: KS statistics, calculated as maximal difference in approximate marginal posterior empirical cumulative distribution functions from 72,000 samples for AGHQ and MCMC, for (a) zero-inflation spatial effects $u(\mathbf{s}_i)$ and (b) incidence spatial effects $v(\mathbf{s}_i), i \in [n]$.

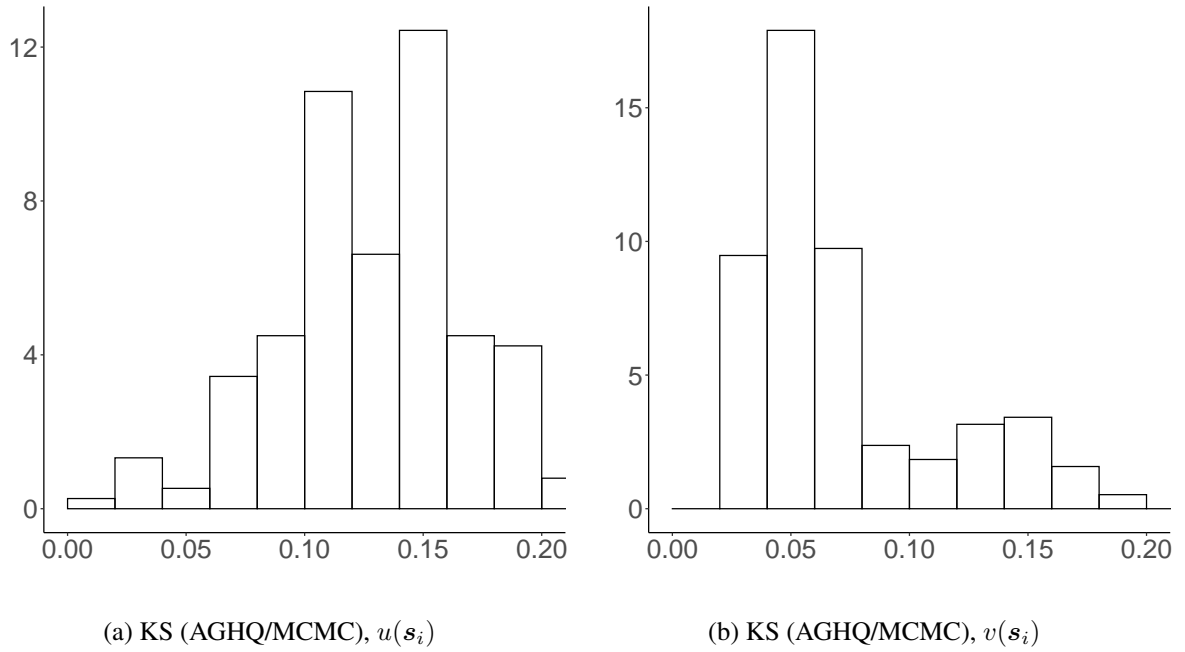


Figure 9: Simulated RMSE (a–c) and average coverage (d–f) for the parameter vector \mathbf{W} (a,d), suitability probabilities $\phi(\cdot)$ (b,e), and (conditional) incidence probabilities $p(\cdot)$ (c,f) for the zero-inflated binomial model of Appendix G.3.

